

# *Analysis of methylation status of CGB genes in common non- trophoblastic cancer*

*Thesis submitted to Middlesex University as partial fulfilment of the  
requirements for the degree of Master by Research*

Ivan Petkov Punev

M00353698

Director of study: Dr Beata Burczynska

Supervisors: Dr Helen Roberts and Dr Celia Bell

Department of Natural Sciences

Faculty of Science and Technology

Date of submission: 21<sup>st</sup> January 2020

## Abstract

hCG is a complex heterodimeric glycoprotein hormone essential during pregnancy. The hormone and its unique  $\beta$ -subunit are recognised tumour markers involved in enabling anti-apoptotic pathways, promotion of invasion and angiogenesis, and supporting tumour proliferation leading to more aggressive cancer and poor prognosis. The limiting factor for the hCG production is the presence of the  $\beta$ -subunit which is encoded by 4 non-allelic genes, *CGB3-9*. These genes are regulated via transcription factors AP2 $\alpha$ , SP1, OCT3/4 and possibly DNA methylation. DNA methylation is a repressive mark found in cytosines in DNA. The aim of this study is to investigate the role of DNA methylation in relation to *CGB3-9* genes activation and hCG/hCG $\beta$  production in non-trophoblastic cancer cell lines. Bioinformatics methods were used to establish the region of interest and predict CpG islands (CGIs) within the promoter region of the target genes. Methylation-sensitive PCR and next generation sequencing were used to assess *CGB3-9* promoter methylation in the cancer cell lines. The transcription level of *CGB3-9* genes was investigated using qRT-PCR with TaqMan probes. Secretion in media of hCG/hCG $\beta$  was investigated with ELISA. The results demonstrated the presence of a CGI associated with *CGB7* which matches previous reports of the transcription of the gene in normal and cancer tissue. Notably, this study confirmed previously reported hypomethylation in trophoblastic cell lines. Hypomethylation of the genes was found in HeLa cell line which matches literature reported transcription studies. However, other results were discordant or inconclusive leading to no significant correlation between methylation and transcription levels. This first sequencing study of *CGB3-9* methylation in non-trophoblastic cancer cell lines was inconclusive for the role of the epigenetic mark in *CGB3-9* genes. Further investigations need to be performed to elucidate the role of methylation.

# Acknowledgments

Foremost, I would like to express my gratitude to my director of study Dr Beata Burczynska and my supervisors Dr Helen Roberts and Dr Celia Bell. Thank you for giving me this opportunity to complete this project and thank you for your patience, guidance and motivation on this learning journey.

I would also like to thank my colleagues and friends from the GAA team, research students and colleagues from the Dept. of Natural Sciences for the advice, stimulating discussions and support which helped me to arrive here.

Last but not least, I want to express my gratitude and appreciation for my family and friends who never stopped believing in me and were there for me through the difficult times.

# Table of Contents

<b>Abstract</b> .....	i
<b>Acknowledgments</b> .....	ii
Table of Contents.....	iii
<b>Abbreviations</b> .....	vi
<b>1. Introduction</b> .....	1
1.1 hCG function and structure.....	1
1.1.1 Normal physiology .....	1
1.1.2 hCG activation of LH/hCG-R and other alternative pathways.....	5
1.1.3 hCG Structure .....	7
1.1.4 Cancer and varied forms of hCG .....	10
1.2 <i>CGB</i> Gene Cluster.....	12
1.2.1 <i>CGB</i> promoter and its regulation .....	14
1.2.2 Regulation via Transcription Factors .....	15
1.3 DNA Methylation and <i>CGB</i> genes .....	16
1.3.1 General function of methylation .....	16
1.3.2 Methylation and <i>CGB</i> genes.....	19
1.3.3 DNA methylation changes in cancer.....	20
1.4 Detection of DNA Methylation.....	21
1.5 Aims.....	23
<b>2. Methods</b> .....	24
2.1 Sample Collection.....	24
2.1.1 Tissue culture .....	24
2.1.2 DNA samples .....	24
2.1.3 RNA samples .....	25
2.1.4 Protein samples.....	25
2.2 <i>CGB in silico</i> .....	26
2.2.1 Multiple sequence alignment.....	26
2.2.2 CpG islands.....	27

2.2.3	Primer design .....	27
2.3	<i>CGB</i> promoter methylation .....	27
2.3.1	Bisulphite conversion.....	27
2.3.2	MSP.....	28
2.3.4	Sequencing .....	28
2.4	<i>CGB</i> expression and secretion .....	29
2.4.1	cDNA.....	29
2.4.2	qRT-PCR.....	29
2.4.3	ELISA .....	30
2.5	Statistical Analysis.....	31
<b>3.</b>	<b>Results</b> .....	<b>32</b>
3.1	Putative promoter Characteristics.....	32
3.1.1	MSA of target region.....	32
3.1.2	CGI prediction .....	33
3.2	Methylation profile.....	35
3.2.1	MSP.....	35
3.2.2	Sequencing primers.....	36
3.2.3	Global profile of <i>CGB3-8</i> methylation .....	37
3.2.4	Differential analyses of methylation .....	44
3.3	Transcription level of <i>CGB3-8</i> .....	50
3.4	Secretion of hCG and hCG-beta.....	51
<b>4.</b>	<b>Discussion</b> .....	<b>53</b>
4.1	MSP analysis did not find differential methylation.....	53
4.2	MiSeq based bisulphite sequencing .....	54
4.3	Trends in DNA methylation of <i>CGB3-8</i> promoter.....	55
4.4	Similarities in DNA methylation of cancer cell lines .....	57
4.5	<i>CGB7</i> has a CGI within promoter .....	59
4.6	Methylation differences within tissue groups .....	61

4.6.1 Trophoblastic versus non-trophoblastic cell lines .....	61
4.6.2 Differences in tissue of origin groups.....	62
4.7 Transcription and translation level of <i>CGB3-8</i> genes.....	66
4.8 Limitations of study .....	70
4.9 Further research .....	72
<b>5. Conclusions</b> .....	<b>75</b>
<b>6. References</b> .....	<b>76</b>
<b>Appendix</b> .....	<b>87</b>
A1. DNA and RNA samples.....	88
A2. <i>In silico</i> analyses .....	89
A2.1 MSA with promoter elements .....	89
A2.2 CpG Island predictions.....	93
A2.3 Primer design and ePCR .....	94
A3. MSP Densitometry .....	102
A4. Sequencing data .....	104
A5. R statistics.....	109
A5.1 MethylKit analysis .....	109
A5.2 PCA.....	110
A6. Analyses of difference .....	111
A6.1 Average Promoter methylation.....	111
A6.2 Average promoter methylation vs cancer type .....	112
A6.3 Average promoter methylation vs cell line origin.....	115
A7. qRT-PCR data.....	126
A7.1 Correlation .....	132
A8. ELISA data .....	133

## Abbreviations

<b>(i)EVT</b>	(Invasive) Extravillous Cytotrophoblast
<b>5mC</b>	5-Methyl Cytosine
<b>aa</b>	Amino Acid
<b>AKT</b>	Protein Kinase B
<b>ANOVA</b>	Analysis Of Variance
<b>AP2<math>\alpha</math></b>	Activator Protein 2 (Alpha)
<b>bp</b>	Base Pair
<b>BS</b>	Bisulphite Sequencing
<b>cAMP</b>	Cyclic Adenosine Monophosphate
<b>CD</b>	Cluster Of Differentiation
<b>cDNA</b>	Complementary DNA
<b>CGA</b>	Chorionic Gonadotropin Subunit Alpha
<b>CGB</b>	Chorionic Gonadotropin Subunit Beta
<b>CGI</b>	CpG Island
<b>c-Jun</b>	Jun Proto-Oncogene
<b>CpG</b>	Cytosine Guanine Dinucleotide
<b>CRE</b>	cAMP Response Element
<b>DAPK</b>	Death Associated Protein Kinase
<b>DNA</b>	Deoxyribonucleic Acid
<b>DNase</b>	Deoxyribonuclease
<b>DNMT</b>	DNA Methyltransferase
<b>EDTA</b>	Ethylenediaminetetraacetic Acid
<b>ELISA</b>	Enzyme Linked Immunosorbent Assay
<b>EMT</b>	Epithelial-To-Mesenchymal Transition
<b>ERK1/2</b>	Extracellular Signal-Regulated Kinases
<b>EZH2</b>	Enhancer Of Zeste 2 Polycomb Repressive Complex 2 Subunit
<b>F</b>	Forward
<b>FBS</b>	Foetal Bovine Serum
<b>FSH</b>	Follicle-Stimulating Hormone
<b>H3K27me</b>	Lysine 27 Histone 3 Methylation
<b>hCG</b>	Human Chorionic Gonadotropin
<b>hCG-H</b>	Hyperglycosylated hCG
<b>HDAC1/2</b>	Histone Deacetylase 1/2
<b>kDa</b>	Kilo Dalton
<b>(h)LH</b>	(human)Luteinising Hormone
<b>LH/hCG-R</b>	LH and hCG Common Receptor
<b>M</b>	Methylated
<b>MSA</b>	Multiple Sequence Alignment
<b>MS-HRM</b>	Methylation Sensitive High Resolution Melting
<b>MSP</b>	Methylation Sensitive PCR
<b>MTA3</b>	Metastasis Associated Protein
<b>NGF</b>	Nerve Growth Factor
<b>NT</b>	Non-Trophoblastic
<b>NuRD</b>	Nucleosome Remodelling Deacetylase
<b>OCT3/4</b>	Octamer Binding Transcription Factor
<b>PBS</b>	Phosphate Buffered Saline
<b>PC</b>	Principal Component
<b>PCA</b>	Principal Component Analysis
<b>PCR</b>	Polymerase Chain Reaction

<b>PDGF</b>	Platelet-Derived Growth Factor
<b>PKA</b>	Protein Kinase A
<b>PPAR<math>\gamma</math></b>	Peroxisome Proliferator Activated Receptor Gamma
<b>PS</b>	Penicillin Streptomycin
<b>qRT-PCR</b>	Quantitative Reverse Transcription PCR
<b>R</b>	Reverse
<b>RE</b>	Restriction Enzymes
<b>RM-ANOVA</b>	Repeated Measures ANOVA
<b>RNA</b>	Ribonucleic Acid
<b>RNase</b>	Ribonuclease
<b>SAM</b>	S-Adenosyl Methionine
<b>SLUG</b>	Snail Family Transcriptional Repressor 2
<b>SMAD2</b>	Mothers Against Decapentaplegic Homolog 2
<b>SNAIL</b>	Snail Family Transcriptional Repressor 1
<b>SNP</b>	Single Nucleotide Polymorphism
<b>SP1/3</b>	Specificity Protein 1/3
<b>ST</b>	Syncytiotrophoblast
<b>T</b>	Trophoblastic
<b>TDG</b>	Thymine DNA Glycosylase
<b>TET</b>	Tet Methylcytosine Dioxygenase
<b>TF</b>	Transcription Factor
<b>TGFBR</b>	TGF- $\beta$ Receptors
<b>TGF<math>\beta</math></b>	Transforming Growth Factor Beta
<b>Th</b>	T-Helper Cell
<b>TSE</b>	Trophoblastic Specific Element
<b>TSH</b>	Thyroid Stimulating Hormone
<b>TSS</b>	Transcription Start Site
<b>TWIST</b>	Twist Family BHLH Transcription Factor 1
<b>U</b>	Unmethylated
<b>UTR</b>	Untranslated Region
<b>VCT</b>	Villous Cytotrophoblast
<b>VEGF</b>	Vascular Endothelial Growth Factor
<b>VEGF-R</b>	Vascular Endothelial Growth Factor Receptor
<b>WG</b>	Week Of Gestation



# 1. Introduction

## 1.1 hCG function and structure

### 1.1.1 Normal physiology

Human chorionic gonadotropin (hCG) is a physiologically significant protein heterodimer highly synthesised in the first three months of pregnancy (Guo *et al.*, 2011). In normal physiology, hCG, or the pregnancy hormone, is released by the placenta. Its main role is to support pregnancy by stimulating progesterone secretion, promoting appropriate implantation, and preventing endometrial apoptosis (Rull *et al.*, 2008).

hCG hormone is only found in humans and subhuman primate species. The hormone prevents corpus luteum regression and maintains its (ovarian) progesterone secretion until the shift in progesterone synthesis to placenta is completed by 9<sup>th</sup> week of gestation (WG) (Fournier, 2016, Rao, 2016). hCG is the first signal released by the conceptus after implantation and it is used to detect pregnancy. hCG and its beta subunit are detected in maternal blood from 1WG and their levels increase until 10-12WG then steadily drop until delivery (Fig. 1). The alpha subunit of hCG keeps increasing until delivery (Fournier, 2016).

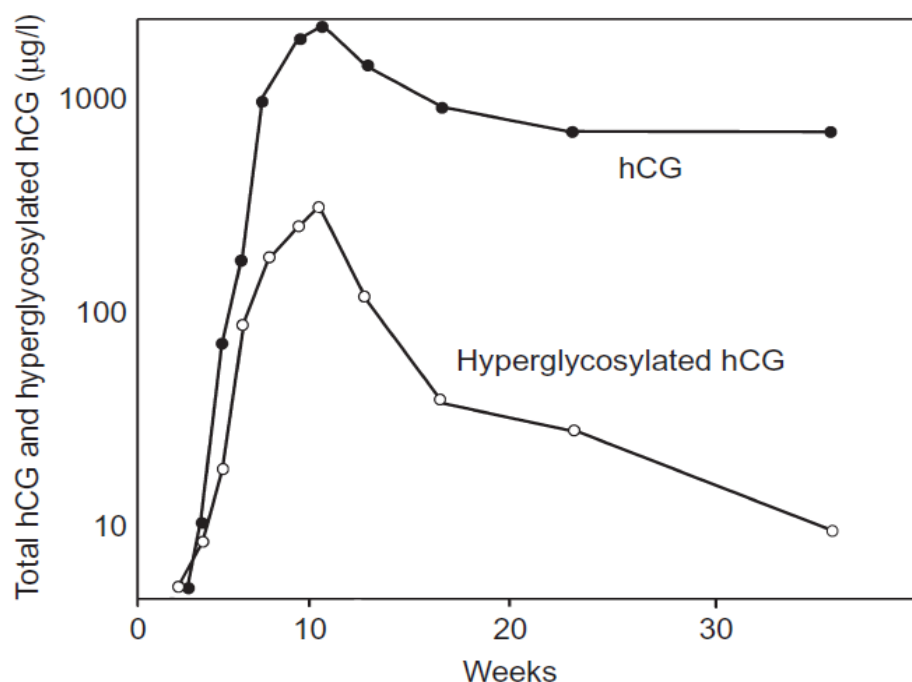


**Fig.1** Levels of hCG and its hyperglycosylated form in the serum during pregnancy. Adapted from (Cole, 2015)

The hCG molecule acts as a ligand activating the LH/hCG-R, a receptor that is shared between hCG and luteinising hormone (LH) (Guo *et al.*, 2011). This is due to high similarity between the 2 hormones. hCG binds to this receptor with higher affinity than LH which leads to hCG being more active *in vivo* (Casarini *et al.*, 2012). These receptors are widely distributed in the body including non-gonadal tissues. However, there is selectivity in the non-gonadal tissues: liver, lungs, kidney, spleen and skeletal smooth muscle in adults do not contain the receptor. This selectivity is not present in the human foetus which may indicate the possibility of a role of hCG in the promotion of tissue differentiation in embryo (Rao,2016).

In pregnancy, a complex interaction between the mother and conceptus occurs. The blastocyst needs to implant or invade the maternal endometrium and establish link between the developing baby and the mother for the purposes of its optimal growth and development *in utero*. This is achieved via the placenta that develops upon implantation from the trophoblast, the outer layer of the blastocyst. The trophoblast matures into the structures: villous cytotrophoblast (VCT), syncytiotrophoblast (ST), and invasive extravillous (cyto)trophoblast (iEVT) (Singh *et al.*, 2010).

The secretion of hCG in the formed placenta is done by the endocrine tissue known as syncytiotrophoblast (Fournier, 2016, Rao, 2016). The ST develops from the trophoblast via the autocrine action of hCG when the blastocyst invades the maternal decidua (endometrium) during implantation (Fig. 2) (Singh *et al.*, 2010). hCG promotes the formation of syncytiotrophoblasts by binding to the common LH/hCG-R which triggers secondary messengers like cAMP and inositol phosphates. This in turn starts the process of villous cytotrophoblast fusion into multinucleated ST (Fournier, 2016).

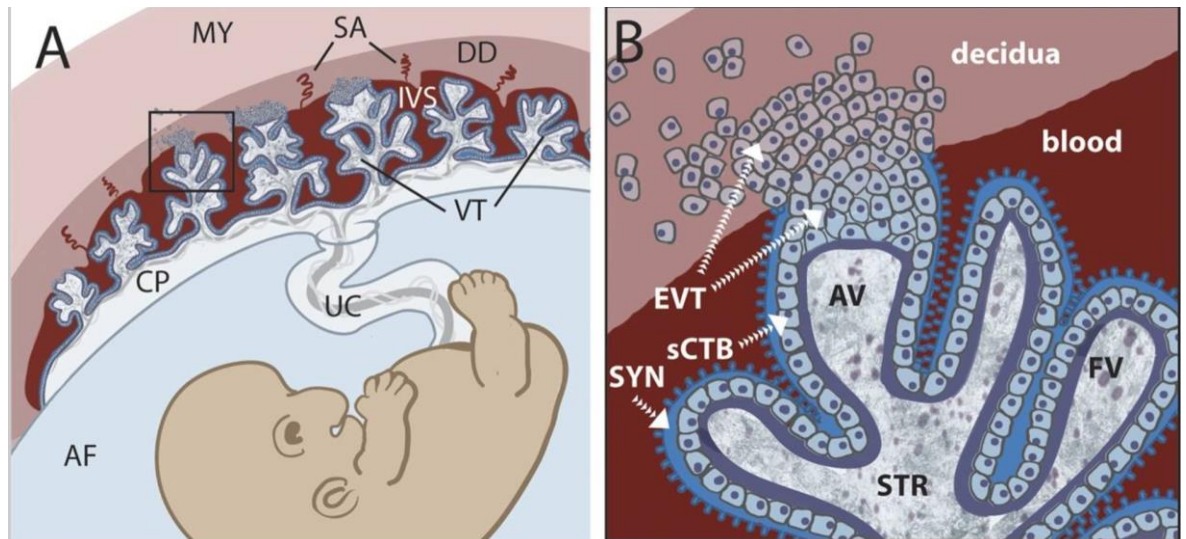


**Fig.2** Placental structure at approximately 6 weeks of gestation. A. Orientation of foetus and placenta. B. Closer view of the interface between mother and foetus. Abbreviations: MY: myometrium; SA: spiral arteries; DD: decidua; IVS: intervillous space filled with maternal blood; VT: villous tree; CP: chorionic plate; UC: umbilical cord; AF: amniotic fluid; AV: anchoring villi; FV: floating villi; SYN: syncytiotrophoblast; sCTB: subsynchronal cytotrophoblast; STR: villous stroma; EVT: extravillous cytotrophoblast. Adapted from Robbins *et al.*, 2012.

The invasion of the endometrium is essential to establish the foeto-maternal link needed for a successful pregnancy. Trophoblast cells cross into the maternal decidua to begin process of remodelling the maternal spiral arteries to establish the vasculature connecting the mother and the baby (Singh *et al.*, 2010). The trophoblast cells taking part in this process are the invasive extravillous trophoblast. Compared to the villous cytotrophoblast these cells express less cell adhesion molecules and more proteinases that degrade the extracellular matrix, allowing their invasive and migratory properties (Singh *et al.*, 2010).

*In vitro* studies have identified that the iEVT exhibits a different isoform of hCG – the hyperglycosylated hCG (hCG-H). Conditioned media from iEVT promotes trophoblast invasion suggesting that hCG-H isoform is responsible for the invasive properties of the trophoblast (Fournier, 2016). In ST conditioned media no hyperglycosylated protein was found and the media did not elicit invasion of the trophoblast. *In vivo* hCG-H concentration increases and peaks during 9WG, and steadily decrease thereafter reaching a plateau at the beginning of 2<sup>nd</sup> trimester corresponding to the end of the trophoblastic invasion. This further supports that hCG-H is responsible for the invasive properties of iEVT. It has also been proposed that the invasive properties may be a result from a pathway independent of LH/CG-R activation (Fournier, 2016).

hCG also promotes angiogenic activity in the placenta, maintains quiescence of myometrium and helps in development of embryonic immunotolerance in the mother (Fournier, 2016, Rull *et al.*, 2008). The angiogenic activity is proposed to be due to hCG inducing upregulation of vascular endothelial growth factor (VEGF) and indirectly triggering angiogenesis. Also, LH/hCG-R has been found to be expressed in vascular endothelial cells. hCG acts on the endothelial cells by promoting their migration, permeability, and proliferation and increasing capillary sprout formation. Further to this direct effect hCG promotes vessel maturation by recruiting perivascular cells. hCG has also been reported to promote spiral artery angiogenesis (Połeć *et al.*, 2014, d'Hauterive *et al.*, 2011). There is some evidence to suggest that the pregnancy hormone may contribute towards the increase of the foeto-placental perfusion by dilation of the uterine blood vessels. This is thought to promote the acquisition of nutrition from the maternal circulation to meet the needs of the developing baby and to help with the foetal waste removal (Rao, 2016).

Upon implantation the hCG molecule contributes to the quiescence of the myometrium (Rao, 2016). Myometrial quiescence involves downregulation of the myometrium gap-junctions. hCG binds directly to myometrial LH/hCG-R to reduce their expression. Also, it has been shown that exogenous hCG inhibits oxytocin-induced labour (Ambrus and Rao, 1994). The decrease of hCG levels towards the end of pregnancy may allow for the activation of the myometrium to promote successful delivery of the baby (Rao, 2016). Further to that, it has been shown that myometrium from term labour contains less LH/hCG-R, thus less chance of inhibition of labour (Ambrus and Rao, 1994).

Maternal immunotolerance is essential for successful pregnancy. The conceptus is a semi-allograft that needs to be protected from the maternal immune system to ensure there is no miscarriage due to immune rejection upon implantation. To ensure this the maternal leukocytes need to be signalled to tolerate the immunologically distinct blastocyst (Tsampalas *et al.*, 2010, Schumacher *et al.*, 2009). The main agents of this tolerance or rejection process are the T-cells. hCG has been shown to downregulate the Th1 cells, CD8<sup>+</sup> T-cells and macrophages which take part in the rejection of non-self-molecules. However, the pregnancy hormone increases the Th2 cells and the ratio of CD4<sup>+</sup>CD25<sup>+</sup>/CD4<sup>+</sup> T-cells in the spleen and pancreatic lymph nodes which helps tolerate the conceptus by the maternal immune system (Tsampalas *et al.*, 2010, Schumacher *et al.*, 2009).

Other roles of the hCG have also been reported. It has been documented that hCG hormone may play a role as anti-HIV agent *in utero* protecting the developing foetus from infection. hCG has also been proposed to reduce the manifestation of autoimmune disorders such as Rheumatoid arthritis and Diabetes Mellitus Type I due to the immunotolerance effects induced by the hormone during pregnancy. It has been suggested that hCG plays a role in the promotion of growth and differentiation of human foetal tissues. hCG has been shown to promote the growth and development of the breast tissue whereby the hormone triggers irreversible differentiation of the epithelial tissue to secretory cells which are immune to carcinogenic triggers (Rao, 2016).

### 1.1.2 hCG activation of LH/hCG-R and other alternative pathways

Activation of the LH/hCG-R by hLH or hCG can trigger several cell-signalling pathways: cAMP/PKA, ERK1/2 and AKT (Fig. 3) (Borisova *et al.*, 2017, Casarini *et al.*, 2012). hCG binding mainly activates the cAMP/PKA pathway by which the secondary messenger cAMP is released to modulate responses stimulating progesterone synthesis in the ovary and morphological changes such as angiogenesis in vascular endothelial cells (Połec *et al.*, 2014, Casarini *et al.*, 2012, d'Hauterive *et al.*, 2011). ERK1/2 and AKT pathways are more often activated by hLH. The activation of the 2 pathways modulates proliferation, differentiation and survival (Casarini *et al.*, 2012).

The receptor is a glycoprotein of 675 amino acids encoded by a single gene. LH/hCG-R has an external domain rich in leucine residues that is responsible for the recognition and binding of hCG/LH coupled to 7 domains spanning through the membrane and an intracellular portion coupled with G-protein (Fig. 3). Once activated by hCG the receptor triggers a signal transduction via the secondary messenger cAMP part of the cAMP/PKA pathway to initiate progesterone secretion and fusion process of VCT (Tsampalas *et al.*, 2010).

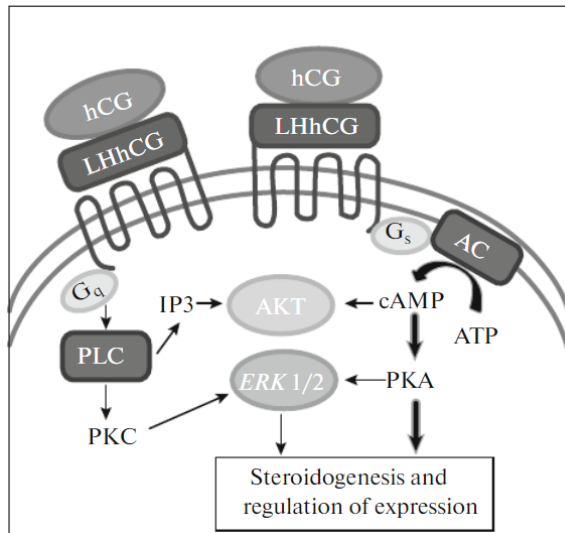


**Fig.3** LH/hCG-R receptor and pathways activated by hCG. Thicker arrows show characteristic pathway used. PKA - protein kinase A, PKC – protein kinase C, AKT—protein kinase B, ERK1/2—serine/threonine MAP kinases. Adapted from (Borisova *et al.*, 2017)

Research has shown that in some instances hCG may act independently of its native LH/hCG-R. Proliferation of uterine natural killer cells, mediated via hCG, has been shown to act via the mannose receptor CD206 (Tsampalas *et al.*, 2010). Murine LH/hCG-R knock out models have shown hyperglycosylated hCG mediated angiogenic activity suggesting alternative receptor activation. It was reported that angiogenic activity is mediated via TGF- $\beta$  receptor (Fournier, 2016). Another study has shown empirically that hCG- $\beta$  subunit is activating the TGF- $\beta$  receptor to induce EMT (epithelial to mesenchymal transition) in colorectal cancer (Kawamata *et al.*, 2018). However, this remains a controversial topic as some of the preparations used in these studies may have been cross contaminated, with for instance, TGF $\beta$ , and other growth factors may have in fact activated the TGF- $\beta$  receptor (Koistinen *et al.*, 2015).

All in all, the underlying processes in the developing conceptus are orchestrated in big part by the hCG hormone. Pregnancy is strictly regulated to ensure normal physiology is maintained (Singh *et al.*, 2010). An imbalance of the hormone can result in various pathologies. Lower hCG levels are associated with ectopic pregnancies or miscarriages. In cases of low hCG shallow implantation can occur and thus preeclampsia can arise (Fournier, 2016; Singh *et al.*, 2010). High levels of hCG in maternal blood can link with trisomy of the embryo or can be a marker of cancer such as choriocarcinoma (Keay *et al.*, 2004).

### 1.1.3 hCG Structure

Human chorionic gonadotropin is a heterodimeric molecule which shares similarities with luteinising hormone, follicle-stimulating hormone (FSH), and thyroid stimulating hormone (TSH). These hormones have a common  $\alpha$  subunit and the  $\beta$  subunit determines their respective biological functions (Rull *et al.*, 2008; Stenman *et al.*, 2004). hCG is also part of the diverse cysteine-knot growth factor superfamily together with TGF- $\beta$ , NGF, PDGF (Cole, 2015, Iyer and Acharya, 2011). hCG is a glycosylated protein of about 37kDa that has 2 subunits which are non-covalently associated. The alpha subunit consists of 92 amino acids and the beta – consists of 145 amino acids (Fournier, 2016, Rao, 2016).

The tertiary structure of the hCG protein is maintained by a cysteine knot in the centre of each subunit. This cysteine knot is formed by 3 disulphide bridges linking the protein molecule of each subunit in a way that forms 3 loops. When the 2 subunits of hCG form the intact protein, they bind non-covalently in an antiparallel manner such that the first and third loop of one subunit and the second loop of the other molecule lie on the same side of the knot (Fig. 4) (Berger *et al.*, 2013).

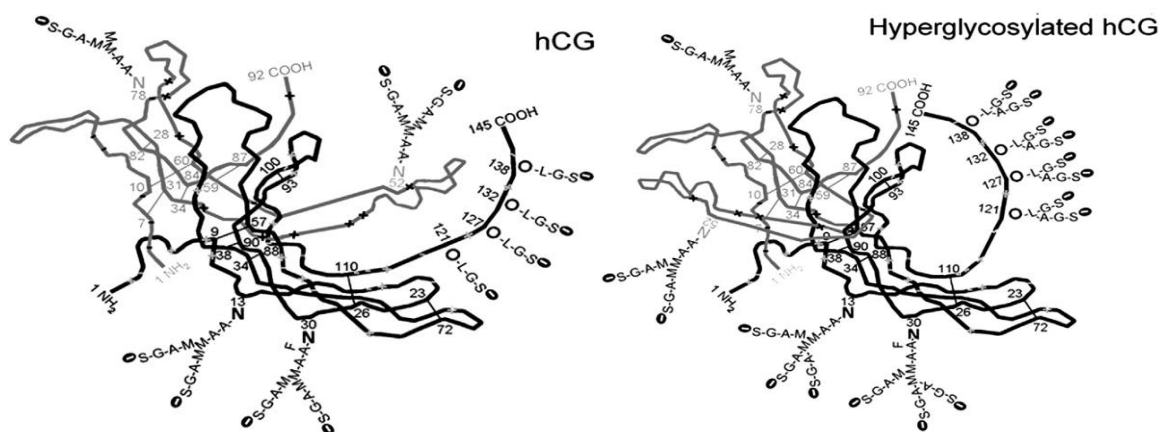


**Fig.4** Structures of hCG and hyperglycosylated hCG with proposed attached sugar moieties. (Cole, 2015)

Additionally, the protein structure is complicated by glycosylation which creates a diverse variety of hCG isoforms. Glycosylation is the covalent binding of a carbohydrate residue to a peptide. It determines the folding, receptor binding and half-life of the hCG molecule (Berger *et al.*, 2013). The sugar branches in hCG can be O-linked oligosaccharide containing N-acetylgalactosamine linked to a serine

residue or N-linked oligosaccharide containing N-acetylglucosamine residue linked to asparagine residue. The alpha subunit has 2 N-glycosylation sites, and the beta - 2 N-glycosylation and 4 O-glycosylation sites located in Carboxyl terminus of the polypeptide (Fournier, 2016).

Depending on the site of production, whether it is during pregnancy or in cancer, hCG has different sugar moieties, conferring different functions (Fournier, 2016; Cole, 2007). Studies investigating the difference in the hCG isoforms have reported important sites on the protein molecule that seem to distinguish between hCG and its highly glycosylated form hCG-H. The serine residues 127, 132, and 138 presenting with predominantly bi-antennary O-linked oligosaccharides are typical for the hCG-H whereas monoantennary O-linked oligosaccharides are more consistent with hCG (Fig. 4) (Cole, 2007).

hCG-H is a family of glycoproteins with 40-43 kDa molecular weight. hCG-H has tri-antennary N-linked oligosaccharide and double molecular size (hexasaccharide) O-linked oligosaccharides. As previously mentioned, it has been reported that hCG-H is important for the invasive properties of the iEVT in normal pregnancy and associated with successful embryo implantation (Fournier, 2016). The larger hCG-H isoform has been reported in choriocarcinoma, testicular germ cell malignancies and other invasive diseases supporting possible role of the hCG-H in promoting cellular invasion (Cole, 2007).

Due to high amount of glycosylation the protein dimer of hCG-H does not fold properly resulting in exposing the central cysteine knot. This knot is very similar to structures found in TGF- $\beta$  and other members of the cysteine knot growth factor family (Berger *et al.*, 2013). The exposed cysteine knot in hCG-H may interact with TGF- $\beta$  receptors to reduce trophoblast apoptosis during the 1<sup>st</sup> trimester and enhanced invasion associated with secretion of metalloproteinases (Fournier, 2016).

Given the involvement of hCG in pregnancy and pathological conditions such as miscarriages and cancer, it is important to be able to detect the hormone for prognostic and diagnostic purposes (Iles *et al.*, 2010, Uuskula *et al.*, 2010). Discovering immunologically and biologically important epitopes to design antibodies for hCG is essential for the hormone's detection with methods such as the commonly employed ELISA. However, the variety of hCG isoforms due to glycosylation and thus folding poses a challenge in the epitope identification. A



further complication is the fact that the genes coding for hCG (*CGB3-9* genes) have evolved from the *LH* gene (*CGB4*). The hLH protein shares > 85% similarity with hCG. The main difference between the 2 different proteins is in the extended carboxyl terminus of hCG. This poses the challenge of designing an antibody that is specific only to hCG (Berger *et al.*, 2013).

hCG metabolism in the body generate different fragments or variants that have been applied in different assays in aiding diagnosis. There are 6 established variants which have been internationally defined: intact hCG, free  $\beta$ -subunit, free  $\alpha$ -subunit, nicked hCG, nicked  $\beta$ -subunit,  $\beta$ -subunit core fragment. (Table 1) (Berger *et al.*, 2013, Stenman *et al.*, 2006). Assays based on one or multiple of these variants can give valuable information for the detection of pregnancy status and progression and cancer. hCG and its subunits can be detected in serum and urine. The nicked forms of hCG and its  $\beta$ -subunit are mainly found in urine but can be found in serum. The  $\beta$ -subunit core fragment comprises main hCG immunoreactivity in urine (Stenman *et al.*, 2006).

**Table 1** hCG and hCG-related variants. Adapted from (Berger *et al.*, 2013)

Symbol	Molecular definition
hCG	Intact $\alpha\beta$ heterodimer, bioactive
hCG <sub>n</sub>	Nicked $\alpha\beta$ heterodimer, nicks in the region of aa hCG $\beta$ 44-48
hCG $\beta$	Intact noncombined free hCG $\beta$ -subunit, aa hCG $\beta$ 1-145
hCG $\beta$ <sub>n</sub>	Nicked hCG $\beta$ , nicks in the region of aa hCG $\beta$ 44-48
hCG $\beta$ <sub>cf</sub>	Core fragment of hCG $\beta$ ; aa hCG $\beta$ 6-40 linked to hCG $\beta$ 55-92
hCG $\alpha$	Noncombined free $\alpha$ -subunit of hCG; aa hCG $\alpha$ 1-92
Less well-defined hCG variants	
hCG $\beta$ CTP	Carboxylterminal extension of hCG $\beta$ , aa hCG $\beta$ 109/114-145
-CTPhCG	hCG $\beta$ truncated core hCG, missing most of the hCG $\beta$ CTP (aa hCG $\beta$ 121-145)
-CTPhCG $\beta$	hCG $\beta$ truncated core hCG $\beta$ (aa hCG $\beta$ 1-120), missing most of the hCG $\beta$ CTP

Therefore, it is important to design monoclonal antibodies for the detection of the different molecules such as intact hCG, hCG $\beta$ , or metabolites such as the nicked hCG. These molecules share some epitopes but also have some unique ones due to their difference in folding. Extensive research has been performed to identify epitopes detecting one or combination of the hCG variants without cross-reactivity with similar molecules such as LH (Berger *et al.*, 2013).

### 1.1.4 Cancer and varied forms of hCG

Trophoblastic cancers, like choriocarcinomas and hydatidiform moles, and germ cell tumours, such as dysgerminomas and non-seminomatous germ cell tumours, are found to have elevated levels of intact hCG. Raised hCG and its  $\beta$ -subunit have also been confirmed in patients with non-trophoblastic tumours such as bladder cancer, gastrointestinal cancer and breast cancer (Guo *et al.*, 2011; Iles *et al.*, 2010; Stenman *et al.*, 2004). hCG elevation has been correlated with poor outcome in variety of different tumours from various origins including trophoblastic and non-trophoblastic. In the case of bladder cancer the elevation of the beta subunit is associated with a more aggressive cancer, with poor prognosis and resistance to available cancer therapies (Iles *et al.*, 1996). Intact hCG and also the free  $\beta$  subunit of hCG are used as a sensitive tumour marker for trophoblastic and testicular germ cell tumours (Rull *et al.*, 2008).

Some cancers express the hCG in small amounts thought to act as an autocrine growth factor. These small amounts are quickly eliminated and usually not detected in circulation. Some evidence of this role is found in non-trophoblastic lung cancers and trophoblastic neoplasms (Rao, 2016). hCG $\beta$  is also found to play a role as a cancer growth factor by blocking TGF $\beta$ -induced apoptosis rather than stimulation of mitosis and cancer proliferation (Iles *et al.*, 2010). This effect is thought to occur due to structural similarity between hCG $\beta$  and TGF $\beta$  as both can form homodimers and act as growth stimulating factors via their receptors (Cole, 2015). The autocrine mechanism behind this is thought to be due to the hCG- $\beta$  molecule blocking the apoptosis induced by TGF- $\beta$  pathways. Antibody against the  $\beta$ -subunit of hCG reverses the effect of cell growth. Study has confirmed this possibility of apoptosis blocking by showing that the  $\beta$ -subunit can bind to TGF- $\beta$  receptors (TGFBR type 2) and act as antagonist. This further confirms previous research where the  $\beta$ -subunit has been proposed to competitively bind to TGFBR2 to prevent apoptosis activation (Cole, 2007).

A similar role in the inhibition of apoptosis due to hCG- $\beta$  has been found *in vitro* in cervical cancers. In Jankowska *et al.*, (2008) reduction of the beta subunit increases programmed cell death rate confirming its action of growth factor by blocking of apoptosis. In ovarian cancer cell lines expressing hCG- $\beta$  it has also been observed that when apoptosis-related proteins were investigated there was an upregulation of the pro-survival protein BCL-XL and decrease of the pro-

apoptotic protein Bad active form which suggests decreased apoptosis in the cells (Guo *et al.*, 2011).

Further proof of tumour proliferation role of hCG beta has been observed in ovarian cell lines (Guo *et al.*, 2011). Introduction of  $\beta$ -hCG vector into ovarian non-tumorigenic cell lines leads to overexpression inducing increased proliferation in those cells and potential *in vitro* tumour transformation. The overexpression of the beta subunit upregulates cyclins E and D1 together with their partner kinases Cdk-2 and Cdk-4 and cdk-6. This leads to progression through the G2 checkpoint of the cell cycle leading to increased cellular proliferation. Furthermore, the cells showed to be anchorage-independent suggesting increasing tumourigenicity and invasiveness (Guo *et al.*, 2011). Injecting xenografts of these cell lines in nude mice (*in vivo*) showed that the hCG $\beta$  overexpressing cells developed into tumours further supporting the *in vitro* data of the  $\beta$ -hCG mediated transformation of the surface epithelial cells into tumour cells (Guo *et al.*, 2011).

A study in colorectal carcinoma has also reported epithelial transformation due to hCG $\beta$  (Kawamata *et al.*, 2018). In the study transfected cell lines overexpressing hCG $\beta$  were tested for EMT markers SLUG, SNAIL, TWIST, phosphorylated SMAD2 and E-cadherin. Their results show that the markers change their expression as observed during epithelial transformation. They further propose that the EMT process occurs due to TGFBR activation since incubation with inhibitors for the type 1 and 2 TGFBR reversed to normal the levels of EMT markers SNAIL and TWIST. In the study they also report the overexpression of the  $\beta$ -subunit of hCG increased invasiveness and migratory property of the cells (Kawamata *et al.*, 2018).

The hyperglycosylated form of hCG has also been reported to play a role in carcinogenesis. In trophoblastic disease, the hyperglycosylated hCG form has been associated with invasive properties. In cases of trophoblastic cancers hCG-H presence has been detected (Cole, 2007). *In vitro* studies with choriocarcinoma cell lines and testicular germ cell carcinoma cell lines have high levels of hCG-H and some amounts of hCG- $\beta$  but no detectable regular hCG. The cell lines present with increased cellular growth, invasive properties, tumour formation. Similar trend was observed in *in vivo* models with nude mouse xenografts. These properties were lost after the cells were incubated with monoclonal antibodies against hCG-H confirming the invasive and metastasis-inducing properties of the

molecule. Furthermore, the hyperglycosylated form seems to have low interaction with the regular LH/CGR in comparison with the regular isoform suggesting activation of a different receptor to induce the invasive autocrine functions (Cole, 2007).

As mentioned above hCG-H and the beta subunit share a specific cysteine knot structure with a few other cytokines like TGF- $\beta$  (Iyer and Acharya, 2011). This similarity has initiated research surrounding the possible interactions of hCG-H with the receptors of these cytokines and more specifically TGF- $\beta$ . TGF- $\beta$  and its pathway are involved in trophoblast invasion in normal and pathophysiology. hCG-H as well as the free  $\beta$ -subunit have both been proposed to interact with TGFBR to enhance cell proliferation and invasion through modulation of the apoptosis mechanism induced by TGF- $\beta$  (Cole, 2015, Iles *et al.*, 2010). As to why both hCG-H and free  $\beta$ -subunit behave in such manner is that both present hyperglycosylation which in turn changes the protein structure to expose the cysteine knot which then interacts with the TGFBR. In the case of trophoblastic disease there is presence of  $\alpha$ -subunit and this allows for hCG-H to be formed. However, non-trophoblastic malignancies tend to produce only the  $\beta$ -subunit in hyperglycosylated form which still has the cysteine knot. There has been research suggesting the existence of hCG- $\beta\beta$  homodimer, which is suggested to act as a growth factor similar to the homodimer of TGF- $\beta$  (Iles *et al.*, 2010, Cole, 2007)

Further role of hCG in cancer relates to tumour angiogenesis. As mentioned previously hCG works in tandem with VEGF to establish the neovascularisation in the placenta (Połec *et al.*, 2014, d'Hauterive *et al.*, 2011). As such it is thought similar process should occur in cancer. Arieta *et al.*, (2009) reports hCG as independent angiogenic factor in testicular germ cell tumours not related to VEGF expression. Further to that both VEGF and hCG are considered part of the cysteine knot growth factor family together with TGF- $\beta$ . Therefore, it is possible that hCG may play a role in angiogenesis via the VEGF-R (Iles *et al.*, 2010).

## 1.2 CGB Gene Cluster

As established so far hCG has important roles both in normal and pathological states. However, understanding of the molecular mechanisms activating the gene and subsequently protein production, are still unclear. The complexity of the hCG protein structure is reflected in the genetics of the hormone. The common alpha subunit is encoded by single gene *CGA* on chromosome 6q21.1-23 and the gene

is expressed in large excess (Fournier, 2016, Cole, 2015). However, the beta subunit is encoded by a cluster of genes located on chromosome 19(19q13.32) and clustered together with the hLH- $\beta$  gene (Fig.5). The beta subunit is unique for hCG; however, it is still showing high similarity with luteinising hormone (Berger *et al.*, 2013).

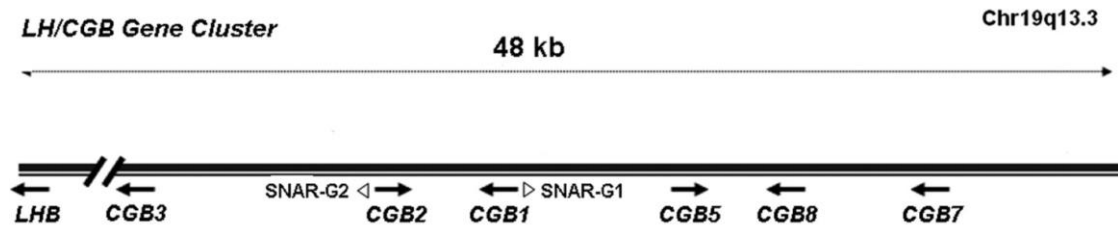


**Fig.5** LHB/CGB gene cluster. Diagram representing the relative positions of the genes Adapted from Burczynska *et al.*, 2014.

There are 6 number of genes referred to as CGB1-9 divided into two types. The CGB genes are highly homologous but transcribed at different levels in trophoblastic tissues. Parrott *et al.* (2011) groups CGB3-9 as type I genes and CGB1/2 as type II. All CGB genes have 3 exons but type I and II genes produce different transcripts. Type I genes produce one transcript with the exception of CGB7 which has splice variants. Type I genes produce the mRNA needed to translate the hCG $\beta$  subunit 145aa. Type II genes have been found to have multiple splicing variants varying from the type I gene transcript (Rull *et al.*, 2008). This is because the CGB1-2 genes have a specific long insert of approx. 730 base pairs in the 5' untranslated region (UTR). This leads to Type II producing a transcript corresponding to predicted 132 aa sequence of unknown protein (Rull and Laan, 2005).

Type I genes are 4 genes and 2 alleles encoding for the biologically active hCG $\beta$  subunit. CGB6 is an allele of CGB7 and CGB9 is an allele to CGB3 (Stenman *et al.*, 2004). CGB3-9 genes can further be grouped in two types based on the translated beta subunit protein. CGB7 (1) has 3 aa difference from type 2 proteins (CGB3, 5, 8) (Fournier, 2016; Berger *et al.*, 2013). CGB6/7 genes are expressed at a low level in non-trophoblastic tissues, where CGB3/9, CGB5, and CGB8 are actively transcribed in placenta, testis and malignant tumours (Stenman *et al.*, 2004).

The most abundantly expressed in pregnancy are the CGB5, 3 and 8 genes (type I) (Glodek *et al.*, 2014). According to some studies CGB5 is with highest

expression in the placenta (Fournier, 2016). Rull and Laan (2005) reported *CGB8* as the most transcriptionally active during pregnancy. However, these differences may be owed due to different polymorphic variant of tested genes or individual differences in trophoblastic differentiation. *CGB7* has low expression profile in comparison to the other Type I genes (Rull and Laan, 2005).

*CGB1* and 2 (type II) were considered to be pseudogenes (Stenman *et al.*, 2004). However, recent research shows that these genes are transcribed in placental tissue and common epithelial cancers; but their protein products have not yet been identified (Burczynska *et al.*, 2014; Glodek *et al.*, 2014). Type II genes are expressed in higher levels in the testes compared to other *CGB* genes (Rull *et al.*, 2007). Their proposed role is in the development of the male reproductive tract in the foetus (Parrott *et al.*, 2011).

The cluster of the beta subunit genes is proposed to have evolved from the *LHB* gene. This happened in recent evolutionary history whereby the *LHB* gene was duplicated and mutated to give rise to the *CGB1-9* genes. In comparison with the *LHB* gene, the *CGB* genes have shifted transcription start site and extended transcription at 3' of the last exon corresponding to the protein's C-terminus (Fournier, 2016; Rao, 2016; Berger *et al.*, 2013).

### 1.2.1 *CGB* promoter and its regulation

Since the placental  $\alpha$  subunit is available in excess, the limiting factor of hCG synthesis is the  $\beta$  subunit which production is influenced by the trophoblast via cAMP (Cole, 2015). The expression of genes coding for hCG $\beta$  (*CGB*) is proposed to be controlled by epigenetic modifications and availability of transcription factors AP2 $\alpha$ , SP1, and SP3 mainly (Glodek *et al.*, 2014; Adams *et al.*, 2011).

As the *CGB* gene family has evolved from *LHB* via a proposed duplication event, the type I genes share a highly similar putative promoter region (Hallast *et al.*, 2007). The *CGB* genes' promoter does not have canonical regulatory elements or TATA box which has posed challenges to identify protein binding sites and how the gene is activated. Initial studies used the similarity with *LHB* gene to identify conserved elements. However, the promoter of *LHB* has been found out to be distinct from that of the *CGB* genes (Johnson and Jameson, 1999).

Empirical approaches were applied to elucidate the sequences required for the activity of *CGB* genes. These identified two enhancer regions upstream of the

transcription start site (TSS) that is responsive to cAMP (CREs) (Fig. 6). In these regions there are also sequences required for basal transcription. These have been found to interact with the ubiquitous Transcription Factors (TFs) AP2 $\alpha$ , SP1 and SP3. The 5' CRE has 2 binding sites for AP2 $\alpha$  and between them an SP1/SP3 binding site. The 3' CRE has 1 AP2 $\alpha$  and one SP1 binding site (Cole, 2015; Johnson and Jameson, 1999; Pestell *et al.*, 1994).

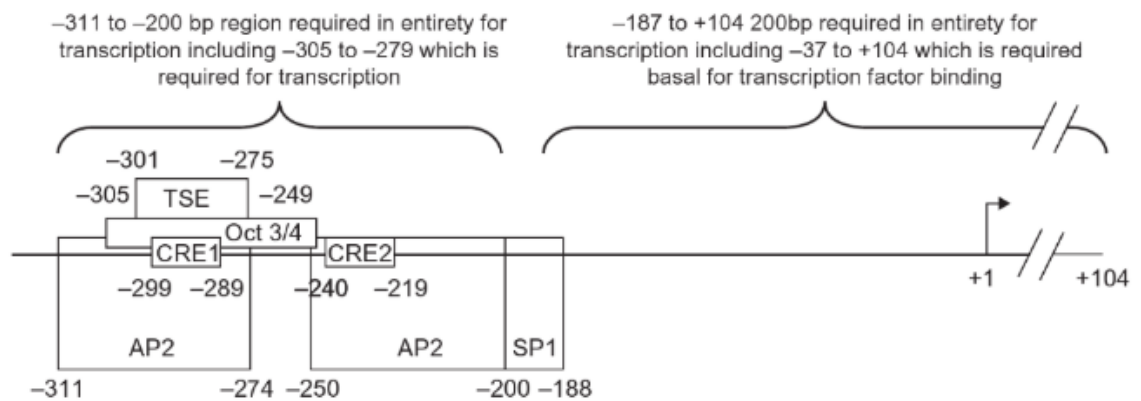


**Fig.6** Putative promoter region of *CGB5* indicating promoter elements and TF binding sites. Adapted from Cole, 2015.

The type II genes *CGB1/2* appear to have a different promoter structure. They have an insertion of DNA of approx. 730bp that replaces the proximal 52 bp of the putative promoter and the 5' UTR in the *CGB3-9* genes. This insert therefore creates a different putative promoter fragment just before the alternative 5'UTR and new exon 1 for the type II genes. This also creates a frameshift for the open reading frame by 1bp for exons 2 and 3 of the type II genes (Hallast *et al.*, 2007).

### 1.2.2 Regulation via Transcription Factors

AP2 $\alpha$  and SP1 act to promote expression of the genes encoding for hCG $\beta$  in the placenta (Adams *et al.*, 2011). AP2 $\alpha$  and SP1 are important in sustaining basal expression but AP2 $\alpha$  has a further role of enhancing cAMP responsiveness. AP2 $\alpha$  competes with SP1 in the 5' CRE. SP1 seems to have a stronger binding to the 5' CRE which competes away the AP2 $\alpha$  binding. Even though AP2 $\alpha$  and SP1 sequences seem to not overlap, both molecules cannot bind together at the 5' CRE. In the 3' CRE SP1 and AP2 $\alpha$  can bind together without the competition seen in the upstream CRE (Fig. 6). (Cole, 2015; Johnson and Jameson, 1999).

AP2 $\alpha$  function has been further proved in mutation studies. Disabling AP2 $\alpha$  binding reduces cAMP responsiveness and decreases the transcription of *CGB* genes. Interestingly, when mutations are introduced in the SP1 sites the cAMP

responsiveness increases. However, both TFs are required for the basal expression of *CGB* genes (Johnson and Jameson, 1999).

Further confirmation of AP2 $\alpha$  role in sustaining hCG level was done by Glodek *et al.* (2014). AP2 $\alpha$  expression levels decrease significantly in pregnancies ending in miscarriage compared with normal pregnancy outcome. The same study shows that hCG serum levels also decrease in miscarriage; thus, a decrease in expression of both hCG and AP2 $\alpha$  correlate positively with complications in pregnancy and can result in miscarriage (Glodek *et al.*, 2014).

The transcription factor SP3 has been shown to act as a repressor of the *CGB* genes (Glodek *et al.*, 2014). It is part of the same family as SP1 and competes for the same binding sites to reduce basal transcription (Johnson and Jameson, 1999). Another repressor of the *CGB* genes is c-Jun. c-Jun can actively bind to the CREs present in the *CGB* promoter to render transcription of the genes terminated (Cole, 2015; Pestell *et al.*, 1994). Oct3/4 has also been reported by Lui and Roberts, (1996) as suppressor of *CGB* gene transcription. Oct3/4 binds to a region between the 2 CRE elements uncompleted by another molecule showing potent repressing abilities (Fig. 6) (Johnson and Jameson, 1999; Lui and Roberts, 1996).

## 1.3 DNA Methylation and *CGB* genes

### 1.3.1 General function of methylation

Epigenetic modifications are a form of gene regulation where heritable changes to gene expression are introduced without changing the DNA sequence. These modifications can be grouped in distinct categories: chromatin remodelling, histone modification, DNA methylation, and microRNA silencing (Tammen *et al.*, 2013). DNA methylation is widespread across different organisms and is the most widely studied epigenetic mark (Cui and Xu, 2018).

Generally, DNA methylation refers to the addition of a methyl group to cytosine at the 5' position which does not affect the DNA sequence (Fig. 7). Recent research has discovered methylation at 6' of adenosine associated with transcriptional activation (Geer *et al.*, 2015). Here, DNA methylation refers to the methylated cytosine residues. It is a repressive mark inhibiting the transcriptional initiation.



The 5-methylcytosine followed by a guanine is termed CpG dinucleotide (Cui and Xu, 2018).

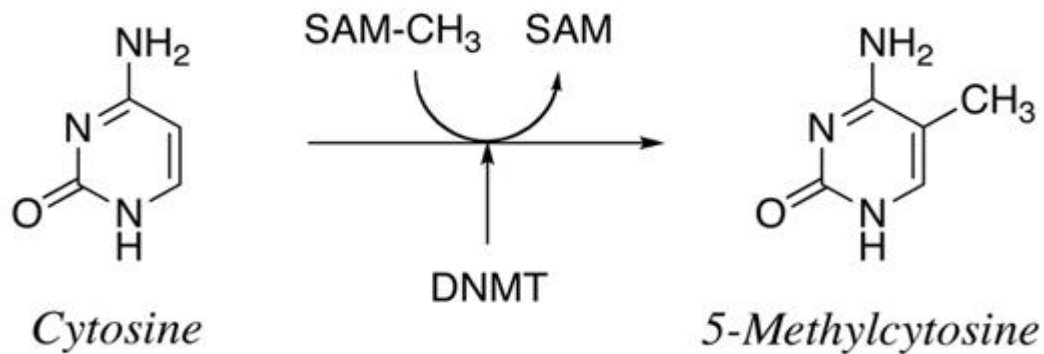


**Fig.7** Formation of 5mC molecule by addition of methyl group (-CH<sub>3</sub>) to cytosine. The reaction is catalysed by DNMT. Adapted from Gibney and Nolan, 2010.

Some regions of the DNA contain CpGs in large quantities known as CpG islands (CGIs), usually within the 5' untranslated region (5' UTR) of a gene promoter. More than half of vertebrate's genes are associated with such short (approx. 1kb) regions. Most CGIs associated with TSS are not methylated. Methylation of CGI at TSS is associated with long term silencing like germ cell expressed genes. They can also be found in intergenic regions and within gene bodies where CGIs are on occasion methylated. CGIs are thought to be more prevalent than CpG poor sites as they are never or shortly methylated leading to a decreased possibility of deamination. Methylated CpGs are mutagenic and can undergo spontaneous deamination converting the Cytosine to Uracil (Jones, 2012; Illingworth *et al.*, 2010).

DNA methylation is established and maintained by a class of enzymes called the DNA methyltransferases (DNMTs). DNMTs catalyse the addition of a methyl group to cytosine from the methyl donor S-Adenosyl methionine (SAM) (Varela-Rey *et al.*, 2014). There are 3 main enzymes identified: DNMT1, DNMT3a and 3b. DNMT1 maintains the established pattern of methylation as it has strong preference for hemimethylated DNA. DNMT3A and 3B are considered the *de novo* methyltransferases which establish the pattern of methylation in early development (Cui and Xu, 2018; Koh *et al.*, 2011).

Removing the methyl group from DNA can be achieved actively or passively. Passive demethylation is the termination of DNA methylation maintenance and allowing for cell division and DNA replication to decrease the amount of 5mC (Guo *et al.*, 2014). Active demethylation has recently been described. It involves

the enzymes TET methylcytosine dioxygenases and TDG. Active demethylation is not achieved by simply removing the methyl group. Most cases it involves a complex process of oxidation that will lead to replacement of the whole base via the Base Excision Repair mechanism or some form of DNA repair or cell division (Guo *et al.*, 2014; Koh *et al.*, 2011).

CpG rich regions in the vertebrate's genome are commonly associated with more than half of the protein producing genes. The other part of the genome is considered to be CpG depleted and about 70% of these CpGs are methylated. Comparing with CGI methylation, non-CGI CpGs have more dynamic methylation and are less uniform and rather tissue specific (Jones, 2012; Illingworth *et al.*, 2010).

Position of methylation is also important in determining the function of it. Methylation has mainly been studied when it is located at the TSS acting as a silencer. However, methylation can be found within the gene in intergenic regions and may have different function in splicing, or when associated with enhancers and insulators (Jones, 2012; Illingworth *et al.*, 2010).

As an epigenetic mark, DNA methylation fluctuates and can be reversed. Most dynamic changes in methylation are observed during embryogenesis (Guo *et al.*, 2015). The Tet enzymes and passive demethylation remove the mark to induce the totipotent state of the cell allowing proper embryogenesis. Lack of Tet enzymes can be detrimental in that period. If not present TET3 enzyme prevents the ability of demethylation of *Oct4* leading to delayed embryogenesis. Similarly, when the epigenetic reprogramming is complete and the establishment of the methylation towards the end of embryogenesis takes place DNMTs are essential. Lack of DNMTs and thus of methylation is incompatible with life (Guo *et al.*, 2015; Guo *et al.*, 2014; Li, 2002).

The reason why DNA methylation is important is when it comes to chromosome stability. Repeat regions are methylated like in centromeres to prevent alteration during processes like chromosomal segregation during cell division. Furthermore, methylation is thought to block transposable elements and thus promoting genomic stability. This silencing of the transposable elements however does not affect the transcriptional elongation. Lack of *de novo* methylation DNMT3A enzyme prevents from development of normal blood cells. This further proves that

5mC is essential for cellular differentiation and development. (Jones, 2012; Li, 2002).

DNA methylation also works with other epigenetic marks such as histone modifications, genomic imprinting and X-inactivation to carry out its functions. Upon methylation of CGI a histone modification follows to render this part of the DNA transcriptionally inactive (Grigoriu, *et al.*, 2011; Wojdacz and Dobrovic, 2007). Nucleosomal DNA is the substrate for *de novo* DNMTs meaning the histone modifications can influence the introduction of methylation by these enzymes. During the process of X-inactivation, DNA methylation packages the chromosome tightly for long-term silencing. Also, methylation is part of Genomic imprinting, taking part in ensuring monoallelic expression of imprinted genes (Jones, 2012; Li, 2002).

### 1.3.2 Methylation and *CGB* genes

It has been reported that in the promoter sequence of the *CGB* genes, CpG dinucleotides are present and these are therefore sites for potential epigenetic gene regulation via methylation (Grigoriu *et al.*, 2011). Under normal physiological conditions (i.e. non-pregnant females and males), the *CGB* genes are highly hypermethylated, which prevents binding of transcription factors and consequent transcription (Grigoriu *et al.*, 2011). When the promoter is hypomethylated, as it occurs during pregnancy, access is granted to transcription machinery and consequently expression of genes coding for hCG is promoted. The placental *CGB* genes show very low methylation levels during the first trimester and this steadily increases until delivery (Grigoriu *et al.*, 2011; Campaign *et al.*, 1993). This corresponds to the serum hCG level fluctuation in pregnancy which also increases until week 12 and then stabilises (Cole and Butler, 2015)

*CGB* aberrant promoter methylation has been linked with miscarriages and adverse pregnancy outcomes (Hanna *et al.*, 2013). Glodek *et al.*, (2014) show that chorionic tissues from miscarriages have higher promoter methylation compared to normal pregnancies. Therefore, hCG $\beta$  is expressed less in miscarriage leading to inability to reach full term pregnancy. The aberrant methylation may reflect problems with the embryo such as chromosomal abnormalities (Glodek *et al.*, 2014).

Additionally, a more specialised type of methylation, gain of imprinting, might be part of the regulation of *CGB*. It relates to the mechanism where only one allele of

a gene (paternal or maternal) is expressed and the other is silenced by methylation (Uuskula *et al.*, 2010). Uuskula *et al.* (2010) have investigated further the methylation of *CGB5* proposing methylation allelic polymorphism (gain of imprinting) that plays a role in pregnancy success. The study concluded that there is link between the methylation allelic polymorphism and miscarriages. Normal term pregnancy shows biallelic expression of the gene but when the paternal genes are silenced by methylation there is increased susceptibility to pregnancy termination (Uuskula *et al.*, 2010).

### 1.3.3 DNA methylation changes in cancer

DNA methylation has been shown to play a role in the development of cancer. Normally, intergenic regions containing transposable elements are highly methylated to maintain genome stability. However, one of the first signs of carcinogenesis is when these mobile regions (transposons) lose their methylation in an event known as global hypomethylation (Robertson, 2005). This allows them to move in the genome and cause genome instability, aberrant gene regulation, and generation of antisense transcripts. At the same time, CGIs associated with tumour suppressor genes become hypermethylated. This causes silencing leading to loss of their protective function. Gene specific hypomethylation may also occur, assisting in the adaptation of tumour cells (Jones, 2012; McCabe *et al.*, 2009; Robertson 2005).

During pregnancy it has been observed that there are changes in the methylation of the *CGB* promoter where it becomes hypomethylated (Grigoriu *et al.*, 2011). It stands to reason that similar changes are observed in cancers. Campain *et al.*, (1993) showed that choriocarcinoma cell lines present hypomethylation in the *CGB* promoter like that observed in normal pregnancy cells. In the same study by Campain *et al.*, (1993) non-trophoblastic cancerous tissues from glioblastoma multiform and lung cancer cell lines show decreased methylation of the *CGB* but the promoters are not as hypomethylated as in choriocarcinoma. Interestingly, only the glioblastoma cell line showed ectopic hCG $\beta$  release (Campain *et al.*, 1993). Further, based on the findings of Campain *et al.* (1993) it may be speculated that gene specific hypomethylation may contribute to the overexpression of *CGB* genes.

A more recent paper investigated DNA methylation of *CGB* in ovarian cancer (Śliwa *et al.*, 2019). The researchers found that the promoter of the *CGB* genes was demethylated when comparing between normal and cancerous ovarian tissue. In their study they also investigated the expression level of the *CGB* genes and associated transcription factors. It was observed that the *CGB3-9* genes were expressed at higher levels in the cancer samples. However, no significant correlation was found between DNA methylation and the expression of the genes in this specific cancer type (Śliwa *et al.*, 2019).

## 1.4 Detection of DNA Methylation

A variety of methods can be utilised to establish the methylation pattern of *CGB* genes. The analysis in Campain *et al.* (1993) is based on selective cleavage of DNA at methylated or unmethylated cytosines by restriction enzymes (RE). However, RE analysis is restricted to specific sites and relies on high quality DNA as well as full digestion by the enzymes (Ammerpohl *et al.*, 2009; Fraga and Esteller, 2002). Currently, bisulphite sequencing (BS) is considered the gold standard in DNA methylation research. Bisulphite modification of DNA introduced more possibilities for methylation analysis since it converts unmethylated cytosines to uracils via deamination across the whole DNA molecule which allows wider gene analysis of all possible CpGs. The most widely applied method for specific locus investigation in research is Methylation Specific PCR (MSP) but this method is prone to false positives and has no quantitative output (Wojdacz and Dobrovic, 2007).

Methylation-sensitive high-resolution melting (MS-HRM) PCR, bisulphite pyrosequencing and MiSeq are examples of quantitative methods applied in DNA methylation analysis (Soto *et al.*, 2016; Colyer *et al.*, 2012; Wojdacz and Dobrovic, 2007). MS-HRM PCR is a relatively new method executed in a closed system that diminishes the possibility of errors. It is a modification of the HRM qPCR methodology developed for single nucleotide polymorphism (SNP) analysis which is able to differentiate 1 nucleotide change (Wojdacz and Dobrovic, 2007). MS-HRM is based on the different amplicon melting temperatures which are dependent on nucleotide content. Following PCR amplification the products are subjected to a steady temperature increase leading to their melting. The decrease of fluorescence upon disintegration of the products is recorded by the machine to produce graphical data. Using different ratios of negative and positive control a

standard curve is produced which is used to quantify the percentage of methylation (Wojdacz and Dobrovic, 2007).

Pyrosequencing is one of the established quantitative techniques providing fast and reliable results with the opportunity for high-throughput analysis (Ammerpohl *et al.*, 2009). The technique is considered as one of the first platforms for Next generation sequencing (Fakruddin *et al.*, 2013). It overcomes the need for bacterial cloning, an essential part of the labour intensive BS procedure. Pyrosequencing also provides more straightforward results for the methylation status of a CpG site compared to BS which relies on a lot of data conversion to convey this information due to the bacterial cloning (Reed *et al.*, 2009). It has been reported that pyrosequencing has a reasonably high sensitivity of detecting 5% methylation comparing to genomic sequencing which has considerably lower sensitivity of detecting 20% methylation (Wojdacz and Dobrovic, 2007).

Bisulphite pyrosequencing requires DNA to be converted with bisulphite as the initial step (Mikeska *et al.*, 2011). The target sequence is then amplified from the converted DNA via PCR with bisulphite sequencing primers. The key part of the amplification step is that one of the primers is biotinylated. The PCR product from the labelled primer is separated and subsequently incubated with sequencing primer. The sequencing primer is shorter than a regular PCR primer and is used as the starting point for the pyrosequencing assay. Pyrosequencing is described as a sequence by synthesis method. Upon the incorporation of a new nucleotide to the sequencing primer luminescence is emitted from the released pyrophosphate which is detected by the machine performing the method (Colyer *et al.*, 2012; Mikeska *et al.*, 2011). This allows for detection of methylation as an SNP at CpG dinucleotides where incorporation of a C denotes methylation and incorporation of a T denotes no methylation. In turn, this provides a quantitative analysis of all CpG dinucleotides covered in the PCR product (Mikeska *et al.*, 2011; Reed *et al.*, 2009).

MiSeq is a newer Illumina-based platform for next generation sequencing. It is also sequencing by synthesis method but with the feature of “bridge” amplification (Soto *et al.*, 2016). Libraries fed to this system need to contain amplicons that are barcoded. These barcodes prime with adaptors on a solid phase to immobilise the amplicon while the sequencing is running creating a bridge. During amplification fluorescently labelled nucleotides are fed and machine detects their incorporation.

Like pyrosequencing, MiSeq is a high-throughput system but uses shorter reads in its analysis. However, Illumina based platforms are currently most used and pyrosequencing support for Roche platforms ended in 2016. MiSeq has moderate cost and compared with other Illumina products has the fastest run times and provides the longest reads (Soto *et al.*, 2016). Methylation studies have employed MiSeq platform to reliably detect at a single nucleotide level the changes in DNA methylation in the context of disease (Roh *et al.*, 2018; Dukal *et al.*, 2017; Xiong *et al.*, 2017).

Currently, there is a gap in knowledge regarding changes in the methylation pattern of *CGB* genes in non-trophoblastic cancers. Glodek *et al.* (2014); Grigoriu *et al.* (2011) and Uskuula *et al.* (2010) have shown that methylation changes in the hCG $\beta$  genes are detrimental for successful pregnancy. However, limited studies have been performed to assess this in the context of non-trophoblastic cancers (Campain *et al.*, 1993; Śliwa *et al.*, 2019). Investigating the potential DNA methylation changes will shed light on possible novel molecular mechanisms involved in re-activation of the *CGB* genes in cancer.

## 1.5 Aims

This project aims to investigate the role of the repressive epigenetic mark (DNA methylation) on the production of hCG and its free  $\beta$  subunit in non-trophoblastic cancer cell lines. This will be achieved by the analysis of the methylation status in the promoter region of *CGB3-9* genes via next generation sequencing. This will be followed by the quantification of the expression level of the *CGB3-8* genes by qRT-PCR and establishing the level of the proteins hCG and its beta subunit secreted in culture media. The methylation status of the *CGB3-8* promoter will be correlated to the expression and secretion of the human chorionic gonadotropin to establish the role of the suppressive mark in non-trophoblastic cancers cell lines.

## 2. Methods

### 2.1 Sample Collection

#### 2.1.1 Tissue culture

Samples used in this study were acquired through cell culturing of 16 different cell lines. All of them are established cell lines already available within the laboratory at Middlesex University. Investigated samples included non-trophoblastic (NT) cancer cell lines, trophoblastic (T) cancer cell lines, normal colon cell line, and a mouse fibroblast cell line (Table 2). The trophoblastic cell lines were included as positive control, CRL-1790 - normal cell line control, and 3T3 – negative control. Cell lines were all grown with 10% Foetal bovine serum (FBS) and 1% penicillin-streptomycin (PS) at 37°C and 5% CO<sub>2</sub>. Table 2 shows culture media used for different cell lines. After the cell lines have become 80% confluent, the cells were collected using trypsinisation and then further processed for total DNA and RNA extraction. Cell pellets collected were stored at -80°C

**Table 2** Investigated cell lines, their respective tissue of origin and used culture media

#	Cell Line (cancer type)	Tissue of origin	Culture media
1	MDA-MB-468 (NT)	breast cancer	RPMI 10%FBS 1%PS
2	MCF-7 (NT)	breast cancer	RPMI 10%FBS 1%PS
4	HeLA (NT)	cervical cancer	DMEM 10%FBS 1%PS
5	HT-3 (NT)	cervical cancer	RPMI 10%FBS 1%PS
6	C-33a (NT)	cervical cancer	RPMI 10%FBS 1%PS
8	BeWo (T)	choriocarcinoma	DMEM 10%FBS 1%PS
9	JEG-3 (T)	choriocarcinoma	RPMI 10%FBS 1%PS
10	HCT116 (NT)	colon cancer	DMEM 10%FBS 1%PS
11	CRL-1790	normal colon	EagleMEM 10% FBS 1%PS
12	3T3	mouse fibroblast	RPMI 10%FBS 1%PS
13	OAW42 (NT)	ovarian cancer	RPMI 10%FBS 1%PS
14	OVCAR-3 (NT)	ovarian cancer	RPMI 10%FBS 1%PS
15	HEY-T30 (NT)	ovarian cancer	RPMI 10%FBS 1%PS
16	SKOV-3 (NT)	ovarian cancer	RPMI 10%FBS 1%PS

#### 2.1.2 DNA samples

DNA was extracted from collected cell pellets. The DNA was extracted using column purification technology. The protocol supplied by the manufacturer was used for the extraction (DNA mini kit, Thermo Fisher Scientific). The cells suspended in 200µl PBS were lysed together with 20µl proteinase K and 20µl RNase-A. The lysate was incubated at 55°C for 10 min and 200µl ethanol was added. The mixture was then spun through the columns at 10,000g. The bound



DNA was washed twice with 500µl Wash buffer and then eluted with 100µl EDTA-Tris by maximum speed centrifugation for 1.5min. DNA concentration and purity were checked with Qubit 3 and NanoDrop 2000 respectively (Table A1, Appendix A1). The DNA was then subsequently used for bisulphite conversion or sent for sequencing, DNA was stored at -20°C.

### 2.1.3 RNA samples

RNA was extracted from the collected cell pellets using column purification technology (RNA mini kit, Thermo Fisher Scientific). The extraction followed the manufacturer's protocol. The cells were lysed with 1% beta-mercaptoethanol lysis solution (volume dependent on cell number in pellet) and homogenised mechanically using 20-gauge needle. The homogenate was mixed with equal volume 70% ethanol and was passed through the column. The bound RNA was washed twice with 700µl Wash buffer I and 500µl Wash buffer II. The column membrane was dried by centrifugation and RNA was eluted in RNase free water. RNA concentration and purity were then checked with Qubit 3 and NanoDrop respectively (Table A2, Appendix A1). The RNA samples were stored at -80°C. Prior to further use in expression studies RNA was also treated with DNase I, Amplification grade (Thermo Fisher Scientific) to remove any possible DNA contaminant. 2µl DNase I in buffer was used to treat 1µg of RNA by incubating for 15min at RT. The enzyme was inactivated using 65°C heat and then 1µl of 25mM EDTA was added to stop the reaction. The cleaned-up RNA was then used in expression studies.

### 2.1.4 Protein samples

Conditioned media from cell lines was collected prior to trypsinisation of confluent cells (Table 3). Trypsinised cells were counted using a haemocytometer. The media was used in ELISA to detect free beta hCG and intact hCG. The media was stored at -80°C.

**Table 3** Growth characteristics of cell lines from which conditioned media was collected

Cell Line	Time growing (days)	Volume of media (ml)	Cells counted ( $10^6$ cells)
HEY-T30 (HEY)	4	10	0.64
SKOV-3	4	10	4
Ovcar-3	4	9	0.688
CRL-1790	10	18	0.7
BEWO	4	20	8.3
OAW42	7	10	2.1
MCF-7	6	22	6.67
MDA-MB-468	4	19	8.5
3T3	3	20	6.8
HELA	3	18	9
C-33A	4	20	5
JEG-3	3	20	10.5

## 2.2 *CGB in silico*

### 2.2.1 Multiple sequence alignment

The sequences of the *CGB* genes and *LHB* gene were acquired from the ENSEMBL database and aligned with ClustalW software to identify the region of interest (Madeira *et al.*, 2019). The database used was Human genome version GRCh38.p10. For the Multiple sequence alignment (MSA) the 1<sup>st</sup> exon and 1000bp upstream of the Transcription start site (TSS) were used (Table 4). *CGB6* and 9 were not used as they are allele forms of *CGB7* and 3 respectively. As *CGB7* has multiple splicing variants, the *CGB7* transcript variant 2 was used. Based on previous reports in literature, the putative promoter elements were added on the MSA (Cole, 2015; Kerschgens *et al.*, 2011; Hallast *et al.*, 2007).

**Table 4** *CGB* and *LHB* genes and their location on chromosome 19 used for MSA

Gene	ENSEMBL ID	Strand	Location
<i>CGB1</i>	ENSG00000267631	Reverse	chr19:49,036,526-49,037,895
<i>CGB2</i>	ENSG00000104818	Forward	chr19:49,030,912-49,032,270
<i>CGB</i>	ENSG00000104827	Reverse	chr19:49,023,957-49,025,333
<i>CGB5</i>	ENSG00000189052	Forward	chr19:49,042,884-49,044,224
<i>CGB7</i>	ENST00000377280	Reverse	chr19:49,055,361-49,056,780
<i>CGB8</i>	ENSG00000213030	Reverse	chr19:49,048,725-49,050,107
<i>LHB</i>	ENSG00000104826	Reverse	chr19:49,017,067-49,018,081

### 2.2.2 CpG islands

The *CGB3-8* sequences in table 3 were also checked for possible CpG islands within the promoter region. The sequences used in the MSA were used in the Newcpgreport (Madeira *et al.*, 2019). The window was set to 200 bases, with minimal length of 200bp for CpG Island and 0.6 observed/expected ratio with minimum 50%CG content.

### 2.2.3 Primer design

Primers to be used in Next generation sequencing (NGS) were designed on MethPrimer to accommodate the region of interest within the *CGB3-8* promoter (Li and Dahiya, 2002). Due to the length of region of interest and slightly different sequences for each gene different sets of primers were designed. The designs were based on the bisulphite converted *CGB3* sequence. The preliminary primers were then run through ePCR software (BiSearch) where the expected products of each primer pairs were predicted (Arányi *et al.*, 2006).

## 2.3 *CGB* promoter methylation

### 2.3.1 Bisulphite conversion

Bisulphite conversion was done to prepare the DNA samples for the investigation of methylation level via either MSP or next generation sequencing. 500ng of DNA was used per conversion reaction as per manufacturer protocol (Diagenode, s.a.). The DNA was mixed with 130µl conversion reagent and placed in a thermocycler using the cycling program mentioned in table 5. Following this conversion column purification was used to collect the bisulphite converted DNA. The converted DNA was added to the column with 600µl of binding buffer. After the DNA was bound it was washed with 100µl buffer, desulphonated, and washed 2 more times with 200µl wash buffer. Then the converted DNA was eluted to be used in downstream reactions. Bisulphite converted DNA was stored in -20°C.

**Table 5** Conditions used to bisulphite convert DNA

Stage	Temperature	Time
Denaturation	98°C	8min
Conversion	54°C	60min
Final hold	4°C	∞ (up to 20h)

### 2.3.2 MSP

Bisulphite converted DNA was used in Methylation sensitive PCR (MSP) to establish the level of methylation in the *CGB* promoter region initially. The selected cell lines for MSP were HeLa, C-33a, HEY, SKOV-3, CRL-1790. The methylated (M) and unmethylated (U) primers used were from a previous publication (Glodek *et al.*, 2014). The housekeeping gene used was Death Associated Protein Kinase (DAPK). Primer sequences are mentioned in Table 6. The MSP was performed with HS polymerase mastermix as set in the instructions (PCR Biosystems). The cycling conditions used are detailed in table 7. Products were run on 2% agarose gel and stained with SafeView to visualise on Li-cor. Densitometry analysis was performed using the software ImageJ.

**Table 6** Primer sequences used in MSP

Primer ID	Binding strand	Sequence
DAPK	Forward	5'ATTGGGAAGGTTAAGGYGGAGGGAAATTTGGT3'
	Reverse	5'CCCCAAACRAAACAATCCCCAAAACACATTCTA3'
CGB3-9_M	Forward	5' TGTTTAGTTTGATGGTATCGC 3'
	Reverse	5' ATACCCGAAACGATCCCC 3'
CGB3-9_U	Forward	5'AATTGTTTAGTTTGATGGTATTGT 3'
	Reverse	5' AAAATACCCAAAACAATCCCC 3'

**Table 7** Cycling conditions for MSP

Step	Temperature	Duration
Initial denaturation	95°C	10min
<b>40 cycles</b>		
Denaturation	95°C	30s
Annealing	58°C(M) 55°C(U) 59°C(DAPK)	30s
Extension	72°C	30s
Final extension	72°C	5min
Final hold	4°C	∞

### 2.3.4 Sequencing

Sequencing was performed externally using the MiSeq Illumina platform (Bart's and the London Genome Centre - Queen Mary University, London). DNA samples from cultured cell lines were sent. In addition, DNA extracted from normal breast and cervix tissue was also sent to be sequenced (BioChain). DNA samples were bisulphite converted and then amplified with PCR to create the library for sequencing. Two sets of primers were selected from previously mentioned designs to accommodate the region of interest in the *CGB3-9* genes (Table 8). The PCR products were then ligated with adaptors to perform the sequencing. The reads from the sequencing were mapped to the respective *CGB* genes.

Methylation of the CpG sites within the region of interest was given a Beta value using Bismark software. The value is the percent of methylated reads out of the total reads at each CpG.

**Table 8** Primers for sequencing

Primer pair ID	Binding strand	Sequence
CGB3-9_1 (Pair 6)	Forward	5' GGGGAAGGGATTAAGTTTAGA 3'
	Reverse	5' ACTATACTACCAAAAAAACCCTTA 3'
CGB3-9_2 (Pair 7)	Forward	5' GGGTATTTTGGTTTGAGGG 3'
	Reverse	5' CCTCAACCCTCCTCTACTT 3'

## 2.4 CGB expression and secretion

### 2.4.1 cDNA

1µg of DNase treated RNA was converted to cDNA using SSIV kit (Thermo Fisher Scientific). RNA samples were ligated with random hexamer for 10min at 65°C. The reverse transcriptase was then added and placed in thermocycler for 10min at 25°C, 10min at 55°C and 10min at 80°C to create cDNA.

### 2.4.2 qRT-PCR

qRT-PCR with TaqMan probes was employed to assess the transcription level of the CGB3-8 genes. 200ng of the cDNA was used during the reaction. FastStart Essential DNA Probes Master (Thermo Fisher Scientific) was used as instructed by manufacturer to amplify the cDNA. Due to the similarity of the genes 1 primer set and 1 probe from a previous publication was used to assess the CGB3-8 transcription (Śliwa *et al.*, 2019). Sequences are stated in Table 9. GAPDH TaqMan Assay from Thermo Fisher Scientific was used as the housekeeping gene. Samples were plated in duplicate on a 96-well plate and run on the LightCycler 96 machine with the conditions mentioned in Table 10. Each run also included No Template Control and No Reverse Transcriptase Control. Relative CGB3-8 expression was calculated based on the  $2^{-\Delta\Delta Ct}$  method whereby the expression was normalised to GAPDH expression (Livak and Schmittgen, 2001).

**Table 9** Primer and probe sequences used in qRT-PCR

ID	Sequence
CGB3-9_RT F	5'- GTGTCSAGCTCACYCCAGCATCCTA- 3'
CGB3-9_RT R	5'- AGCAGCCCCTGGAACATCT -3'
TaqMan Probe	6FAM-CCGAGGTYTAAAGCCAGGTACACSAGGC-BHQ

**Table 10** Cycling conditions used to perform qRT-PCR

Step	Temperature	Duration
Pre-incubation	95°C	10min
<b>45 cycles of 3 step amplification:</b>		
Denaturation	95°C	10s
Annealing	60°C	30s
Extension	72°C	1s
Cooling	37°C	10s

### 2.4.3 ELISA

Sandwich-based ELISA was employed to observe the secretion of hCG and hCG-beta in the cell line media. Intact hCG and free beta hCG kits were used from Demeditec Diagnostics (Germany). Both ELISA kits are pre-coated with the respective monoclonal antibody and standard protocol provided by the manufacturer was followed.

#### 2.4.3.1 Free beta hCG

ELISA was performed as instructed by the manufacturer. Six standards ranging from 1.25ng/ml - 50ng/ml were used to create a standard curve. 50µl of the provided standards, controls, and conditioned media samples were loaded on the provided coated wells and diluted with 100µl zero buffer, then incubated at 37°C for 30min. Plate was washed five times with wash solution and 150 µl enzyme conjugate containing the anti-beta-hCG ab conjugated to horseradish peroxidase was added to each well. After a further incubation at 37°C for 30min the plate was washed 5 times and 100µl substrate was added. After 20min 100µl stop solution was employed to block the reaction and the wells were read at 460 nm. To account for background noise readings a second reading at 640nm was performed. The free beta hCG ELISA was run 2 times – once samples were in triplicate and once - in duplicate. Obtained values from standard were used to build a standard curve using the 4-parameter fit model. Sample concentration were calculated and then expressed as ng/ml.

#### 2.4.3.2 Intact hCG

Similarly, the intact hCG ELISA was performed as per manufacturer instructions. Four standards ranging between 5-500 mIU/ml were used to build standard curve. 25 µl of the provided standards, controls and conditioned media samples were loaded on the provided wells. After 100µl of the enzyme conjugate containing the

monoclonal anti-hCG antibody was added to each well and the plate was incubated for 30min at room temperature and washed 5 times with distilled water. 100µl Substrate solution was added to develop colour for 10 min and the reaction was stopped by adding 50µl stop solution. The samples were run once in duplicate. As with the previous ELISA plate was read at 460 and 640 nm. Standard curve was built based on the 4-parameter fit model and sample concentration was calculated.

## 2.5 Statistical Analysis

Methylation data was analysed using methylKit and R programming to create histograms, PCA, clustering analysis, and analysis of methylation association (Pearson) (Akalin *et al.*, 2012). Normally distributed data was analysed using parametric tests (Repeated Measures (RM) ANOVA, paired t-test), otherwise non-parametric tests (Mann Witney, Spearman's ranked correlation) were used. The nonparametric Mann Witney was used to analyse for difference in the MSP data. For the statistical analysis of methylation data Beta values of the sequencing were converted to M-values. Methylation data analysed for difference using paired t-test or RM-ANOVA paired with Tukey's test on Prism8. With smaller sample set the non-parametric Kruskal-Wallis test was used paired with Dunn's test on Prism8. Association analysis between the transcription and methylation data was done using Spearman's ranked correlation using Minitab18.

## 3. Results

### 3.1 Putative promoter Characteristics

#### 3.1.1 MSA of target region

The aligned sequences of the *CGB1-9* and *LHB* genes show the close identity of the genes. The region presented in Figure 9 shows the putative promoter region of the *CGB3-8* genes and how it aligns with the *LHB* and *CGB1-2* genes. All *CGB* genes have a conserved promoter sequence which starts to diverge towards the 3' end where the *CGB1-2* specific insert begins. The putative promoter spans approximately 350bp upstream from the transcription start site of the *CGB3-8* genes. It contains 2 cAMP responsive elements (CREs), Trophoblast Specific element (TSE) and a CCAAT box. At the 5' end of the promoter region there are 4 TF binding sites close together: an AP2 $\alpha$  followed immediately by an SP1 and another AP2 $\alpha$  transcription sites after which an Oct3/4 binding site. These 4 sites also coincide with the 5' CRE. The 3' CRE there are 2 more TF binding sites for AP2 $\alpha$  followed by an SP1. Within the marked promoter region there are 57 CpG sites across all genes. The CpGs that are common between all *CGB3-8* genes are labelled A1-A11, the one common between *CGB3*, 8 and 7 is B1, the one on *CGB3*, 5, and 7 – C1, the one on *CGB3* – D1, the one on *CGB5*, 8, and 7 – E1, the one on *CGB5* & 7 – F1, and the one on *CGB7* – G1. MSA of the whole 1000bp 5'upstream region and the 1<sup>st</sup> exon can be found in Appendix A2.1.



### 3.1.2 CGI prediction

The Newcpgreport tool checked the *CGB3-8* promoter genes for possible CGIs (Appendix A2.2) (Madeira *et al.*, 2019). It returned only one CpG island (Fig. 8). The island predicted by the tool was on the *CGB7* gene with length of 720 bp. The software locates it -901 to -182bp from the TSS of the gene. The CG content within the region is 66% and an observed/expected ratio is 0.75. The other CpG genes did not present with a CpG island within the 1000bp region upstream from the TSS.

```
ID  CGB7  1419 BP.
XX
DE  CpG Island report.
XX
CC  Obs/Exp ratio > 0.60.
CC  % C + % G > 50.00.
CC  Length > 200.
XX
FH  Key                Location/Qualifiers
FT  CpG island          99..818
FT                          /size=720
FT                          /Sum C+G=474
FT                          /Percent CG=65.83
FT                          /ObsExp=0.75
FT  numislands          1
```

**Fig.8** Output from Newcpgreport tool for *CGB7* (Madeira *et al.*, 2019). ID row is the user defined ID and length of input sequence, DE- description of test, CC rows – conditions of the test, FH and FT rows present the predicted CpG island in relation to the input sequence.



**Fig.9** Annotated MSA of the CGB3-8 putative promoter region together with CGB1-2 and LHB. Legend: CpG sites are bolded and highlighted in yellow (CG) and labelled above the CGB sequence, 5'UTR of exon 1 is labelled with red font and bolded (CGGCCCATGG), dash black line surrounds the putative promoter of the CGB3-8 (CTGGCATCCTGGCTT), cAMP response elements (CREs) is the underlined region (CTGGCATCCTGGCTT), TSE is written in green font (CCTGCGGGCCTA), CCAAT box is underlined with a double line (TCTCATTGGGCA). AP2 $\alpha$  binding is marked by lower case letters (cggcccatgggc), italicised letters denote SP1 binding (CGGCCCATGGGC), purple font denotes the Oct3/4 binding site (TCTCATTGGGCA); AP2 $\alpha$ , SP1 and OCT3/4 binding is also denoted by a double-headed arrow above CGB1, blue dotted line marks the CGB1-2 putative promoter (.....) and blue outlined letters denote CGB1-2 specific insert (TCTCATTGGGCA)

## 3.2 Methylation profile

### 3.2.1 MSP

Initially the methylation profile was investigated using Methylation Sensitive PCR to check methylation at a CpG located at -550bp from TSS, F1 and A5. Methylated (M) primers showed consistent strong bands across all the cell lines. CRL-1790, HEY, and C-33a showed brighter bands compared to HeLa and SKOV-3. The obtained values from densitometry analysis were analysed for difference between the normal cell line (CRL-1790) and the non-trophoblastic cancer cell lines (HeLa, HEY, SKOV-3, C-33a) using Mann-Whitney (Fig. 10). No significant difference was found ( $p=0.687$ ). Unmethylated (U) primers had weaker bands. HeLa showed brightest U product bands, and the other cell lines had weaker bands for the same product. Densitometry analysis and differential analysis was performed analogically. No significant difference was found ( $p=0.502$ ) between the control and non-trophoblastic cell line. The house keeping gene showed consistent product of similar intensity in all the tested cell lines (Fig. 10). See Appendix A3 for densitometry data and statistical analysis.

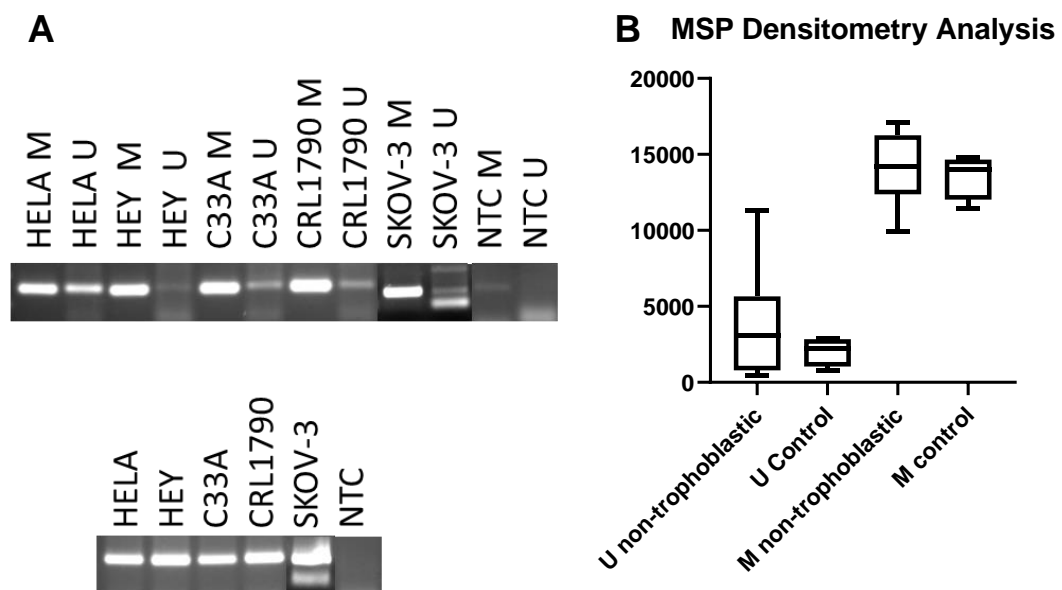


**Fig.10** MSP products and densitometry analysis. A. Methylated, unmethylated and housekeeping gene products run on 2% agarose gels and visualised on Licor. B. Boxplot showing the spread of the values obtained from densitometry analysis for each group – U (unmethylated) non-trophoblastic, U control, M (methylated) non-trophoblastic, M control. Line at the middle of box represents median. U - unmethylated, M – methylated, non-trophoblastic(C-33a, HeLa, HEY, SKOV-3), control (CRL-1790).

### 3.2.2 Sequencing primers

The next step to allow for more detailed analysis of methylation profile was to design sequencing primers. Seven primer pairs were selected from the output of MethPrimer as possible candidates (Table 10) (Li and Dahiya, 2002). The predicted product size of the selected primers varied between 200 and 290bp and the common CpGs covered within the region varied between 8 and 11. Pairs 1 and 6 have a predicted product covering the 5' of the putative promoter but not the 3' end of the region of interest. Pairs 2, 3, 5 and 7 are opposite – they cover the 3' part but not the 5' part of the promoter. Pair 4 covers most of the promoter region. As primer sequences were based on *CGB3*, mismatches after bisulphite conversion were observed (Table 11). Pairs 1, 3, 4, and 5 have 1 mismatch in the binding sites on each of the *CGB5-8* genes for the reverse primer. Pair 2 has 2 mismatches on the reverse primer for *CGB5* binding region. ePCR predicted products of only the target *CGB3-8* genes for pairs 2 and 7 (Table 11). Pair 6 also has predicted product for all target genes but has predicted product for *LHB* as well. Pairs 3 and 5 have predicted product on all *CGB1-8* genes same as pair 4 which has additional predicted product on *LHB*. Pair 1 has 4 predicted products only *CGB3* and 8 from the target genes in addition to predicted product on *CGB1-2*. For default settings and output from ePCR see Appendix section A2.3.

**Table 10** Selected candidate sequencing primers generated from MethPrimer

Pair	Primer Sequence	Start (bp from TSS)	Length (bp)	Product size (bp)	number of common CpGs
1	F: GGGAAGGGATTAAGTTTAGATAATGTT	-353	27	233	10
	R: CTACCAAAAAACCACTTAACCCTA	-121	25		
2	F: TTAATAATTAGTTAAATTATTTGAAGTATA	-278	30	290	11
	R: AAAAAATACTAAACTAAACCTC	11	24		
3	F: TTTAATAATTAGTTAAATTATTTGAAGTAT	-279	30	201	8
	R: CTTAATTTCTACCCAATAAAAAAAA	-79	25		
4	F: GGGAAGGGATTAAGTTTAGATAATGTT	-353	27	275	11
	R: CTTAATTTCTACCCAATAAAAAAAA	-79	25		
5	F: TTAATAATTAGTTAAATTATTTGAAGTATA	-278	30	200	8
	R: CTTAATTTCTACCCAATAAAAAAAA	-79	25		
6	F: GGGGAAGGGATTAAGTTTAGA	-353	20	240	11
	R: ACTATACTACCAAAAAACCACTTA	-113	25		
7	F: GGGTATTTTGGTTTGAGGG	-208	19	219	8
	R: CCTCAACCCTCCTCTACTT	-8	19		

**Table 11** Mismatches of primers with other target genes and predicted products

Pair	Mismatches in CGBs			ePCR predicted products	
	5	7	8	sense strand	antisense strand
1	0	0	0	1.chr19:49031105-49031338 ( <i>CGB2</i> )	1.chr19:49024454-49024687( <i>CGB3</i> ) 2.chr19:49037480-49037713( <i>CGB1</i> ) 3.chr19:49049222-49049455( <i>CGB8</i> )
	1	1	0		
2	0	0	0	1.chr19:49043567-49043858( <i>CGB5</i> )	1.chr.19:49024322-49024612( <i>CGB3</i> ) 2.chr.19:49049090-49049380( <i>CGB8</i> ) 3.chr.19:49055726-49056017( <i>CGB7</i> )
	2	0	0		
3	0	0	0	1.chr.19:49031179-49031380( <i>CGB2</i> ) 2.chr.19:49043566-49043768( <i>CGB5</i> )	1.chr19:49024412-49024613( <i>CGB3</i> ) 2.chr19:49037438-49037639( <i>CGB1</i> ) 3.chr19:49049180-49049381( <i>CGB8</i> ) 4.chr19:49055816-49056018( <i>CGB7</i> )
	1	1	1		
4	0	0	0	1.chr19:49031105-49031380( <i>CGB2</i> ) 2.chr19:49043492-49043768( <i>CGB5</i> )	1.chr19:49017519-49017793( <i>LHB</i> ) 2.chr19:49024412-49024687( <i>CGB3</i> ) 3.chr19:49037438-49037713( <i>CGB1</i> ) 4.chr19:49049180-49049455( <i>CGB8</i> ) 5.chr19:49055816-49056092( <i>CGB7</i> )
	1	1	1		
5	0	0	0	1.chr19:49031180-49031380( <i>CGB2</i> ) 2.chr19:49043567-49043768( <i>CGB5</i> )	1.chr19:49024412-49024612( <i>CGB3</i> ) 2.chr19:49037438-49037638( <i>CGB1</i> ) 3.chr19:49049180-49049380( <i>CGB8</i> ) 4.chr19:49055816-49056017( <i>CGB7</i> )
	1	1	1		
6	0	0	0	1.chr19:49043492-49043732( <i>CGB5</i> )	1.chr19:49017556-49017794( <i>LHB</i> ) 2.chr19:49024449-49024688( <i>CGB3</i> ) 3.chr19:49049217-49049456( <i>CGB8</i> ) 4.chr19:49055853-49056093( <i>CGB7</i> )
	0	0	0		
7	0	0	0	1.chr19:49043619-49043838( <i>CGB5</i> )	1.chr19:49024343-49024561( <i>CGB3</i> ) 2.chr19:49049111-49049329( <i>CGB8</i> ) 3.chr19:49055747-49055966( <i>CGB7</i> )
	0	0	0		

### 3.2.3 Global profile of *CGB3-8* methylation

The sequences generated from the region of interest were mapped back to the promoters of the *CGB3-8* genes and assigned a Beta value (Appendix A4, Table A4). The Beta value corresponds to the percentage methylation – a beta value of 10 denotes 10% methylation at that site. Fig. 11 presents the percentage of the reads mapped to each gene by cell type. *CGB5* and 8 contribute most to the data set, and *CGB7* – the least. *CGB3* and 7 have some CpGs with low or no reads which were excluded from the data. 3T3 negative control mouse cell line did not return any sequencing result.

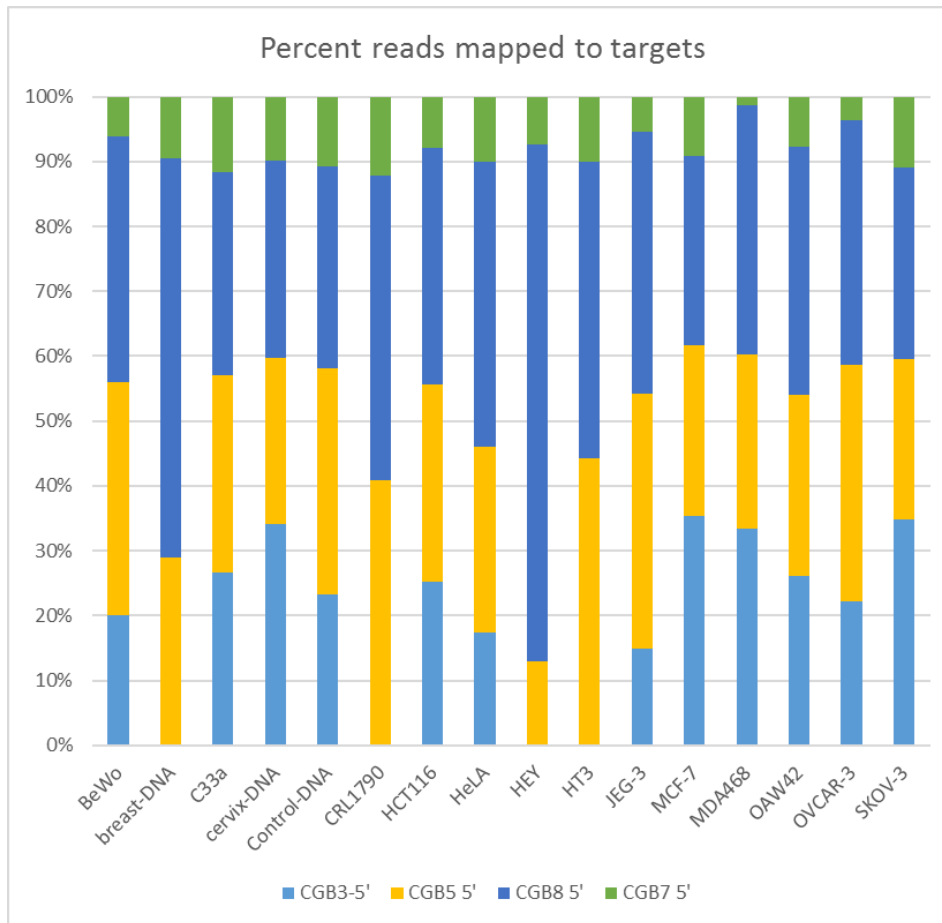


**Fig.11** Percent mapped reads to targets within the *CGB3-8* genes.

At a first glance the methylation reads within the promoter CpGs seem consistent per gene (Fig. 12, Table 12). *CGB3*, 5 and 8 show higher methylation values across the investigated cell lines. The steady high methylation drops between A7 and A8 across most of the cell lines. *CGB7* presents with lower Beta values across the CpGs. When looking at individual cell lines JEG-3 and BeWo stand out as having lower methylation reads for *CGB3* but BeWo has beta value for the other genes as other samples, and JEG-3 maintains lower methylation in the other 3 genes. HeLa seems to have lower beta values at the *CGB3* sites. Observing the histograms in Fig. 13, it shows that predominantly CpG reads range between 90-100% methylation. JEG-3 presents with similar percent methylation reads spanning beta values 20-80% with a peak at 60%. More varied reads of methylation are present in the MCF-7, MDA-MB-468, breast tissue, CRL-1790, and OVCAR-3.

CGB3-8 Methylation heatmap

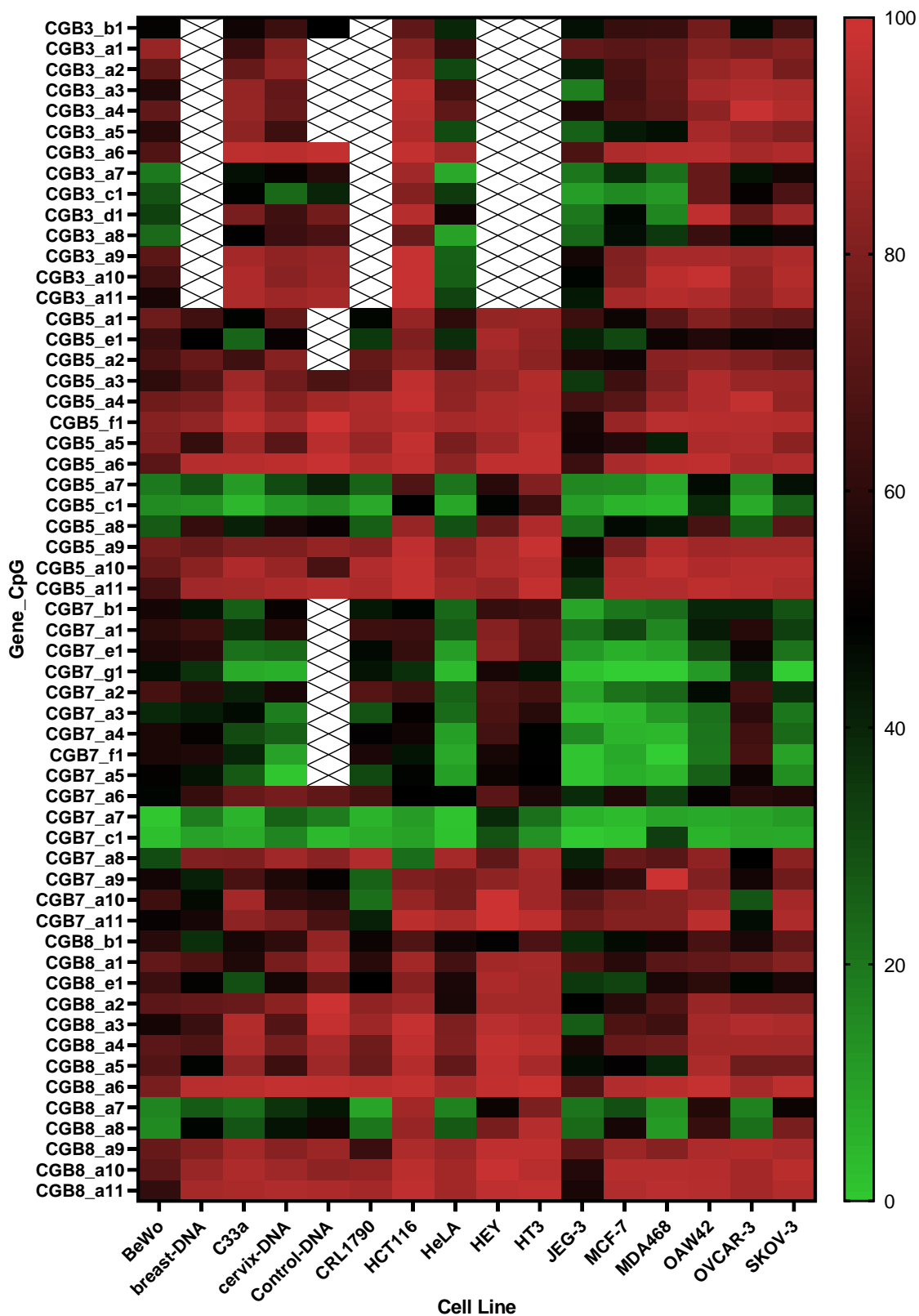


**Fig.12** CpG methylation heat map. The x-axis denotes the cell lines, and the y - denotes the CpG location. Within a gene CpGs are ordered 5'->3'. Green-black-red colour scheme is used to represent the Beta value range (0-50-100%)

**Table 12** Average methylation of the investigated promoter region in the CGB3-8 genes per cell line

<b>Cell line</b>	<b>Tissue origin</b>	<b>CGB3</b>	<b>CGB5</b>	<b>CGB8</b>	<b>CGB7</b>
<b>MCF-7</b>	breast cancer	63%	60%	65%	30%
<b>MDA-MB-468</b>	breast cancer	62%	68%	64%	32%
<b>breast-DNA</b>	breast tissue	NA	67%	65%	49%
<b>C-33a</b>	cervical cancer	75%	66%	70%	44%
<b>HeLa</b>	cervical cancer	42%	65%	67%	34%
<b>HT-3</b>	cervical cancer	NA	90%	91%	62%
<b>cervix-DNA</b>	cervix tissue	72%	70%	72%	42%
<b>BeWo</b>	choriocarcinoma	55%	62%	61%	47%
<b>JEG-3</b>	choriocarcinoma	40%	45%	48%	23%
<b>CRL-1790</b>	colon	NA	66%	66%	44%
<b>HCT116</b>	colon cancer	90%	88%	90%	52%
<b>HEY</b>	ovarian cancer	NA	84%	87%	68%
<b>OAW42</b>	ovarian cancer	85%	80%	82%	43%
<b>OVCAR-3</b>	ovarian cancer	76%	72%	71%	48%
<b>SKOV-3</b>	ovarian cancer	81%	76%	81%	39%
<b>Control-DNA</b>		73%	73%	84%	51%

To observe the similarity between the methylation profiles of the cell lines CGB3-8 promoter Pearson correlation in package methylKit was used (see code in Appendix A5.1). The correlation study (Fig. 13) between the methylation profiles of the different cell lines showed strong correlation between most of them. The correlation was strong within most tissue groups and between them. For instance, OAW42 shows strong correlations with the other ovarian cell lines – SKOV-3, OVCAR-3, HEY, but also with the cervical group cell lines – HeLa, C-33a, and HT-3. It was also observed that some cell lines had weaker correlations with the others. Both HCT116 and HT-3 seem to correlate strongly with a few cell lines, but otherwise correlations are moderate.



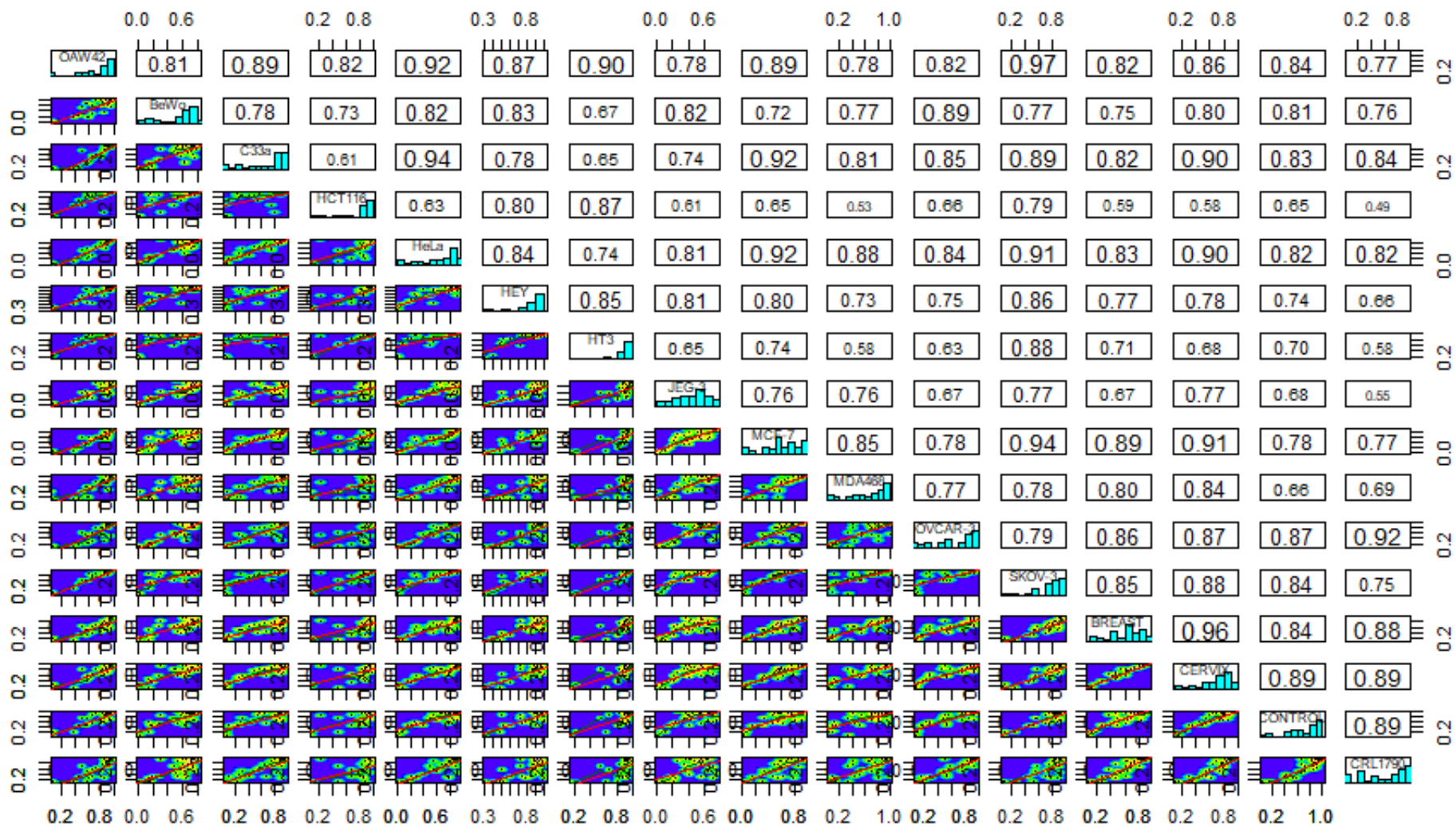


**Fig.13** CpG methylation correlation between samples. Diagonally histograms of CpG percentage reads per cell line are plotted. Right side of diagonal shows the Pearson coefficients between the different samples and the left side – scatterplots of the correlation. Created in methylKit

To further investigate the clustering of the methylation signatures the correlation data was used to build a dendrogram (Fig. 14) (see code in Appendix A5.1). The clustering shows that majority of cell lines have similar methylation profiles. HTC116 shows least correlation with the other cell lines. Together with JEG-3, BeWo, and HEY the 4 cell lines form the cluster furthest away from the other cell lines. OVCAR-3, Control-DNA, and CRL-1790 form a cluster and the rest of the cell lines and tissue DNA form the last cluster which show closer correlation based on methylation footprint.

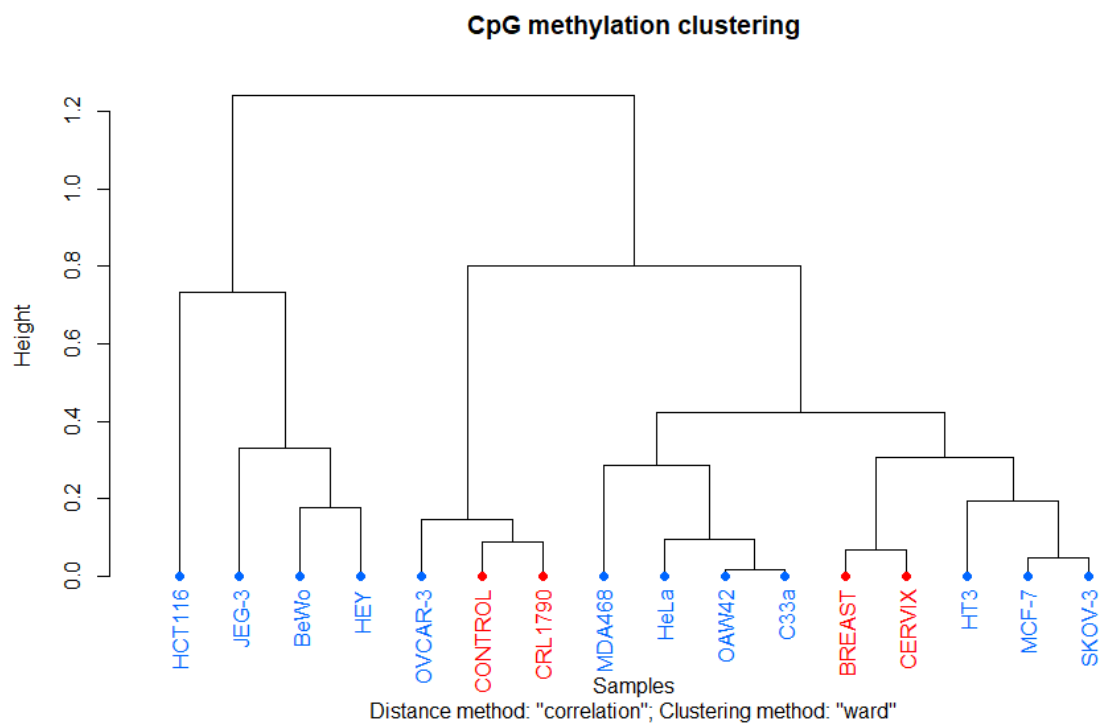


**Fig.14** CpG methylation clustering dendrogram based on correlation data. Produced via methylKit

As the methylation data has high dimensionality Principal Component Analysis (PCA) was applied to observe patterns within the obtained data (see code in Appendix 5.2). PCA reduces the dimensions of the data to 2 principal components (PCs) and retains the maximum variability. In the case of the *CGB3-8* promoter methylation data the PCA retains 63.7% of the data variability (Fig. 15). Most samples stay fairly close together but 4 distinct clusters can be observed. BeWo and JEG-3 do not cluster with any of the other samples.

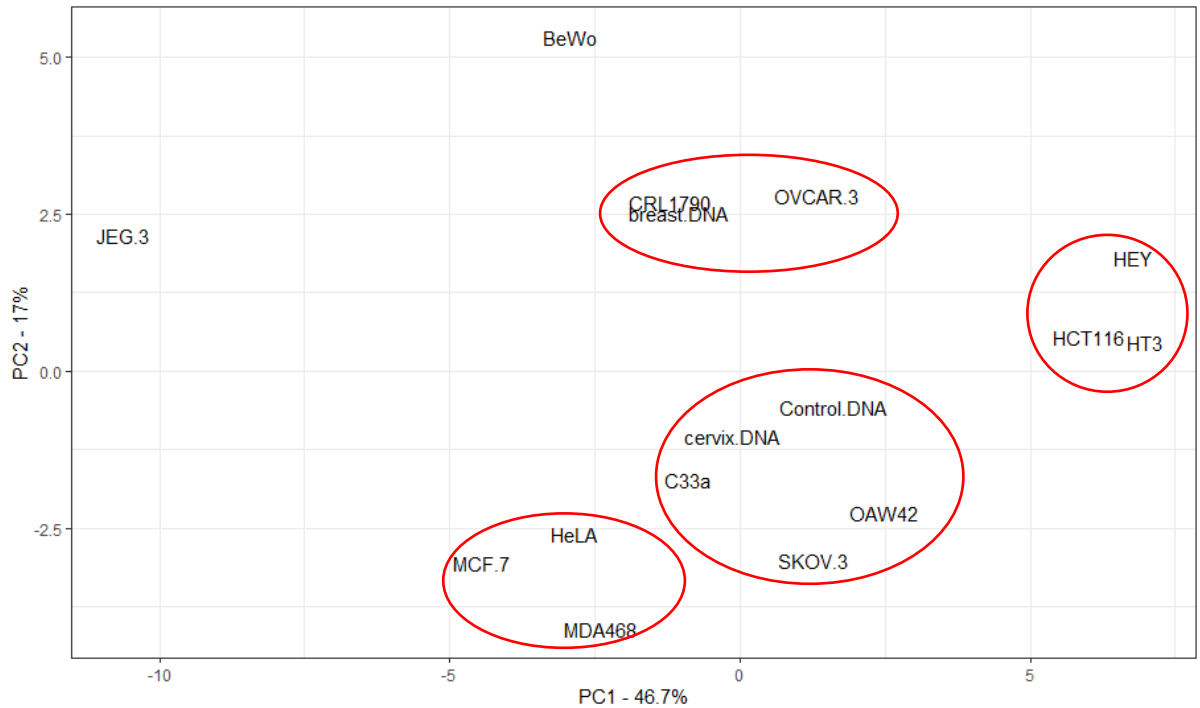


**Fig.15** Principal component analysis of the CpG methylation. Produced using R statistics

Cell line average methylation of region of interest by tissue type was also plotted to observe possible trends in the motif (Fig. 16). As observed previously cell lines maintain their respective higher methylation beta value throughout the promoter region but these values drop between the A7 and A8 CpG. Site D1 which is between A7 and A8 presents with an increase in the percentage methylation for the A7-8 region in the cervical samples (excluding HT-3), ovarian samples (excluding HEY), MCF-7, and Control-DNA. Trophoblastic cell lines present possible lower methylation compared to the control DNA. The 2 cell lines also seem to have distinct motif as beta-values for CpGs at the 5' end do not overlap (Fig. 16A). In the colon group the cancer cell line (HTC116) tends to have higher methylation than the normal colon one (CRL-1790) (Fig. 16B). In the cervical group HT-3 tends to have higher methylation than the other samples within the group which seem to follow similar pattern (Fig. 16C). In ovarian and breast groups samples seem to be following similar pattern of methylation (Fig. 16D).

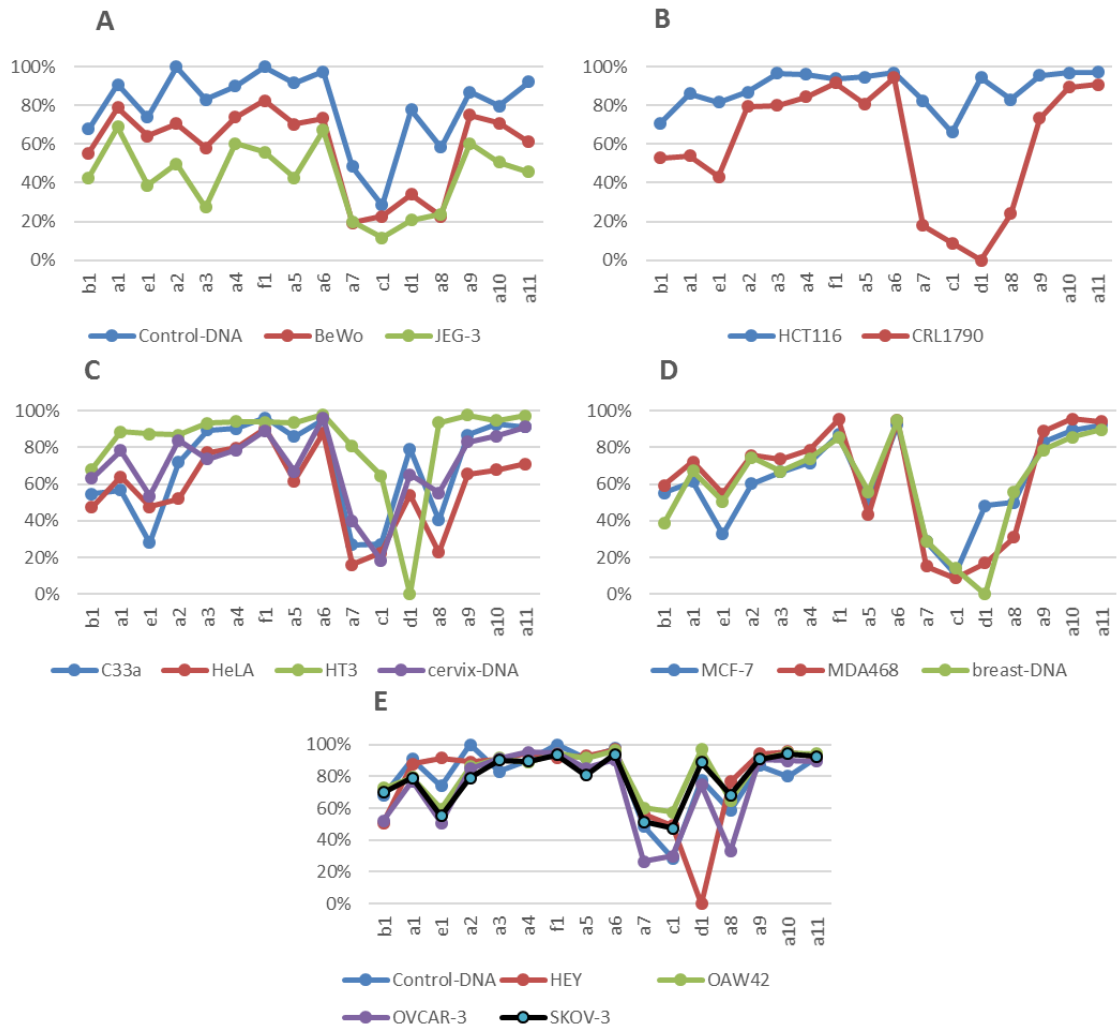


**Fig.16** Samples promoter region averaged methylation grouped by tissue of origin. The x-axis contains the investigated CpGs ordered 5'→3' direction. The y-axis denotes the Beta-value (in %). A. Trophoblastic cell lines and control-DNA B. Colon cell lines. C. Cervical cell lines and cervical tissue. D. Breast cell lines and breast tissue. E. Ovarian cell lines and control-DNA

### 3.2.4 Differential analyses of methylation

To further understand the methylation profile of the region of interest analyses of difference were performed. For these analyses the Beta-value was converted to M-value using the formula  $M = \log_2\left(\frac{\text{beta value}}{1-\text{beta value}}\right)$  to allow parametric statistical analyses as mentioned in Du *et al.* (2010) (Table A5, Appendix A4). Firstly, the promoter methylation per gene was checked for difference. The average promoter M-value per cell line per gene was compared using ANOVA (Appendix A6.1). The results show strong significance of difference ( $p < 0.0001$ ) in the methylation of the genes. Tukey's pairwise comparison test was performed to identify where the difference is. The results show that *CGB7* has significantly lower methylation in

comparison with the other 3 genes ( $p < 0.0001$  for each of the differences with *CGB3*, 5, and 8).

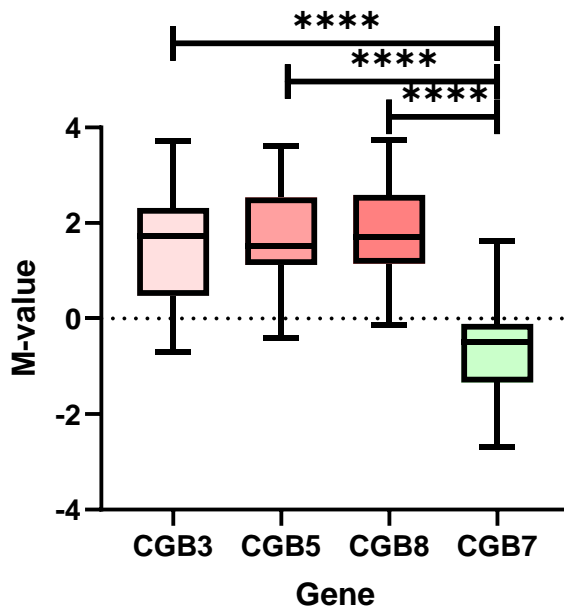


**Fig.17** Box plot of the averaged cell line M-value per investigated *CGB* gene. Lines above the box denote the significance in difference based on Tukey's test.

The next step in the differential analysis was to assess if there is a difference in the methylation profile between trophoblastic and non-trophoblastic cancers and control sample DNAs. Firstly, the averaged M-values of *CGB3*, 5 and 8 genes whole investigated region per cell line were compared (Figs. A23-24, Appendix A6.2). In Fig. 18A it can be seen that the trophoblastic and control samples have narrower spread of the M-value. Trophoblastic samples seem to have lower methylation compared to the other 2 groups. The analysis of difference used was the non-parametric Kruskal-Wallis due to small sample size in the trophoblastic group. A difference of weak significance was returned as result ( $p = 0.0404$ ); however, Dunn's pairwise test showed no significant differences between the groups.

The average methylation of *CGB3*, 5, and 8 was also compared in two specific regions within the investigated promoter (Figs. A25-26, Appendix A6.2). Fig. 18B shows the float bar plot for the 5' TF binding region binding AP2 $\alpha$ -SP1-AP2 $\alpha$ -OCT3/4 transcription factors, which covers the B1, A1-3, and E1 CpG sites. This 5' TF region has more widely spread averaged M-values within the control samples compared to the whole promoter region. The spread of the trophoblastic and non-trophoblastic samples were similar to the whole promoter region. The 5'

TF region was analysed analogically to the whole investigated region. No significant difference was observed.

The second specific region is within the investigated promoter's 3' TF binding site binding AP2 $\alpha$ -SP1 transcription factors and covering A4-6 and F1 CpGs (Fig. 18C). Averaged M-values are widely spread within the normal and non-trophoblastic regions. Trophoblastic samples seem to be having lower methylation as observed in Fig. 18C. The same approach was used to analyse for difference as with the other 2 regions. No significant difference was found between the 3 groups.

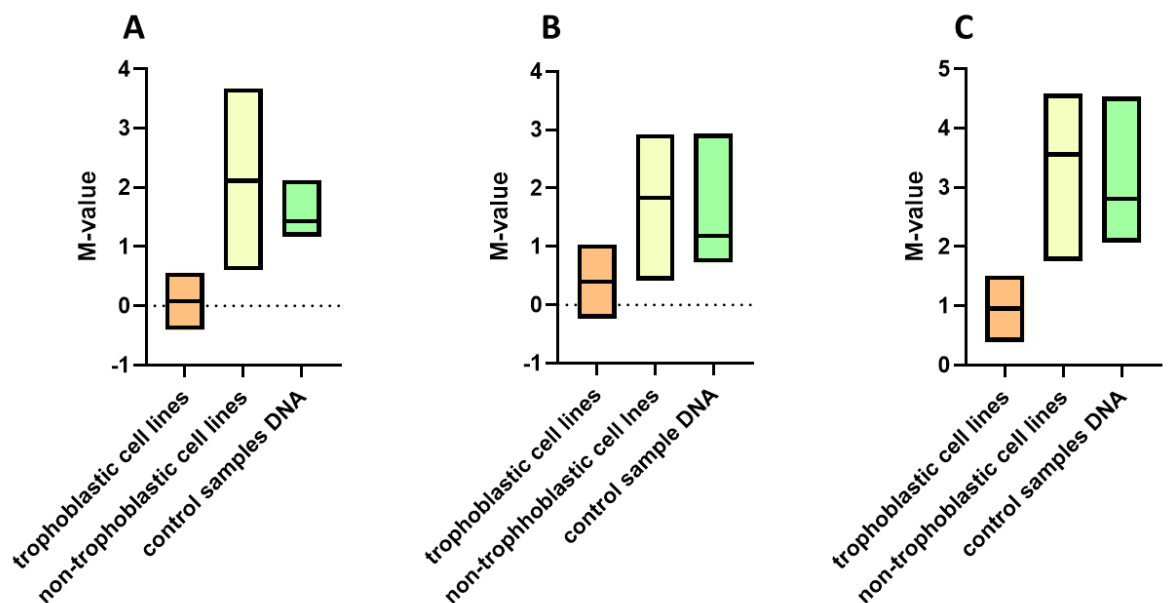


**Fig.18** Float bar plot representing the averaged *CGB3*, 5, and 8 methylation per cell line grouped by cancer type. A. Whole region of interest. B. AP2 $\alpha$ -SP1-AP2 $\alpha$ -OCT3/4 region. C. AP2 $\alpha$ -SP1 region

The same analysis was repeated for the *CGB7* averaged methylation (Figs. A27-29, Appendix A6.2). As seen in Fig. 19 the data is spread wider in the trophoblastic and non-trophoblastic cell lines in comparison to the control samples. Methylation seems to be similar between the sample groups in the whole interest region and in the 5' and 3' TF binding region. As previously, Kruskal-Wallis was applied to test the difference in methylation in the above mentioned regions which yielded no significant result.

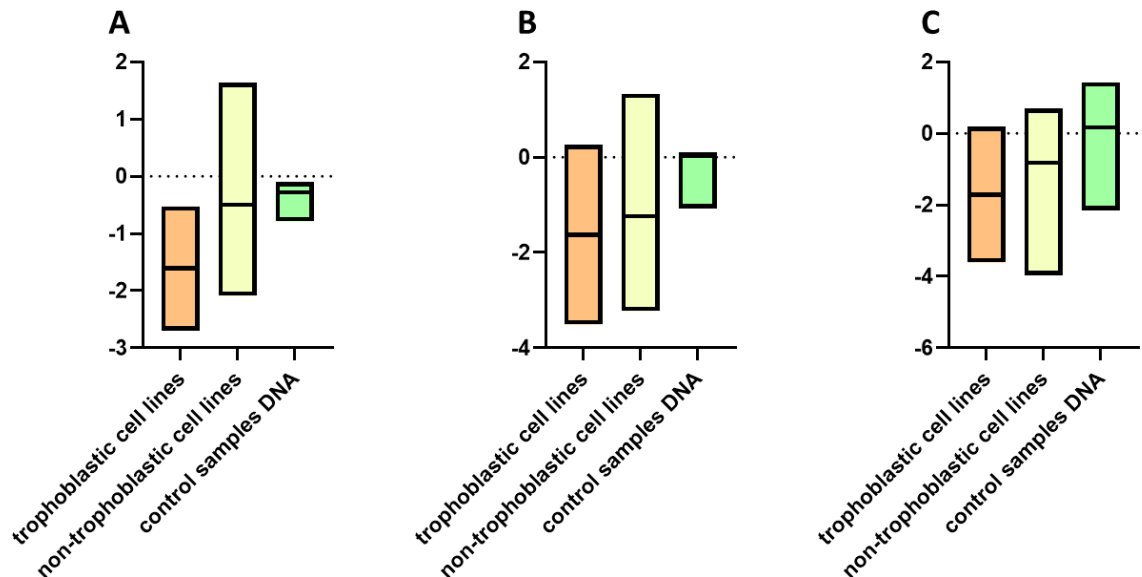


**Fig.19** Float bar plot representing the averaged *CGB7* methylation per cell line grouped by cancer type. A. Whole region of interest. B. AP2α-SP1-AP2α-OCT3/4 region. C. AP2α-SP1 region

The last set of tests to see a difference in the methylation profile analysed the difference in M-values within tissue of origin groups. The M-values for *CGB3*, 5, and 8 were averaged per CpG and samples were grouped by tissue of origin. Also the difference in methylation within the control samples was assessed. Repeated measure ANOVA (RM ANOVA) was used to assess the difference within groups of 3 or more samples. This was paired with Tukey's pairwise comparison to establish where the significant difference lies. For sets of 2 samples paired t-test was used (Appendix A6.3.1-6). No significant difference in the methylation profile was found in the breast and ovarian tissue group (Fig. 20B and E).

In the trophoblastic cell line group, it can be observed that both the cell lines have lower M-values in comparison to the control-DNA (Fig. 20A). The performed RM ANOVA confirms that there is a very strong significant difference ( $p < 0.0001$ ). Tukey's test reveals that control-DNA is significantly more methylated than JEG-3 and BeWo (both with  $p < 0.0001$ ). It also revealed that BeWo is significantly more methylated than JEG-3 ( $p < 0.0001$ ).

In the control samples group the control-DNA seems to have slightly higher methylation (Fig. 20C). The RM ANOVA confirms moderate significant difference between the M-values ( $p = 0.0014$ ). Tukey's test revealed that control-DNA is more methylated with moderate significance than CRL-1790 ( $p = 0.0096$ ) and breast-DNA ( $p = 0.0079$ ) and weak significance from cervix-DNA ( $p = 0.0114$ ).



Observing the cervix group no difference stands out between the samples at a first glance (Fig. 20 D). RM ANOVA shows that there is a difference of weak significance ( $p=0.0125$ ). Tukey's test shows that the difference comes from lower methylation in the HeLa cell line in comparison with C-33a ( $p=0.0014$ ), cervix-DNA ( $p=0.0041$ ), and HT-3 ( $p=0.0209$ ).

In the colon group there were only 2 samples to compare (Fig. 20F). HCT116 seems to be more methylated than the normal colon cell line CRL-1790. Paired t-test confirms that with strong significance ( $p=0.0003$ ).

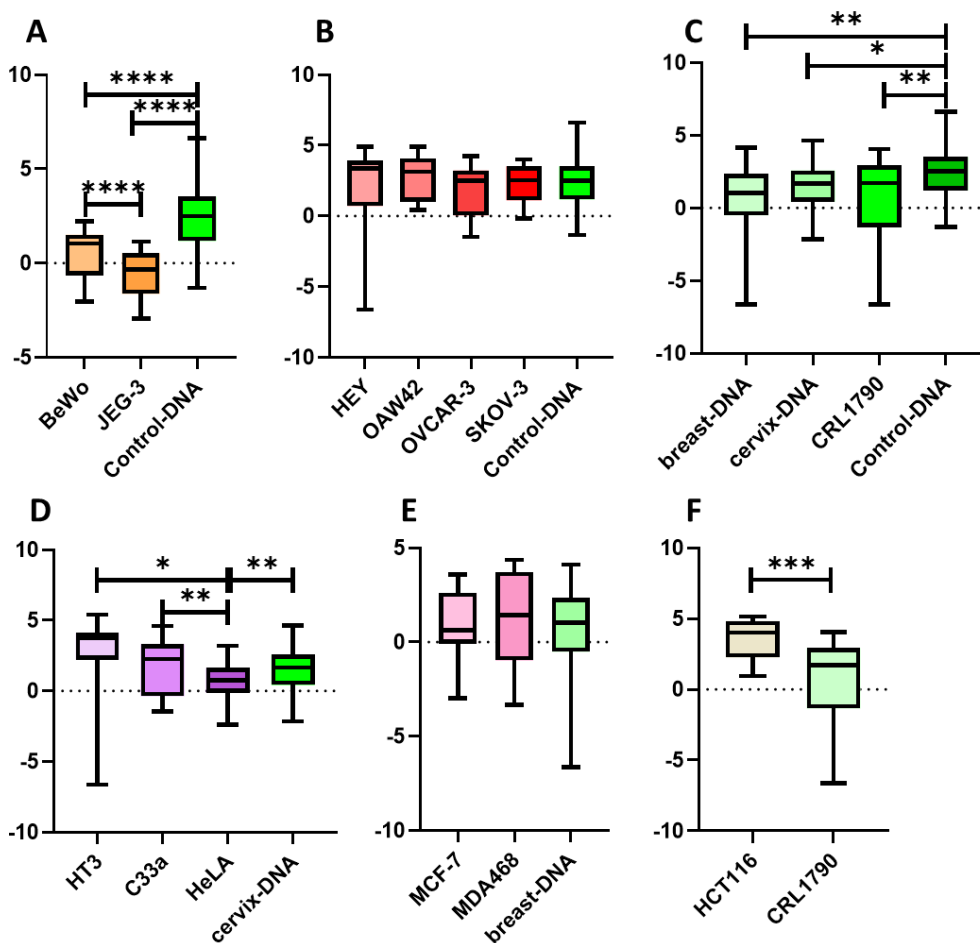


**Fig.20** Boxplot of the average M-values for *CGB3*, 5, and 8 of each sample compared within their respective tissue of origin group. A. Trophoblastic cell lines and control DNA. B. Ovarian cancer cell lines and control DNA. C. Control samples. D. Cervical cancer cell lines and normal cervix tissue. E. Breast cancer cell lines and normal breast tissue DNA. F. Colon samples. Lines above boxes denote significance of difference between groups based on Tukey's test (A-E) or paired t-test (F)

Analogically, the M-values of the *CGB7* gene were analysed for differences in methylation within the samples' tissue of origin group (Appendix A6.3.7-12). Control-DNA sample was excluded from the analysis due to missing data points



preventing the RM ANOVA test. No significant difference was observed in the control DNA samples and colon groups (Fig. 21C and F).

JEG-3 tends to have lower methylation in the trophoblastic group for *CGB7* (Fig. 21A). RM ANOVA confirms difference of moderate significance ( $p=0.0020$ ) within the trophoblastic group. Tukey's test shows that the difference is due to lower methylation of JEG-3 in comparison to CRL-1790 ( $p=0.0120$ ) and BeWo ( $p=0.0126$ ).

In the ovarian group HEY tends to have higher methylation values than the other samples for *CGB7* (Fig. 21B). Statistical test presents moderate difference within the group ( $p=0.0047$ ). Pairwise comparisons reveal that HEY has higher methylation than OAW42 ( $p<0.0001$ ), OVCAR-3 ( $p=0.0002$ ) and OVCAR-3 ( $p=0.0396$ ).

HT-3 cell line from the cervical group appears with slightly higher methylation when observing Fig. 21D. RM ANOVA presents that there is a difference in the samples with strong significance ( $p<0.0001$ ). HT-3 is more methylated than HeLa ( $p<0.0001$ ) and C-33a ( $p=0.0009$ ) with strong significance and cervix-DNA ( $p=0.0106$ ) with weak significance. C-33a is also more methylated than HeLa ( $p=0.0187$ ) according to Tukey's.

Finally, in the breast group breast-DNA seems to have higher methylation than the breast cancer cell lines (Fig 21E). RM ANOVA confirms a weak significance in the difference of  $p=0.0333$  in the group. Tukey's test shows that the difference lies between MCF-7 and breast-DNA ( $p=0.0100$ ) whereby MCF-7 has lower methylation than breast-DNA.

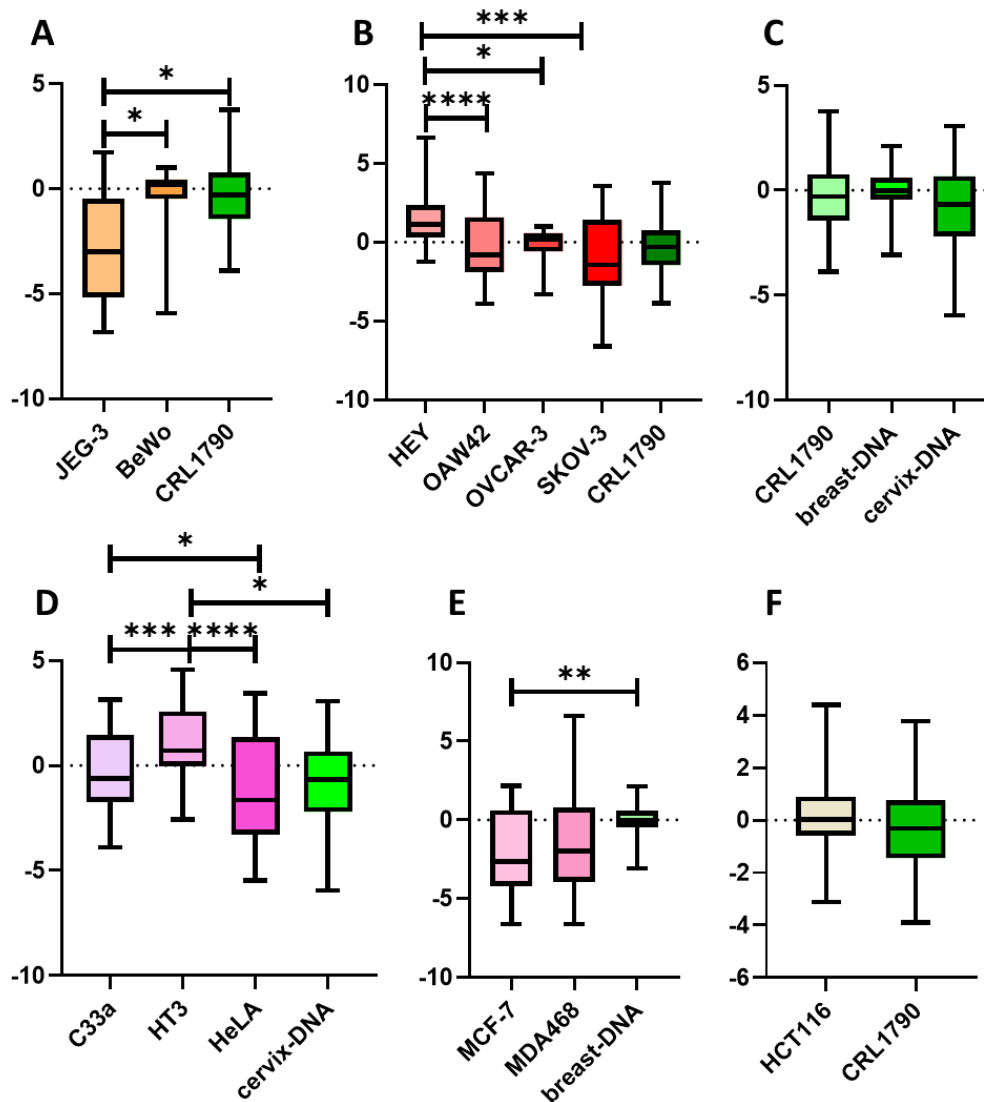


**Fig.21** Boxplot of the M-values for *CGB7* of each sample compared within their respective tissue of origin group. A. Trophoblastic cell lines and control DNA. B. Ovarian cancer cell lines and control DNA. C. Control samples. D. Cervical cancer cell lines and normal cervix tissue. E. Breast cancer cell lines and normal breast tissue DNA. F. Colon samples. Lines above boxes denote significance of difference between groups based on Tukey's test (A-E)

### 3.3 Transcription level of *CGB3-8*

Relative quantification expressed as fold difference for the *CGB3-8* mRNA transcript was calculated by comparing the cancer sample  $C_t$  ( $C_q$ ) values to the normal cell line CRL-1790 (Appendix A7). The trophoblastic cell lines present with very high fold difference in mRNA levels in comparison to the normal cell line (Fig. 22A; BeWo: 1767-fold; JEG-3: 588-fold). From the non-trophoblastic cell lines (Fig. 22B) HTC116 and SKOV-3 have highest mRNA transcript levels – 127- and 121-fold difference, respectively. OAW42, HT-3, and C-33a also tend to have moderately higher transcription level of the *CGB3-8* genes – 65-, 57-, and 30-fold difference respectively. MDA-MB-468, OVCAR-3, MCF-7, and HEY tend to show

slightly higher transcription of the beta-subunit genes – 10-, 8-, 7-, and 2-fold difference respectively. HeLa shows lower transcription level of the *CGB3-8* genes with a 0.29-fold difference from the normal CRL-1790. 3T3 did not produce any product as expected.

The data from the transcription study was compared for association with the methylation level (Appendix A7.1). Spearman’s ranked correlation was used to perform the test. The transcription fold difference was compared to the average whole promoter methylation, 5’ TF binding, and 3’ TF binding regions. No significant association was discovered between the methylation profiles and transcription level.

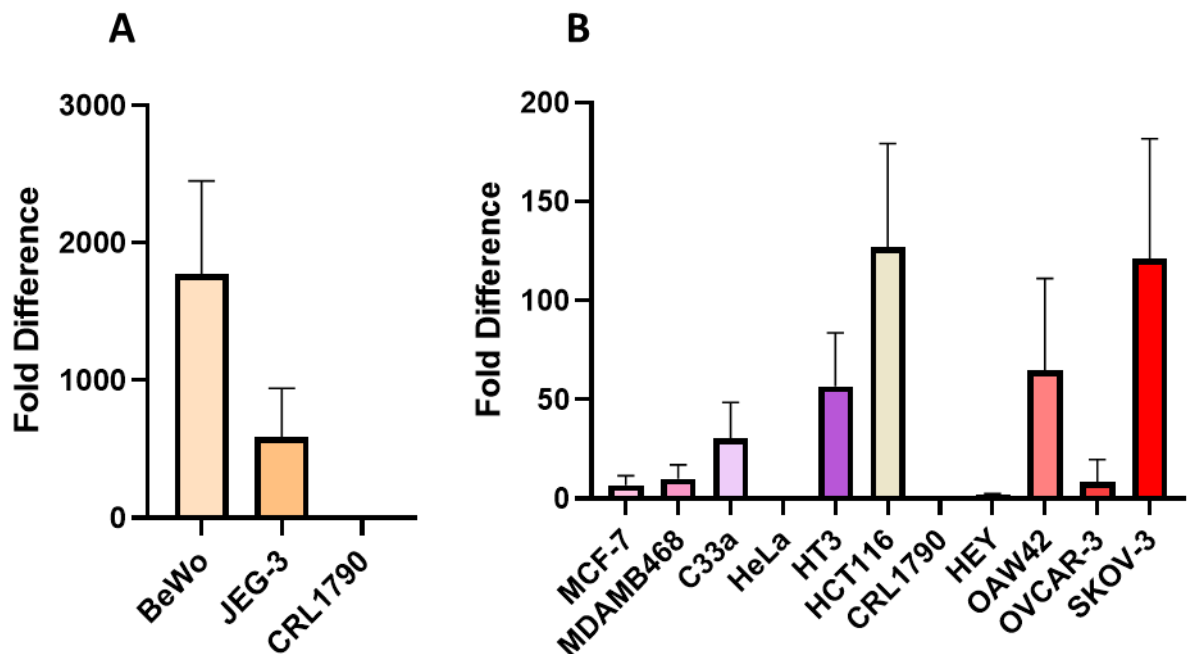


**Fig.22** Bar chart showing fold difference in mRNA transcript in the investigated cell lines. A. trophoblastic cell lines and CRL-1790. B. Non-trophoblastic cell lines and CRL-1790

### 3.4 Secretion of hCG and hCG-beta

The concentration of intact hCG and free hCG-beta was calculated using the standard curves produced by each ELISA and the samples’ optical density. Each ELISA had internal controls provided with the kit (Appendix A8). The calculated concentration for those in each assay matched the expected range provided by manufacturer. In the ELISA for intact hCG, the target molecule was only detected in the 2 trophoblastic samples – BeWo and JEG-3. BeWo media had hCG concentration of 117mIU/ml and JEG-3 -121 mIU/ml. The values were converted

to  $\text{ng}/10^6\text{cells}/24\text{h}$  to adjust for the number of cells and days the media was conditioned. JEG-3 had higher secretion of intact hCG ( $8.39 \text{ ng}/10^6\text{cells}/24\text{h}$ ) than BeWo ( $7.7 \text{ ng}/10^6\text{cells}/24\text{h}$ ).

For the free beta hCG ELISA 4 samples were positive for the free beta subunit. The molecule was found in the media of the 2 trophoblastic cell lines (BeWo –  $3.67\text{ng}/\text{ml}$  and JEG-3 –  $1.78\text{ng}/\text{ml}$ ) and 2 non-trophoblastic cell lines (HEY –  $1.37\text{ng}/\text{ml}$  SKOV-3 –  $4.6\text{ng}/\text{ml}$ ). After adjusting for cells and days in culture HEY seems to secrete the most free beta hCG ( $5.35 \text{ ng}/10^6\text{cells}/24\text{h}$ ), followed by SKOV-3 ( $2.88 \text{ ng}/10^6\text{cells}/24\text{h}$ ), BeWo ( $2.21 \text{ ng}/10^6\text{cells}/24\text{h}$ ), and JEG-3 ( $1.13 \text{ ng}/10^6\text{cells}/24\text{h}$ ). No statistical analysis was performed on the data from ELISA due to the small sample size.

## 4. Discussion

hCG $\beta$  has been studied extensively in relation to its ectopic production in cancers. Presence of hCG $\beta$  is indicative of worsened prognosis and increased metastasis. However, there is still missing knowledge in the molecular mechanism of re-activation in cancer (Zhong *et al.*, 2019; Schüler-Toprak *et al.*, 2017; Szczerba *et al.*, 2016; Kubiczak *et al.*, 2013; Jankowska *et al.*, 2008).

In previous reports (Grigoriu *et al.*, 2011; Campain *et al.*, 1993) *CGB* genes demonstrate hypomethylated profile as the genes are important during pregnancy and actively transcribed. In normal physiology as the genes are not needed, higher methylation of the genes is observed in comparison to the state during pregnancy. This confers the silent state of these genes (Grigoriu *et al.*, 2011). This suggests that reactivation in cancer should also present with decrease of the methylation.

In the present study the main focus was investigation of the methylation profile of the *CGB3-8* genes promoter in non-trophoblastic cancer from epidermal origin. Previous research has found ectopic hCG $\beta$  in bladder, colon, lung, ovarian, cervical and breast cancers (Zhong *et al.*, 2019; Schüler-Toprak *et al.*, 2017; Szczerba *et al.*, 2016; Kubiczak *et al.*, 2013; Jankowska *et al.*, 2008). However, only 3 other studies have been found to investigate methylation in non-trophoblastic cancer tissues and cell lines (Śliwa *et al.*, 2019; Campain *et al.*, 1993; Whitfield and Kourides, 1985).

### 4.1 MSP analysis did not find differential methylation

Initially, studies via MSP were applied to investigate the *CGB3-8* promoter region methylation on a few selected non-trophoblastic cell lines. The selected cell lines are representative of previously reported hCG- $\beta$  positive non-trophoblastic cancers (Sinnappan, 2015; Acevedo *et al.*, 1992). Thus, it was suspected that the cancer cell lines could possess hypomethylated profile in comparison to a normal cell line (CRL-1790). Densitometry analysis of the MSP products did not yield significant difference in the methylation profile of *CGB* genes in the investigated cancer cell lines versus the normal cell line.

However, the applied MSP approach has its caveats that may have not represented the full picture of the *CGB* promoter methylation. Firstly, comes the caveat of sample size and heterogeneity. DNA methylation profile is

heterogeneous between different tissues and within cancer tumours (Wen *et al.*, 2017). The samples investigated via MSP were from 2 different tissues of origin – ovarian and cervical cancer. Therefore, their methylation profile could be quite varied. Combined with the small sample size it may not be a good representation of the wider non-trophoblastic cancer population.

Other limitations of the MSP approach are that the obtained data is semi-quantitative and relative only to the CpGs contained in the primers. The primers for MSP are designed in such a way that they cover the same CpGs – one set detecting their methylated version and one – detecting the unmethylated version (Fraga and Esteller, 2011; Ammerpohl *et al.*, 2009). Therefore, information on any CpG site within the product is not represented, unless the product is sequenced. In this study the MSP targets only 3 CpG sites within the promoter – one located 550bp upstream from TSS and 2 between the Oct3/4 and AP2 binding site – A5 and F1 (Fig. 9). Furthermore, the data obtained cannot be reliably quantitated and MSP does not provide nucleotide level resolution of the sample methylation (Fraga and Esteller, 2011).

## 4.2 MiSeq based bisulphite sequencing

In order to achieve more detailed picture of the DNA methylation within the *CGB3-8* promoter MiSeq (Illumina) based targeted bisulphite sequencing was applied. The first step was to design primers amplifying the region of interest. Bisulphite conversion of DNA changes the original sequences by converting non-CpG cytosines to uracils. CpG cytosines remain ambiguous due to their possible methylation (Li and Tollefsbol, 2011). Bisulphite sequencing primers should be able to amplify methylated and unmethylated sequences with equal efficiency. That is why the primers should not contain CpG sites (Correa *et al.*, 2012; Warnecke *et al.*, 2002). Another criterion is that the length of the product should not be longer than 300bp which is the maximum read length of MiSeq (Soto *et al.*, 2016). Further to that, it is recommended that 2 primer sets are used for the same locus in a way that they overlap. This is to prevent mispriming and amplification of non-desired regions (Correa *et al.*, 2012, Warnecke *et al.*, 2002).

Seven primer pairs based on *CGB3* were selected as possible candidates that fit the above mentioned criteria. A further complication to the primer design was that the oligonucleotides need to amplify 4 different genes simultaneously. To resolve this, the primer sequences were checked for mismatches with the *CGB5-8* genes

and then run in the BiSearch ePCR tool to check for predicted products (Table 11) (Li and Dahiya, 2002). Due to mismatches in the primer sequence and possible amplification of more than the target genes (primer pairs 3-5) or no predicted amplification in all genes of interest (primer pair 1), primer pairs 1-5 designs were not used for the downstream sequencing. Primer pairs 6 and 7 were selected as they had no mismatches and were predicted to amplify all genes of interest. Furthermore, the product sequences also overlap to ensure specific target amplification. However, a possible issue with these pairs was the possible *LHB* product in primer pair 6. Nonetheless, the primer products overlapping and/or mapping of the library post-sequencing should resolve this issue based on single nucleotide differences (Correa *et al.*, 2012; Warnecke *et al.*, 2002).

The selected primers were run in optimised PCR assay to create the library based on bisulphite converted DNA from the studied cell lines and tissue samples which was consecutively sequenced using next generation sequencing MiSeq Illumina platform. The MiSeq platform has been previously employed with methylation studies to reliably obtain methylation status and differences in various genes in conditions ranging from cancers to psychiatric disorders (Dukal *et al.*, 2016; Roeh *et al.*, 2016; Masser *et al.*, 2013; Xiong *et al.*, 2012). It has been shown that this technology is cost-effective, high-throughput, and also sensitive even in samples where target DNA sequence is in low amount (Ward *et al.*, 2016; Luthra *et al.*, 2013). MiSeq has been reported as a tool for accurate absolute 5-methyl cytosine quantification in low diversity samples such as the bisulphite-converted cytosine-poor DNA (Masser *et al.*, 2013).

### 4.3 Trends in DNA methylation of *CGB3-8* promoter

Sample sequencing was performed on total DNA from selected cell lines and internal control DNA sample (labelled control-DNA). The sequencing data was aligned to *CGB3-8* reference sequences using commonly employed Bismark software. The software is a reliable tool for alignment and methylation calling of sequencing data obtained from varied bisulphite-based sequencing methods (Xiong *et al.*, 2012; Krueger *et al.*, 2011). Based on the methylation calling, a beta value is assigned at each site covered by the sequencing which is the percentage of methylated reads from the total reads at a particular CpG site (Du *et al.*, 2011).

The sequencing interrogated the methylation status of a total of 57 CpG sites across the promoter of the *CGB3-8* genes. This included 14 sites in *CGB3*, 5; 13 -

in *CGB8*; and 16 - in *CGB7*. Most mapped reads come from *CGB5* and *CGB8*. The generally observed trend was that *CGB3*, 5 and 8 were more methylated compared to *CGB7* which showed lower DNA methylation across the 13 of the studied cell lines and 2 normal tissue samples.

Looking at the trends of the methylation pattern within samples, it is observed that the positive control trophoblastic cells JEG-3 show varied methylation reads at individual sites (Fig. 13 histograms) but tend to have lower methylation. The other positive control, BeWo, has lower average methylation especially at the *CGB3* gene but higher at *CGB7*. These findings match results from Campain *et al.*, (1993) that claim choriocarcinoma is hypomethylated. Both positive control cell lines are used as models to study human trophoblast *in vitro*, therefore they share some phenotypic features with the placenta (Serranoa *et al.*, 2007; Wolfe, 2006). Grigoriu *et al.*, (2011) performing studies on human placenta DNA methylation, have confirmed hypomethylation of the *CGB3-9* genes in trophoblast cells during gestation.

The negative control cell line 3T3 did not have any reads as expected. 3T3 is a mouse fibroblast cell line which does not have the *CGB* genes as these are only found in human and some primate species (Tuncay *et al.*, 2018; Fournier, 2016; Rao, 2016). In the other non-trophoblastic cell lines interestingly, HeLa presented with lower methylation reads at the *CGB3* gene averaging at 42%. Cell lines and tissues from breast origin (MCF-7, MDA-MB-468, normal breast tissue), the normal colon (CRL-1790) and ovarian OVCAR-3 showed varied methylation reads at investigated CpG sites (Fig. 13). Another interesting feature in the data was that HEY, HT-3 and HCT116 cell lines tend to have higher average methylation in the *CGB7* gene in comparison to the relatively low reads in the other samples (Table 12).

The trends of the averaged methylation for *CGB3-8* genes per CpG site in the different tissue groups present similar as the ones stated above (Fig. 16). Compared to the control-DNA, JEG-3 and BeWo tend to have lower methylation as reported previously (Campain *et al.* 1993). The variability in methylation reads per site is visualised for the breast tissue group, JEG-3, and CRL-1790. Some samples seem to have distinct patterns hinting differences in methylation. In Fig. 16 the lines of JEG-3, BeWo, and control in trophoblast group; the lines of CRL-1790 and HCT116 in colon group; and the HT-3 line in cervical group separate distinctly from the other samples within the respective groups.



Only limited other studies (Campain *et al.*, 1993; Whitfield and Kourides, 1985) have been found from literature to perform some degree of research into the *CGB* genes DNA methylation of non-trophoblastic cancer cell lines. Campain *et al.*, (1993) studies 2 non-trophoblastic cell lines – normal transformed fibroblast from lung (2RA) and ectopically hCG producing glioblastoma (CBT). The research discovered that both present with some degree of demethylation. In Whitfield and Kourides, (1985), D-98 (cervical cancer), Lu-65, and Sand (both lung tumour) cell lines were studied which showed some degree of methylation changes. However, these findings are from more than two decades ago and are based on restriction enzyme analyses of methylation. RE analyses on their own are outdated as they require high quality DNA and are restricted to enzyme recognised sites (Fraga and Esteller, 2011; Ammerpohl *et al.*, 2009). A more recent study investigated methylation of *CGB3-9* genes in ovarian cancer tissue via MSP (Śliwa *et al.*, 2019). It was reported demethylation of the *CGB* genes in cancer tissue corresponds to the increase of mRNA transcript in the diseased samples. However, the methodology used by Śliwa *et al.*, (2019) limits the investigation to only a few sites covered by the primers of the MSP (Fraga and Esteller, 2011; Ammerpohl *et al.*, 2009). In the present research a more reliable method is applied based on bisulphite conversion that can interrogate all CpG sites in the region of interest spanning the *CGB* promoter region of approx. 350bp (Masser *et al.*, 2013).

#### 4.4 Similarities in DNA methylation of cancer cell lines

To further elucidate the methylation profile in the studied cell lines and tissues the data from the sequencing was analysed with the software package methylKit (Akalin *et al.*, 2012). This approach of analysis is based on the R programming language. The package is flexible in its data input and allows for rapid analyses in the realm of DNA methylation from high-throughput methylation sequencing. methylKit can be used to summarise and cluster data from sequencing and visualise patterns from the supplied methylation calls. This allows discerning outliers in the data set and finding similarly methylated samples (Wreczycka *et al.*, 2017; Akalin *et al.*, 2012).

Based on the data in this research Pearson correlation analysis was used initially to understand similarity of the investigated samples methylation profile in the *CGB3-8* genes promoter. The methylation profiles showed high Pearson

coefficient between samples within and between different tissue of origin groups. HCT116 and HT-3 cell lines stand out as they present lower correlation values to the other samples (Fig. 13)

To further clarify the similarity of the samples, two different approaches were applied in methylKit – plotting a dendrogram based on correlation results and principal component analysis (Figs. 14 & 15). In these approaches CpG sites that have missing data have been excluded (Akalin *et al.*, 2012). The dendrogram clusters the majority of the samples relatively close together. HCT116 diverges furthest from the other samples based on its correlation. JEG-3, BeWo and HEY show closer correlation but still their correlation values are different from the rest of the samples. Together the four cell lines cluster furthest away from the rest of the investigated samples. Another more defined cluster is formed between OVCAR-3, Control-DNA, and CRL-1790. These samples' correlation is closer to the majority of the rest of the samples in comparison to the above mentioned cell lines.

The above discussed clustering approach by correlation, however, may not be the most appropriate for this data set. The distance method applied in Fig. 14 to build the dendrogram is solely based on the Pearson coefficient (Akalin *et al.*, 2012). Comparing the averaged methylation data per gene and the dendrogram reveals a few discrepancies. JEG-3 and BeWo cell lines showed lower methylation values compared to HCT116 and HEY with which they are clustered. CRL-1790 stands out in its cluster as the cell line with low methylation values. OAW42 and HT-3 cell lines in the big cluster show higher average methylation per investigated gene compared to the other samples. Therefore, a different approach for clustering might be more appropriate.

Principal component analysis (PCA) is a technique in statistics that can be applied to large data sets with multiple variables attached. It aims to reduce the complexity of data by reducing the number of variables and retaining as much as possible from the original data (Akalin *et al.*, 2012; Jolliffe and Morgan, 1992). This can help distinguish outliers in a data set and show more clearly patterns which may have been omitted by simple observation. The PCA creates new variables, which are linear functions of original variables called principal components (PC). The PCs are ordered so that the first PC has the highest variance among the rest of the PCs, the second PC - has second most variance, and so forth. PCs are

built from a correlation matrix of the original data which aims to standardise it (Jolliffe and Morgan, 1992).

In the present study the data set has a high number of variables which means PCA can be a good approach to cluster the methylation profile for the investigated samples. The PCA plot on Fig. 15 uses PC1 and PC2 derived from the methylation percentage to build a scatter to observe the grouping in the samples (Akalin *et al.*, 2012; Jolliffe and Morgan, 1992). The plot built from these 2 components considers 63.7% of the variability in the data. The cell lines JEG-3 and BeWo do not seem to cluster with any other from the investigated samples. This is comparable to what was observed above (Tale 12, Fig. 12) where JEG-3 shows lower methylation across all investigated *CGB* genes, and BeWo presenting with lower average *CGB3* methylation but relatively higher *CGB7* methylation. HEY, HT-3, and HCT116 cluster together which reflects their higher average methylation values in comparison to the other samples. Observing the next cluster CRL-1790, breast-DNA, and OVCAR-3, shows a profile of high *CGB5*, lower *CGB8*, and lowest *CGB7* methylation relative to the average values of the interested genes. The last two clusters of the rest of the samples are in a relatively close proximity on the plot. In the last two clusters the profile of methylation based on the averaged methylation percentage is high *CGB8*, low *CGB5*, and lowest *CGB7* averaged methylation call. What separates HeLa, MCF-7, and MDA-MB-468 in a defined cluster is the fact that their *CGB7* methylation is lower to the other samples within the two clusters. It is worth noting that the PCA analysis did not take into account *CGB3* reads due to missing or low values in the investigated samples.

## 4.5 *CGB7* has a CGI within promoter

The next step in investigating the *CGB3-8* promoter profile was to establish whether the differences in methylation percentages between the four studied *CGB* genes bared any statistical significance. To achieve this aim the reported beta-values were converted to M-values as previous reports suggested (Weinhold *et al.*, 2016; Du *et al.*, 2011). The M-value is logarithmic conversion of the reported percentage methylation. This removes the statistical limitations posed by using percentages in subsequent differential analyses. The beta-value is more intuitive in interpretation but limits the available methods to distinguish statistically differences in samples (Weinhold *et al.*, 2016; Du *et al.*, 2011).

Comparison of the average methylation of the investigated promoter expressed in M-value revealed a significant difference ( $p < 0.0001$ ) between the *CGB3-8* genes. Tukey's test confirmed that the difference comes from the lower methylation of the *CGB7* compared to the other 3 genes across all samples. This matches the previous results from Fig. 12 and Table 12 where this trend was observed.

Furthermore, the *CGB3-8* genes' promoter sequences were tested *in silico* for presence of CGIs. CGIs are usually defined as regions of at least 200bp length with at least 50% cytosine and guanine content that has observed over expected ratio of minimum 0.6 CpG dinucleotides. These regions are generally unmethylated and found in about 60% promoter regions of human genes (Jones, 2012; Straussman *et al.*, 2009). The returned results show that *CGB7* has a CGI of 720bp length associated with the promoter region and no other from the investigated *CGB* genes. Thus, the results from Newcpgreport tool and the differential analysis of promoter methylation between the genes of interest strongly suggest *CGB7* indeed has a CGI associated with its promoter (Madeira *et al.*, 2019).

As mentioned above CGIs are commonly associated with promoter regions and have relatively uniform low level of methylation. The DNA structure within this site is poor for nucleosome assembly which allows for maintenance of a more relaxed chromatin state to induce transcription (Illingworth *et al.*, 2011). This is further supported by the fact that the CGI are commonly associated with histone 3 lysine 4 trimethylation (H3K4me), an active transcription mark (Thomson *et al.*, 2010). Further to this, CGIs can also be found remotely from promoter regions and termed as "orphan" CGI. They also maintain a mostly unmethylated state with H3K4me. They are proposed to be associated with transcription start site of regulatory molecules like *HOTAIR* and *Xist* – non protein coding RNA transcripts, which take part in regulating chromatin state and X-inactivation respectively (Illingworth *et al.*, 2011).

On occasion CGIs can be methylated in normal tissues which is usually associated with long term silencing (Jones, 2012). This methylation usually occurs in mono-allelic fashion to silence only one allele as seen in genomic imprinting. Another example of CGI methylation in normal tissue is the inactivation of X-chromosome whereby adequate gene dosage is achieved (Portela and Esteller, 2010). However, research of CGI methylation is focused on the aberrant hypermethylation in cancer. This is considered as one of the general changes in

the methylome that occurs during carcinogenesis (Robertson, 2005). CGI hypermethylation in cancer is linked with a wide range of genes associated with DNA repair (*MGMT*), cell cycle (*Rb*), cell adherence (*E-cadherin*), and apoptosis (*DAPK1*) (Portela and Esteller, 2010; Esteller, 2007). These are all pathways which when dysregulated help the establishment of a neoplastic tumour (Portela and Esteller, 2010; Esteller, 2007).

However, in the current study *CGB7* demonstrates low methylation state across all samples. This suggests activity of the gene in both normal and cancerous cells. Stenman *et al.*, 2004 reports transcriptionally active *CGB7* at low levels in non-trophoblastic tissues. Zimmermann *et al.*, (2012) also claims *CGB7* is expressed in breast, lung, bladder, and colon. Their study investigates *CGB* expression in normal endometrium. The findings in Zimmermann *et al.*, (2012) confirm hCG expression in the normal endometrium in secretory phase derived from the *CGB7* and its allele form *CGB6*. Another study by Giovangrandi *et al.*, (2001) investigates the transcriptional activity of the *CGB* genes in normal and cancerous breast tissue. They confirm the detection of *CGB7* transcripts in both tissue types; however, there is no change in the transcription level of the *CGB7* gene between normal and cancerous state (Giovangrandi *et al.*, 2001). Therefore, it could be stated that the detected low level expression of *CGB7* in previously mentioned studies possibly is due to the CGI within the *CGB7* promoter maintaining the transcriptionally available state of DNA.

## 4.6 Methylation differences within tissue groups

### 4.6.1 Trophoblastic versus non-trophoblastic cell lines

After assessing the differences between *CGB3-8* genes promoter methylation, the differences between normal samples, trophoblastic and non-trophoblastic cancers were considered. As mentioned above M-value was used in the statistical tests. Two sets of tests for difference were used – one aimed at the *CGB3*, 5, and 8 results, and one aimed at the *CGB7* results to account for their different methylation. Each set of tests tested 3 different groups of averaged M-values – one for the whole region of interest, one for the TF binding sites at the 5' part of the region of interest, and one for the 3' TF binding site of the region of interest. The 5' part corresponds to CpGs found in the vicinity of 4 TF sites ordered AP2 $\alpha$ -SP1-AP2 $\alpha$ -OCT3/4, and the 3' – to the 2 TF binding sites AP2 $\alpha$ -SP1 (Fig. 9). This was done to assess if the methylation of the whole promoter or a specific TF

binding region contributes to the possible reactivation of the beta subunit in non-trophoblastic caners.

These tests of differences found weakly significant differences ( $p=0.404$ ) only in the average methylation of *CGB3*, 5, and 8 in the whole promoter. However, Dunn's test could not point to significant difference between the control, trophoblastic, and non-trophoblastic samples. The limitation in these sets of statistical tests was the small sample size of trophoblastic and normal samples. Even though no differences were established, an interesting trend is seen in the spread of the data in the different groups (Figs. 18 & 19). In the *CGB3*, 5, 8 averaged M-values the trophoblastic group in all 3 regions tends to lower average methylation in comparison to normal and non-trophoblastic groups, and the non-trophoblastic group maintains wider spread in the 3 regions compared to the other 2 groups (Fig. 18). The trophoblastic tendency of lower methylation matches what has been found by Campain *et al.*, 1993 as discussed previously.

In the *CGB7* group, the tendency for lower methylation of trophoblastic samples is not obvious, but the wider spread of the non-trophoblastic group is maintained (Fig. 19). The previously mentioned lower methylation of the *CGB7* genes and the fact that there is no significant difference is concordant with the findings in Zimmermann *et al.*, (2012) which suggest that *CGB7* consistent transcript is present in low levels in normal and non-trophoblastic tissue. The *CGB7* results also further support the presence previously mentioned CGI associated with the gene as islands tend to keep more uniform methylation across tissues (Illingworth *et al.*, 2010).

#### 4.6.2 Differences in tissue of origin groups

The PCA analysis demonstrated that samples from same tissue of origin cluster with samples from different origin. Furthermore, in the set of difference tests done just prior it was noticed how widely spread the values of the 5mC content within the non-trophoblastic group are in comparison to the other 2 groups. Therefore, the significance of these differences between samples within tissue of origin groups needs to be considered. Again two sets of difference tests were used – one set aimed at *CGB3*, 5, and 8 averaged values, and one – at *CGB7* values. In this instance the M-value per site in each sample was used. The selected test of difference was parametric RM-ANOVA which allows comparing the difference in repeated measures of a variable (CpG site) at different conditions (cell line)

(Singh *et al.*, 2013). Normality assumption was violated in some cases of the test; however, previous research has shown ANOVA is robust enough to handle this (Harwell *et al.*, 1992).

In the positive control group (JEG-3 and BeWo) methylation differences were as expected for *CGB3*, 5 and 8. Both choriocarcinoma cell lines were compared to the control-DNA for the *CGB3*, 5 and 8, and CRL-1790 was used as normal reference for *CGB7* RM-ANOVA analysis. The control DNA was found to be more methylated at *CGB3*, 5 and 8, with a strong significant difference ( $p < 0.0001$ ) for both choriocarcinoma cell lines. These findings are concordant with the reports by Campaign *et al.* (1993) and Grigoriu *et al.* (2011) that show hypomethylation in the *CGB* genes for choriocarcinoma and trophoblast tissue respectively.

Interestingly, JEG-3 showed also significantly lower methylation ( $p < 0.0001$ ) than BeWo. This is also observed in the PCA plot where the two cell lines have been plotted at different locations, not clustering with other samples. This could be due to the difference in the two cell lines' characteristics. Serranoa *et al.* (2007) reports that even though the two cell lines are active producers of intact hCG, they differ in the degree of differentiation and proliferation. JEG-3 is more differentiated than BeWo, but proliferation of the cells is at higher rate in BeWo (Serranoa *et al.*, 2007). This difference in phenotype could be reflected also in the methylation of the cells as this mark is fluctuating (Guo *et al.*, 2014). Furthermore, JEG-3 was found to be less methylated than CRL-1790 and BeWo for *CGB7*. This matches with previous observations - *CGB7* appears to have higher average methylation in BeWo than JEG-3 which could be contributed to the reported phenotypic differences in the selected choriocarcinoma cell lines (Guo *et al.*, 2014; Serranoa *et al.*, 2007).

In the normal samples or control group, including the cervix tissue, breast tissue, CRL-1790 and Control-DNA, differences were observed as well. The control-DNA used as reference from the sequencing facility was more methylated than all other normal samples. All normal samples send for sequencing – CRL-1790, breast-DNA, and cervix-DNA are from epidermal origin. However, the tissue of origin for the control-DNA was not reported back which would help in understanding the reasons for the observed difference. As mentioned previously DNA methylation fluctuates in its pattern between different tissues (Wen *et al.*, 2017). Therefore, it is likely that the control-DNA is from a different tissue type which would contribute to the observed difference in methylation. The normal samples group analysis of

difference for *CGB7* did not contain control-DNA due to missing reads. There was no significant difference in *CGB7* methylation between the 3 samples in the normal samples group.

Observing the tests of difference in the non-trophoblastic cervical tissue group, a few differences can be observed. HeLa presents with a hypomethylated profile when compared to the other cervix samples in *CGB3*, 5 and 8. This is also observed in the clustering from the PCA where HeLa is separately grouped with MCF-7 and MDA-MB-468. The average methylation values (Table 12) also show that the cell line exhibits lower *CGB3* methylation, comparable with JEG-3 and BeWo. This is suggesting that HeLa should have active transcription of the *CGB* genes mentioned above. Articles Jankowska *et al.*, (2008); Chen *et al.*, (1996); and Goldstein *et al.*, (1990) report the presence of *CGB* mRNA transcript in HeLa cells. However, these transcripts are relatively low compared to the choriocarcinoma cells (Chen *et al.*, 1996).

Observing the results in the same tissue group for *CGB7* showed that HT-3 is hypermethylated in comparison to the normal cervical tissue and the other two cervical cancer cell lines. A similar trend was observed in the *CGB3*, 5, and 8 genes but was not significant. As mentioned before HT-3 is also part of the cluster with HEY and HCT116 in the PCA, that tend to have higher average methylation values. Thus, it is expected that there should be reduction of the transcript of *CGB* genes and in particular less transcripts from *CGB7*. However, Acevedo *et al.*, (1992) reported that free hCG-beta has been found associated with the membrane of the HT-3 cells in low amounts suggesting active transcription of the genes. The other notable result was that *CGB7* appears to be significantly more methylated on C-33a in comparison with HeLa but no difference found with the normal cervical tissue. Furthermore, C-33a and the cervical tissue are clustering together on the PCA. This is further confirmation that HeLa is hypomethylated in the cervical group.

In the colon tissue group, a significant difference between the cancerous and normal tissue was only found for the *CGB3*, 5 and 8 averaged M-values. The cancerous cell line HCT116 presented with significantly higher methylation. This matches what was observed in the PCA where HCT116 is grouped with more methylated on average HT-3 and HEY cell lines. This would indicate that the investigated *CGB3*, 5 and 8 genes are likely silenced in this colorectal cancer cell line. However, HCT116 has been reported to produce low levels of *CGB* mRNA



transcript when compared to the choriocarcinoma JAR (Li *et al.*, 2018; Sohr and Engeland, 2011). No significant differences were found in the colon group for *CGB7*.

Interestingly, no significant differences were observed in the ovarian group for the methylation status of *CGB3*, 5, and 8 methylation averages. This contradicts the PCA plot which groups the 4 ovarian cancer cell lines in 3 different clusters. One possible reason for that is that the PCA does not include data from *CGB3* methylation. The only significant difference in the ovarian group comes in the *CGB7* gene methylation, where the HEY cell line shows hypermethylation in comparison to the other cancer cell lines. This is concordant with the PCA grouping where HEY clusters together with HCT116 and HT-3 that show higher average methylation which was confirmed statistically for the *CGB3,5* and 8 (HCT116) and *CGB7* (HT-3). The higher methylation of HEY in *CGB7* suggests that the gene expression would be silenced. Sinnappan (2015) reports that HEY is a potent producer of hCG $\beta$  mRNA. However, the study does not discern from which gene the transcripts come from so the effect of methylation on *CGB7* transcript is not confirmed.

One of the few studies done on *CGB* methylation in cancer investigates the methylation changes in ovarian tissue (Śliwa *et al.*, 2019). The study is suggesting that DNA methylation plays a role in the *CGB* expression in ovaries (Śliwa *et al.*, 2019). Śliwa *et al.*, (2019) analysed methylation within *CGB* promoter via MSP. Their results find significant difference between the unmethylated product of cancer and normal ovary, whereby the cancer tissue is significantly demethylated. These findings were not confirmed by the current study. This is possibly due to the different approach in analysis – here the all CpGs of the sequenced promoter are considered, and the MSP in Śliwa *et al.*, (2019) focusses on a few CpG sites found only in their designed primers (Fraga and Esteller, 2011; Ammerpohl *et al.*, 2009). Furthermore, ovarian tissue from both healthy and cancer samples expresses *CGB3-9* transcripts but the level of these transcripts is significantly increased in cancer tissues (Śliwa *et al.*, 2019). Therefore, it could be speculated that possibly other CpG sites in the *CGB* promoter in normal tissue have lower methylation enabling the *CGB* activation (Grigouriu *et al.*, 2011). Thus, the observed difference in methylation by Śliwa *et al.* (2019) cannot be accounted for when considering the whole promoter as is done in this study (Śliwa *et al.*,

2019). The applied approach here should provide a more accurate picture due to the number of methylation sites analysed.

The last tissue group to discuss for the methylation sequencing differences is the breast tissue. No significant differences in methylation were found in the samples for *CGB3*, 5, and 8 genes. Interestingly, the PCA plot groups the cancer cell lines in different clusters from the normal breast-DNA. However, looking into the average methylation values the most difference is observed in the *CGB7* gene. There was only significant difference in the pattern of MCF-7 which has presented with lower methylation than the control breast-DNA for *CGB7*. As mentioned above Giovangrandi *et al.*, (2001) has already reported that *CGB7* is active in both normal and cancerous tissues. Therefore, the lower methylation in MCF-7 seems to have no impact on *CGB7* expression.

#### 4.7 Transcription and translation level of *CGB3-8* genes

In order to understand whether the DNA methylation has direct effect on *CGB3-8* genes, the transcription and translation of the hCG-beta subunit was assessed via qRT-PCR and ELISA. mRNA transcript for the *CGB3-9* gene was detected in all samples with the exception of the negative control, 3T3. The positive control samples from choriocarcinoma had the highest relative transcription level (BeWo-1767 and JEG-3- 588 fold difference). These findings are concordant with the observed methylation pattern found in this study and previous reports (Grigoriu *et al.*, 2011; Campain *et al.*, 1993). The transcription pattern is as expected since the cell lines are from trophoblast origin and behave in a similar fashion to what is observed in pregnancy, i.e. active *CGB* transcription (Serranoa *et al.*, 2007; Acevedo *et al.*, 1995; Whitfield and Kourides, 1985).

The observed transcription level for the non-trophoblastic cancer was quite diverse. Previous studies agree that all non-trophoblastic cancers show *CGB3-9* gene activity either by the detection of the mRNA transcript or the beta subunit itself (Śliwa *et al.*, 2019; Li *et al.*, 2018; Sinnappan, 2015; Sohr and Engeland, 2011; Jankowska *et al.*, 2008; Chen *et al.*, 1996; Acevedo *et al.*, 1992; Goldstein *et al.*, 1990). One study in particular uses a fairly different approach to assess the level of hCG $\beta$  in cancer cell lines – flow cytometry (Acevedo *et al.*, 1992). In this particular study polyclonal and monoclonal antibodies target different fragments of the intact hCG molecule or its subunits that are associated with the cellular membrane. Due to the differences in applied methods and the employment of

relative quantification of mRNA transcripts, accurate comparisons with this project cannot be achieved.

Correlation using Spearman's ranked test was used to assess any association between the observed methylation and level of *CGB* expression. The test did not present any significant correlation between the transcription level and average methylation of the cell lines in the promoter region, 3' TF binding and 5' TF binding region. Studies by Whitfield and Kourides (1985) and Śliwa *et al.*, (2019) which explored DNA methylation in *CGB3-9* genes also report no association between the methylation and expression level of the hCG $\beta$  genes. This agrees with the correlation results in this project. A possible reason for the lack of association in this study is the contradictory results of averaged methylation and transcription level data. For instance, HCT116 cell line shows high average methylation of ~90% (hypermethylation for *CGB3*, 5, 8) suggesting no transcription. However, in the transcription study HCT116 has the highest fold difference in non-trophoblastic tissues (Fig. 22)

Comparing data between methylation and transcription at tissue of origin level may show some associations which may not be detected by the statistical tests. Unexpectedly, HeLa cells show transcription level of *CGB3-9* genes lower than the normal CRL-1790, even though methylation analyses reveal HeLa hypomethylation. As previously mentioned, HeLa is transcriptionally active (Jankowska *et al.*, 2008; Chen *et al.*, 1996; Goldstein *et al.*, 1990). Acevedo *et al.* (1995) further reports that hCG $\beta$  is produced in HeLa cells and the main contributor to the product was identified as *CGB3*. This finding supports the methylation data obtained from the sequencing in this study. The unexpected transcriptional result may be due to issues in contamination of HeLa cells in our lab, as recently colleagues have reported changed phenotype of the cell line. Proposed reasons for this change is cross-contamination with another cell line.

The other cell lines in the cervical group C-33a and HT-3 do not show significant methylation changes from the normal cervix DNA. However, Acevedo *et al.*, (1992) reports free beta subunit association with the membrane of C-33a and HT-3 corresponding to 47.5% and 15.4% of the studied populations confirming the activity of the genes. This correlates with the transcription data in this study where HT-3 and C-33a have moderately high level of transcription compared to the normal CRL-1790 with the difference that HT-3 has higher transcription than C-33a. HT-3 did present hypermethylation in the *CGB7* sites; however, the

transcriptional assay does not discern between different gene transcripts and its role cannot be assessed.

Further to that, Jankowska *et al.* (2008) presents a study on gynaecological cancers where hCG $\beta$  and LH/hCG-R transcription level are evaluated in ovarian, endometrial, and cervical cancer. Their study found that all cancer samples were positive for the *CGB3-9* transcript. The normal tissue used in the study did not detect any activity of the *CGB* genes suggesting that expression of the hormone subunit is typical for cancer tissue. In the same study the LH/hCG-R is co-expressed in cancers suggesting possible autocrine/paracrine role of the free  $\beta$  hormone subunit. Furthermore a consecutive study by the same group report that in cervical carcinoma U1 snRNA blocking of hCG $\beta$  expression results in increased apoptosis (Jankowska *et al.*, 2008).

In the other investigated gynaecological cancer, ovarian cell lines SKOV-3 is showing highest transcriptional activity followed by OAW42, OVCAR-3 and HEY has lowest relative expression in the group. Śliwa *et al.* (2019) and Sinnappan (2015) confirm expression of the *CGB3-9* genes at a low level in normal and higher level in cancerous ovarian cells. The fact that *CGB* genes are expressed in both normal and cancerous could be a reason why methylation data that shows no significant difference in ovarian cells. Sinnappan (2015) further shows that HEY and SKOV-3 have the most active *CGB3-9* genes in their sample, and OVCAR-3 has low level of expression. This contradicts the results in the present study where HEY has lowest transcription level. This could be due to differences in applied qRT-PCR assays.

Tissues from ovarian cancer patients have revealed increased transcript levels of hCG $\beta$  mRNA in comparison to healthy tissue (Zhong *et al.*, 2019). In the same study it was also established that this increase matched with the protein level increase in the cancer tissue samples. The increase of hCG $\beta$  level in these samples was found to be associated with worse patient prognosis denoted by advanced tumour stages and increased metastasis. However, exact mechanism of how hCG acts on ovarian cancer progression needs to be elucidated (Zhong *et al.*, 2019).

The studies Szczerba *et al.* (2016) and Kubiczak *et al.* (2013) have also confirmed samples of ovarian cancer tissues positive for hCG $\beta$  expression. In the studies transcript of the *CGB3-9* genes were found both in normal and cancerous tissue.

The cancerous tissue presented with higher level of *CGB* gene activity. However, they also report that the level of activity in the analysed samples was highly varied due to cellular heterogeneity and genetic instability typical for cancerous cells. Szczerba *et al.* (2016) and Junker and Oudenaarden (2014) further suggest that induced overexpression of *CGB5* modulates apoptosis regulated genes *BCL2*, *BAX* and *BRIC5* so that apoptosis in ovarian cancer is suppressed.

In the breast cancer group the 2 cell lines MCF-7 and MDA-MB-468 are transcribed similarly at low levels compared to most other investigated cell lines. Acevedo *et al.* (1992) reports presence of membrane associated free hCG $\beta$  confirming that the genes are transcriptionally active in the cell line. Giovangrandi *et al.* (2001) investigates the expression of the genes in breast cancers and confirms that elevated *CGB3*, 5 and 8 transcription is associated only with malignant tumours. Methylation data did not confirm hypomethylation in the *CGB3*, 5 and 8 genes to suggest the activation of these genes.

Furthermore, Giovangrandi *et al.* (2001) proposes that the beta subunit of hCG is acting as a tumour growth factor independently from the classic receptor in breast cancer. A different report states that beta-hCG presence in breast cancer is associated with apoptosis inhibition and down regulation of epithelial cell adhesion to allow tumour migration and metastasis. However, intact hCG has a protective role on breast tissue against malignancy. Early completion of full term pregnancy changes the breast epithelium protecting it from malignant changes. The paradoxical nature of hCG and its beta subunit on breast cancer remains controversial (Schüler-Toprak *et al.*, 2017).

In the colon group the transcription level of HCT116 has the highest relative transcription level of all non-trophoblastic cell lines used in this study. Data from previous studies confirm the presence of mRNA transcripts in the cell line but due to the relative approaches applied no comparison of the values can be done (Li *et al.*, 2018; Sohr and Engeland, 2011). This is in contrast with the methylation data which show HCT116 is hypermethylated in the *CGB3*, 5 and 8 genes.

Li *et al.*, (2018) further comments on the role of hCG $\beta$  in colorectal cancer which is mainly in tumour invasion and migration but no effect on tumour proliferation. This is thought to be due to triggering of epithelial-to-mesenchymal transition (EMT), a process in which the cell loses its epithelial characteristics such as the cuboidal cell shape and adhesiveness to become more spindle shaped and able

to migrate. Kawamata *et al.* (2018) is another report confirming findings that hCG $\beta$  activates EMT via TGF $\beta$  receptor in colorectal carcinoma. The study tests this *in vitro* using western blot and qPCR to show that overexpressing cells display EMT associated changes. The EMT associated changes were reversed in the studied cell line by addition of TGF $\beta$  receptor inhibitor (Kawamata *et al.*, 2018).

The last piece of information collected for this study was the protein level of hCG $\beta$  in the cell line conditioned media. The positive control trophoblastic cell lines behaved as expected and showed positive results for intact and free beta hCG. This matches previous reports of the cell lines as potent hCG producers (Serranoa *et al.*, 2007). The negative control 3T3 had no protein detected. ELISA data showed positive results for free hCG $\beta$  in only two of the non-trophoblastic samples – SKOV-3 and HEY. All other cell lines were negative and below detection limit for hCG $\beta$  of 0.2 ng/ml. Transcription data for SKOV-3 from this study is relatively high in the tested samples and matches the detection of the beta subunit in the media. However, HEY showed little transcriptional activity in this study but displayed the highest level of free hCG $\beta$  per million cells over 24h. Wu *et al.* (2019) and Sinnappan (2015) show that hCG $\beta$  protein is produced by both of the cell lines. Findings in (Sinnappan, 2015) report that SKOV-3 produces more of the hCG $\beta$  protein as detected in culture media.

As the other samples did not show positivity for the protein ELISA data could not be used for statistical analysis to evaluate translation associations with transcription and methylation. The transcription data suggests that at least HT-3, HCT116, and possibly C-33a should express some level of the protein. Possible reasons for this discrepancy could be an artefact from repeated freezing-thawing. As previously mentioned tumours tend to be heterogeneous and only select few cells secrete the hCG $\beta$  leading to too low of a concentration to be detected in the media (Szczerba *et al.*, 2016; Junker and Oudenaarden, 2014). Rao (2016) further reports that small amounts of secreted hCG can be quickly eliminated/absorbed from circulation leading to no detection. It is possible that this could have happened in the cultured cell lines.

## 4.8 Limitations of study

One limitation of this study is the lack of replicates of the sequenced samples. The study used a single set of cell line and tissue samples for the sequencing. Yet, tumour cells are heterogeneous and unstable in nature (Szczerba *et al.*, 2016;

Junker and Oudenaarden, 2014). DNA methylation fluctuates and the heterogeneity of tumour cells may be reflected in the DNA methylation (Jones, 2012). Replicate samples of each cell line could address the issue of heterogeneous methylation by increasing the chance to capture the variety in the profiles and establish significant methylation motifs that may have a biological role. Furthermore, no validation study has been coupled with the sequencing performed here. Combining the sequencing with a second approach can show whether the data is reproducible and sensitive (Roeh *et al.*, 2016; Luthra *et al.*, 2013).

Further to this, each possible methylation site at a given cell can be either methylated or not. However, there are multiple reads per site which are reported as beta-value. A beta value of 60% indicates that 60% of the total reads showed methylation but the other 40% are not methylated (Du *et al.*, 2011). That could be a possible reason why some samples with higher average methylation percentage or beta value still show transcription. To address that some sequencing approaches apply cut-off ranges based on beta value to define methylated, unmethylated and heterogeneous samples (Warden *et al.*, 2013).

Additionally, DNA methylation is not well studied in regards to non-CGI associated promoters such as CGB3, 5 and 8. CGIs show clear inverse correlation between transcription initiation and DNA methylation (Jones, 2012). However, Weber *et al.* (2007) stated that methylated non-CGI sites still possess transcriptional activity. This statement is not in agreement with other research where it is presented that the methylation of DNA behaves similarly between CGI and non-CGI associated TSS (Han *et al.*, 2011).

The recommended approach for DNA sequencing analysis is using R programming based packages (Wreczycka *et al.*, 2017; Weinhold *et al.*, 2016; Akalin *et al.*, 2012). However, limited expertise in R programming prevented the full utilisation of the available functions of methylKit or other similar tools. As reported these can provide comprehensive analysis that identifies differentially methylated regions and differentially methylated cytosines. This may recognise other motifs which may have been omitted by conventional statistics (Wreczycka *et al.*, 2017; Akalin *et al.*, 2012).

In the transcription study the major limitation is the use of a universal primer pair to amplify multiple genes. This does not allow checking for the transcript levels of

specific CGB genes. Therefore, the methylation data obtained per gene needed to be averaged and possibly masking some associations between the specific gene methylation and transcription. This is especially important with the *CGB7* gene which as observed and reported in Giovangrandi *et al.*, (2001) behaves differently than the rest of the *CGB* genes.

#### 4.9 Further research

This is the first study of methylation profile in the promoter of the *CGB3-9* genes in non-trophoblastic cancer cell lines employing next generation sequencing method. The study was coupled with qRT-PCR analysis and ELISA to establish how methylation of the promoter affects downstream gene expression. As such the data from the methylation study could only be inferred from the obtained transcription levels and the ones reported in literature. Śliwa *et al.* (2019); Uuskula *et al.* (2010); Glodek *et al.* (2014); Campain *et al.* (1993); and Whitfield and Kourides (1985) are the only found previous reports of the *CGB3-8* genes methylation specifically. However, the studies apply varied approaches in analysis of methylation status and utilise different cancer and non-cancer samples making comparison between the methylation data difficult.

Free hCG beta is a tumour marker which is associated with poor prognosis and overall lower survival time (Rull *et al.*, 2008, Iles *et al.*, 2010; Stenman *et al.*, 2004). hCG $\beta$  can be produced by numerous common non-trophoblastic cancers as already established (Schüler-Toprak *et al.*, 2017; Sinnappan, 2015; Kubiczak *et al.*, 2013; Jankowska *et al.*, 2008; Iles *et al.*, 1996). Understanding the mechanisms which are involved in the transcriptional regulation can shed a light on the development on both diagnostic tools and possible therapeutic targets to combat aggressive cancers (Śliwa *et al.*, 2019). As previously reported methylation pattern of the *CGB* genes changes between the cancerous and normal tissues (Śliwa *et al.*, 2019; Campain *et al.* 1993); however, no association is found between the transcription and methylation data (Śliwa *et al.*, 2019; Whitfield and Kourides, 1985). The obtained data in this project showed some discrepancies where hypermethylated regions have active transcription. Other methylation results could not be compared to see if there is significance due to the approach of the transcription study where a universal primer set was used for all *CGB3-8* genes and thus, no discrepancy between the individual gene transcripts. Therefore, future research needs to be carried out to validate the information



obtained here and elucidate the role of DNA methylation in non-trophoblastic cancers.

DNA methylation does not exist as an isolated mark – it is involved with the other epigenetic mechanisms such as histone modifications and non-coding RNAs (Grigoriu, *et al.*, 2011; Thomson, 2010; Wojdacz & Dobrovic, 2007). An example is the lysine 4 methylation at histone 3 which is the active mark associated with CGI overlaying the already hypomethylated (active) CGI (Thomson, 2010). Therefore, it could be speculated that the methylation observed in *CGB3-8* genes may be a consequence of other epigenetic marks that dictate the methylation pattern. For instance in cancers, histones, as with DNA methylation, have global changes – these are less defined but typically loss of the active acetylation marks is observed. The methyltransferase EZH2 is overexpressed in several cancers which alters the H3K27me profile in the genome. In turn, this histone methyltransferase interacts with DNMTs and by extension controls DNA methylation (Portela and Esteller, 2010).

Another aspect of *CGB* transcriptional control is the TFs involved in its expression. The studies by Glodek *et al.* (2014) and Śliwa *et al.* (2019) use combined approach to assess the methylation level and compare it with TFs levels in the samples. AP2 $\alpha$  levels have been correlated positively with transcriptional activation of the *CGB* genes. Pairing methylation studies with transcriptional factor level may provide insights into the relationship of the two. Furthermore, not all TFs are directly influenced by DNA methylation directly – establishing how DNA methylation and TFs influence each other could further elucidate the transcription mechanism of hCG $\beta$  genes (Portela and Esteller, 2010).

Other TFs that have been found to interact with *CGB* genes are PPAR $\gamma$  and MTA-3. PPAR $\gamma$  is a nuclear receptor involved in trophoblast differentiation and invasion (Handsuh *et al.*, 2009). Handsuh *et al.* (2009) showed different behaviour depending on the site of the trophoblast: in VCT activation of PPAR $\gamma$  leads to higher amount of free hCG $\beta$  and secretion of hCG. In iEVT PPAR $\gamma$  activation decreased the transcript and hCG secretion. Fournier *et al.*, 2011 showed similar findings to Handsuh *et al.*, (2009) with regards to PPAR $\gamma$  differential regulation of trophoblast cell subtypes. Further to the nuclear receptor association with increased hCG expression and secretion in VCT, it was reported PPAR $\gamma$  plays a role in villous trophoblast differentiation to ST (Fournier *et al.*, 2011).

MTA3 has been shown to repress hCG gene expression mediated via HDAC1/2 component of NuRD in BeWo cell line. Forskolin treatment in BeWo decreased MTA3 and increased hCG expression (*CGB5*) suggesting inverse relationship between MTA3 and hCG expression in trophoblast (Chen *et al.*, 2013). Cytotrophoblasts show higher staining for MTA3 than syncytiotrophoblasts, which are usually associated with higher amount of hCG secretion between the 2 sites, further suggesting inverse correlation between MTA3 and hCG expression in placenta (Chen *et al.*, 2013). MTA3 may have a role in proliferation and differentiation in cytotrophoblast as it shows stable concentration until CTs are fully differentiated to EVT or ST (Horii *et al.*, 2015). MTA3 is required for terminal differentiation as its knockdown leads to decrease in hCG secretion and reduction of mRNA transcripts (Horii *et al.*, 2015). Understanding where these 2 factors (MTA3 and PPAR $\gamma$ ) bind in the promoter and their interaction with DNA methylation can present novel insights in the transcriptional regulation of the *CGB* genes.

## 5. Conclusions

This study focused on the role of DNA methylation in the activation of the *CGB3-8* genes whose protein products have functions as anti-apoptotic, angiogenic, growth and invasion stimulating factors in cancers. The results from this study showed that the *CGB7* gene is hypomethylated compared to *CGB3-9*. This, coupled with *in silico* predictions strongly suggests *CGB7* has a CGI associated with its promoter which is further confirmed in the literature where it was reported low levels of *CGB7* mRNA were present in normal tissues and in breast cancer.

Comparing the methylation profiles of the studied non-trophoblastic cell lines and tissues revealed 4 distinct groups, separate from the trophoblastic cancer cell lines, which did not assemble with each other. Other notable finds show hypomethylation of JEG-3 and BeWo cell lines which matches the expression and secretion data obtained by this study and is further supported by literature. Hypomethylation of HeLa was also detected which has confirmed previously reported transcription studies but did not match the expression data in this study. The results from the methylation sequencing showed no significant correlation with the data from expression studies.

This is the first study investigating the *CGB3-8* promoter methylation in non-trophoblastic cancer cell lines. The results did not show conclusive methylation changes associated with non-trophoblastic cancer. Further studies should be completed to fully understand the role of *CGB* gene family DNA methylation in non-trophoblastic cancer.

## 6. References

- Acevedo, H. F., Krichevsky, A., Campbell-Acevedo, E. A., Galyon, J. C., Buffo, M. J., and Hartsock, R. J. (1992) 'Expression of membrane-associated human chorionic gonadotropin, its subunits, and fragments by cultured human cancer cells', *Cancer*, 69(7), pp. 1829–1842, doi: 10.1002/1097-0142(19920401)69:7<1829::aid-cncr2820690727>3.0.co;2-0
- Acevedo, H.F., Tong, J.Y. and Hartsock, R.J. (1995) 'Human chorionic gonadotropin-beta subunit gene expression in cultured human fetal and cancer cells of different types and origins' *Cancer*, 76, pp.1467-1475. doi:10.1002/1097-0142(19951015)76:8<1467::aid-cncr2820760826>3.0.co;2-a.
- Adams, C., Henke, A., and Gromoll, J. (2011) 'A novel two-promoter-one-gene system of the chorionic gonadotropin beta gene enables tissue-specific expression', *Journal of Molecular Endocrinology*, 47(3), pp. 285-298. doi:10.1530/JME-11-0026.
- Akalin, A., Kormaksson, M., Li, S., Garrett-Bakelman, F.E., Figueroa, M. E., Melnick, A. and Mason, C.E.(2012) 'methylKit: a comprehensive R package for the analysis of genome-wide DNA methylation profiles', *Genome Biology*, 13, doi:10.1186/gb-2012-13-10-r87.
- Ambrus, G. and Rao, C. V.,(1994) 'Novel regulation of pregnant human myometrial smooth muscle cell gap junctions by human chorionic gonadotropin', *Endocrinology*, 135(6), pp. 2772-2779, doi:10.1210/endo.135.6.7988470
- Ammerpohl, O., Martin-Subero, J. I., Ritcher, J., Vater, I., and Siebert, R. (2009) 'Hunting for the 5th base: Techniques for analyzing DNA methylation', *Biochimica et Biophysica Acta- General Subjects*, 1790(9), pp. 847-862, doi:10.1016/j.bbagen.2009.02.001.
- Arányi, T., Váradi, A., Simon, I. and Tusnády, G.E. (2006) 'The BiSearch web server', *BMC Bioinformatics*, 7, doi:10.1186/1471-2105-7-431
- Arrieta, O., Michel Ortega, R.M., Ángeles-Sánchez, J., Villarreal-Garza, C., Avilés-Salas, A., Chanona-Vilchis, J.G., Aréchaga-Ocampo, E., Luévano-González, A., Jiménez, M.A. and Aguilar, J.L.(2009) 'Serum human chorionic gonadotropin is associated with angiogenesis in germ cell testicular tumors', *Journal of Experimental & Clinical Cancer Research*, 28(1), doi:10.1186/1756-9966-28-120.
- Berger, P., Paus, E., Hemken, P.M., Sturgeon, C., Stewart, W.W., Skinner, J.P., Harwick, L.C., Saldana, S.C., Ramsay, C.S., Rupprecht, K.R., Olsen, K.H., Bidart, J.M. and Stenman, U.H.(2013) 'Candidate epitopes for measurement of hCG and related molecules: the second ISOBM TD-7 workshop', *Tumor Biology*, 34(6), pp. 4033-57, doi:10.1007/s13277-013-0994-6
- Borisova, M., Moiseenko, D., and Smirnova, O. (2017) 'Human Chorionic Gonadotropin: Unknown about Known', *Human Physiology*, 43, pp. 93-104, doi:10.1134/S0362119716060050.
- Burczynska, B., Kobrouly, L., Butler, S. A., Naase, M., and Iles, R. K. (2014) 'Novel insights into the expression of CGB1 & 2 genes by epithelial cancer

cell lines secreting ectopic free hCG $\beta$ ', *Anticancer Research*, 34(5), pp.2239-2248, Available at: <http://ar.iiarjournals.org/content/34/5/2239.long> (Accessed: 16 December 2019)

- Campaign, J. A., Gutkin, D. W., and Cox, G. S. (1993) 'Differential DNA Methylation of the Chorionic Gonadotropin beta-subunit Multigene Family', *Molecular Endocrinology*, 7(10), pp.1331-1346, doi:10.1210/mend.7.10.7505395
- Casarini, L., Lispi, M., Longobardi, S., Milosa, F., La Marca, A., Tagliasacchi, D., Pignatti, E. and Simoni, M.(2012) 'LH and hCG action on the same receptor results in quantitatively and qualitatively different intracellular signalling', *PLoS One*, 7(10), pp. e46682, doi:10.1371/journal.pone.0046682.
- Chen, Y. H., Chen, T.M. and Hsieh, C.Y. (1996) 'The expression of the human chorionic gonadotropin beta subunit gene depends on negative control'. *Cell Biochem. Funct.*, 14, pp. 297-301, doi:10.1002/cbf.686.
- Chen, Y., Miyazaki, J., Nishizawa, H., Kurahashi, H., Leach, R., and Wang, K. (2013) 'MTA3 regulates *CGB5* and Snail genes in trophoblast', *Biochemical and biophysical research communications*, 433(4), pp.379-384, doi:10.1016/j.bbrc.2013.02.102.
- Cole, L. (2015). *Human Chorionic Gonadotropin (hCG)*. 2nd edn. Edited by L. Cole and S. Butler. San Diego: Elsevier.
- Cole, L.A. (2007) 'Hyperglycosylated hCG', *Placenta*, 28(10), pp. 977-986 doi:10.1016/j.placenta.2007.01.011.
- Colyer, H., Armstrong, R., Sharpe, D., and Mills, K. (2012) *Detection and Analysis of DNA Methylation by Pyrosequencing*. In R. Dumitrescu, and M. Verma (Eds.), *Cancer Epigenetics* (pp. 281-292). Humana Press. doi:10.1007/978-1-61779-612-8\_17.
- Correa, P. A., Pujol-Borrell, R. and Colobrana, R.(2012) 'Bisulfite genomic sequencing to uncover variability in DNA methylation: Optimized protocol applied to human T cell differentiation genes', *Inmunología*, 31(4), pp. 97-105 doi:10.1016/j.inmuno.2012.09.002.
- Cui, D., and Xu, X. (2018) 'DNA Methyltransferases, DNA Methylation, and Age-Associated Cognitive Function', *International journal of molecular sciences*, 19(5), doi:10.3390/ijms19051315.
- d'Hauterive, S.P., Hüge, F., Polese, B., Berndt, S., Gaspard, O., Munaut, C., Foidart, J.M., Geenen, V. and Gridelet V.(2011) 'Immune tolerance and angiogenesis during embryo implantation: the role of hCG', *Journal of Reproductive Immunology*, 90(2), pp. 161-162, doi:10.1016/j.jri.2011.06.057.
- Du, P., Zhang, X., Huang, C. , Jafari, N., Kibbe, W.A., Hou L. and Lin, S.M. (2010) 'Comparison of Beta-value and M-value methods for quantifying methylation levels by microarray analysis', *BMC Bioinformatics*, 11, doi:10.1186/1471-2105-11-587.
- Dukal, H., Schendel, D., Lang, M., Mossner, M., Jann, J.C., Frank, J., Treutlein, J., Witt, S. and Ia Rietschel, M. (2017) 'T22 - Next-Generation Bisulfite Sequencing Of *Cacna1c* With Illumina Miseq', *European*

*Neuropsychopharmacology*, 27, pp. S445,  
doi:10.1016/j.euroneuro.2016.09.510.

- Esteller, M.(2007) 'Epigenetic gene silencing in cancer: the DNA hypermethylome', *Human Molecular Genetics*, 16(R1) pp. R50–R59, doi:10.1093/hmg/ddm018
- Fakruddin, Mazumdar, R., Chowdhury, A., Hossain, N., Mohajan, S., and Islam, S. (2013) 'Pyrosequencing-A Next Generation Sequencing Technology', *World Applied Sciences Journal*, 24(12), pp. 1558-1571, doi:10.5829/idosi.wasj.2013.24.12.2972.
- Fournier, T. (2016) 'Human chorionic gonadotropin: different glycoforms and biological activity depending on its source of production', *Annales d'Endocrinologie*, 77(2), pp. 75-81 doi: 10.1016/j.ando.2016.04.012.
- Fournier, T., Guibourdenche, J., Handschuh K., Tsatsaris V., Rauwel B., Davrinche C. and Evain-Brion D. (2011) 'PPAR $\gamma$  and human trophoblast differentiation', *Journal of Reproductive Immunology*, 90(1), pp. 41-49 doi: 10.1016/j.jri.2011.05.003.
- Fraga, M. F., and Esteller, M. (2002) 'DNA methylation: a profile of methods and application', *BioTechniques*, 33(3), pp. 632-649 doi:10.2144/02333rv01.
- Gibney, E. and Nolan, C.M. (2010) 'Epigenetics and gene expression', *Heredity*, 105, pp. 4-13, doi:10.1038/hdy.2010.54.
- Giovangrandi, Y., Parfait, B., Asheuer, M., Olivi, M., Lidereau, R., Vidaud, M. and Bièche, I (2001) 'Analysis of the human CGB/LHB gene cluster in breast tumors by real-time quantitative RT-PCR assays', *Cancer Letters*, 168 (1), pp. 93-100, doi:10.1016/S0304-3835(01)00496-7.
- Glodek, A., Kubiczak, M. J., Walkowiak, G. P., Nowak-Markwitz, E., and Jankowska, A. (2014) 'Methylation status of human chorionic gonadotropin beta subunit promoter and TFAP2A expression as factors regulating CGB expression in placenta', *Fertility and Sterility*, 102, pp. 1175-1182 doi:10.1016/j.fertnstert.2014.06.016.
- Goldstein, S., Jones, R., Hardin, J., Glenn D. Braunstein, and Reis, R.J.S. (1990) 'Expression of  $\alpha$ - and  $\beta$ -Human Chorionic Gonadotropin Subunits in Cultured Human Cells'. *In Vitro Cellular & Developmental Biology*, 26(9), pp. 857-864. Available at: [www.jstor.org/stable/4296528](http://www.jstor.org/stable/4296528) (Accessed date 10.01.2020)
- Greer, E.L., Blanco, M.A., Gu, L., Sendinc, E., Liu, J., Aristizábal-Corrales, D., Hsu, C.H., Aravind, L., He, C. and Shi, Y.(2015) 'DNA methylation on N6-adenine in *C. elegans*', *Cell*, 161(4), pp 868–878, doi:10.1016/j.cell.2015.04.005.
- Grigoriu, A., Ferreira, J. C., Choufani, S., Baczyk, D., Kingdom, J., and Weksberg, R. (2011) 'Cell specific patterns of methylation in the human placenta', *Epigenetics*, 6(3), pp. 368-379. doi:10.4161/epi.6.3.14196.
- Guo, F., Li, X., Liang, D., Li, T., Zhu, P., Guo, H., Wu, X., Wen, L., Gu, T.P., Hu, B., Walsh, C.P., Li, J., Tang, F. and Xu G. L.(2014) 'Active and Passive Demethylation of Male and Female Pronuclear DNA in the Mammalian Zygote', *Cell Stem Cell*, 15(4), pp. 447-459, doi:10.1016/j.stem.2014.08.003.

- Guo, F., Yan, L., Guo, H., Li, L., Hu, B., Zhao, Y., Yong, J., Hu, Y., Wang, X., Wei, Y., Wang, W., Li, R., Yan, J., Zhi, X., Zhang, Y., Jin, H., Zhang, W., Hou, Y., Zhu P, Li, J., Zhang, L., Liu, S., Ren, Y., Zhu, X., Wen, L., Gao, Y. Q., Tang, F. and Qiao, J. (2015) 'The Transcriptome and DNA Methylome Landscapes of Human Primordial Germ Cells', *Cell*, 161(6), pp. 1437-1452, doi:10.1016/j.cell.2015.05.015.
- Guo, X., Liu, G., Schauer, I.G., Yang, G., Mercado-Uribe, I., Yang, F., Zhang, S., He, Y. and Liu, J. (2011) 'Overexpression of the beta subunit of hCG promotes the transformation of human ovarian epithelial cells and ovarian tumorigenesis', *The American journal of pathobiology*, 179(3) , pp. 1385-1393 doi:10.1016/j.ajpath.2011.05.018.
- Hallast, P., Rull, K. and Laan, M. (2007) 'The evolution and genomic landscape of CGB1 and CGB2 genes', *Molecular and cellular endocrinology*, 260-262(9), pp. 2–11, doi:10.1016/j.mce.2005.11.049.
- Han, H., Cortez, C. C., Yang, X., Nichols, P. W., Jones, P. A., and Liang, G. (2011) 'DNA methylation directly silences genes with non-CpG island promoters and establishes a nucleosome occupied promoter', *Human molecular genetics*, 20(22), pp. 4299–4310, doi:10.1093/hmg/ddr356.
- Handsuh, K., Guibourdenche, J., Cocquebert, M., Tsatsaris, V., Vidaud, M., Evain-Brion, D. and Fournier, T. (2009) 'Expression and Regulation by PPAR $\gamma$  of hCG alpha and beta subunits: Comparison between villous and invasive extravillous trophoblastic cells', *Placenta*, 30(12), pp. 1016-1022, doi:10.1016/j.placenta.2009.09.006.
- Hanna, C.W., McFadden, D.E. and Robinson, W.P. (2013) 'DNA Methylation Profiling of Placental Villi from Karyotypically Normal Miscarriage and Recurrent Miscarriage', *The American journal of pathology*, 182(6), pp. 2276-2284 doi: 10.1016/j.ajpath.2013.02.021.
- Harwell, M.R., Rubinstein, E.N., Hayes, W.S. and Olds, C.C.(1992) 'Summarizing Monte Carlo results in methodological research: the one- and two-factor fixed effects ANOVA cases' *J. Educ. Stat.* 17, pp. 315-339, doi:10.2307/1165127.
- Horii, M., Moretto-Zita, M., Nelson, K. K., Li, Y., and Parast, M. M. (2015) 'MTA3 regulates differentiation of human Cytotrophoblast stem cells', *Placenta*, 36(9), pp. 974-980, doi: 10.1016/j.placenta.2015.07.122.
- Iles, R., Delves, P., and Butler, S. A. (2010) 'Does hCG or hCG-beta play a role in cancer cell biology?', *Molecular and Cellular Endocrinology*, 329(1-2), pp. 67-70. doi:10.1016/j.mce.2010.07.014.
- Iles, R., Persad, R., Trivedi, M., Sharma, K., Dickinson, A., Smith, P. and Chard, T. (1996) 'Urinary concentration of human chorionic gonadotrophin and its fragments as a prognostic marker in bladder cancer', *British Journal of Urology*, 77(1), pp. 61-69, doi:10.1046/j.1464-410X.1996.82910.x.
- Illingworth, R. S., Gruenewald-Schneider, U., Webb, S., Kerr, A. R., James, K. D., Turner, D. J., Smith, C., Harrison, D.J., Andrews, R. and Bird, A. P. (2010) 'Orphan CpG islands identify numerous conserved promoters in the mammalian genome', *PLoS genetics*, 6(9), e1001134, doi:10.1371/journal.pgen.1001134.

- Iyer, S. and Acharya, K.R. (2011) 'Tying the knot: the cystine signature and molecular-recognition processes of the vascular endothelial growth factor family of angiogenic cytokines', *The FEBS Journal*, 278(22), pp. 4304-4322. doi:10.1111/j.1742-4658.2011.08350.x.
- Jankowska, A., Gunderson, S. I., Andrusiewicz, M., Burczynska, B., Szczerba, A., Jarmolowski, A., Nowak-Markwitz, E. and Warchol, J. B. (2008) 'Reduction of human chorionic gonadotropin beta subunit expression by modified U1 snRNA caused apoptosis in cervical cancer cells', *Molecular cancer*, 7, doi:10.1186/1476-4598-7-26.
- Jankowska, A., Andrusiewicz, M., Grabowski, J., Nowak-Markwitz, E., and Warchol, J.b. (2008) 'Coexpression of human chorionic gonadotropin beta subunit and its receptor in nontrophoblastic gynecological cancer', *International Journal of Gynecologic Cancer*, 18(5), pp. 1102-1107 doi:10.1111/j.1525-1438.2007.01151.x.
- Johnson, W. and Jameson, J. L.(1999) 'AP-2 (Activating Protein 2) and Sp1 (Selective Promoter Factor 1) Regulatory Elements Play Distinct Roles in the Control of Basal Activity and Cyclic Adenosine 3',5'-Monophosphate Responsiveness of the Human Chorionic Gonadotropin- $\beta$  Promoter', *Molecular Endocrinology*, 13(11), pp. 1963–1975, doi:10.1210/mend.13.11.0386.
- Joliffe, I., and Morgan, B. (1992). Principal component analysis and exploratory factor analysis. *Statistical Methods in Medical Research*, 1(1), pp. 69-95, doi:10.1177/096228029200100105.
- Jones, P.A.(2012) 'Functions of DNA methylation: islands, start sites, gene bodies and beyond', *Nature Reviews Genetics*, 29(17), pp.484-492 doi:10.1038/nrg3230.
- Junker, J.P. and Oudenaarden, A. (2014) 'Every Cell Is Special: Genome-wide Studies Add a New Dimension to Single-Cell Biology', *Cell*, 157(1), pp8-11, doi:10.1016/j.cell.2014.02.010
- Kawamata, F., Nishihara, H., Homma, S., Kato, Y. Tsuda, M., Konishi, Y., Wang, L., Kohsaka, S., Liu, C., Yoshida, T., Tanino, M., Tanaka, S., Kawamura, H., Kamiyama, T. and Taketomi, A., (2018) 'Chorionic Gonadotropin- $\beta$  Modulates Epithelial-Mesenchymal Transition in Colorectal Carcinoma Metastasis', *The American Journal of Pathology*, 188(1), pp. 204-215, doi:10.1016/j.ajpath.2017.08.034.
- Keay, S.D., Vatish, M., Karteris, E., Hillhouse, E.W. and Randeva, H.S. (2004) 'REVIEW: The role of hCG in reproductive medicine', *British Journal of Obstetrics & Gynaecology*, 111(11), pp. 1218-1228, doi:10.1111/j.1471-0528.2004.00412.x.
- Kerschgens, J., Renaud, S., Schütz, F., Grasso, L., Egener-Kuhn, T., Delaloye, J.F., Lehr, H.A., Vogel, H. and Mermod, N. (2011) 'Protein-Binding Microarray Analysis of Tumor Suppressor AP2 $\alpha$  Target Gene Specificity', *Plos One*, 6(8), e22895. doi: 10.1371/journal.pone.0022895.
- Koh, K.P., Yabuuchi, A., Rao, S., Huang, Y., Cunniff, K., Nardone, J., Laiho, A., Tahiliani, M., Sommer, C.A., Mostoslavsky, G., Lahesmaa, R., Orkin, S.H., Rodig, S.J., Daley, G.Q. and Rao, A. (2011) 'Tet1 and Tet2 Regulate 5-Hydroxymethylcytosine Production and Cell Lineage Specification in



- Mouse Embryonic Stem Cells', *Cell Stem Cell*, 8(2), pp. 200-213, doi:10.1016/j.stem.2011.01.008.
- Koistinen, H., Hautala, L., Koli, K. and Stenman, U.H.(2015) 'Absence of TGF- $\beta$  Receptor Activation by Highly Purified hCG Preparations', *Molecular Endocrinology*, 29(12), pp. 1787-91, doi:10.1210/me.2015-1187.
- Krueger, F. and Andrews, S.R.,(2011) 'Bismark: a flexible aligner and methylation caller for Bisulfite-Seq applications', *Bioinformatics*, 27(11) pp.1571-1572, doi:10.1093/bioinformatics/btr167.
- Kubiczak, M., Walkowiak, G. P., Nowak-Markwitz, E. and Jankowska, A. (2013) 'Human Chorionic Gonadotropin Beta Subunit Genes *CGB1* and *CGB2* are Transcriptionally Active in Ovarian Cancer', *International Journal of Molecular Sciences*, 14(6), pp. 12650-12660, doi10.3390/ijms140612650
- Li, E. (2002) 'Chromatin modification and epigenetic reprogramming in mammalian development', *Nature Reviews Genetics*, 3, pp. 662–673, doi:10.1038/nrg887.
- Li, J., Yin, M., Song, W., Cui, F., Wang, W., Wang, S. and Zhu, H. (2018) 'B Subunit of Human Chorionic Gonadotropin Promotes Tumor Invasion and Predicts Poor Prognosis of Early-Stage Colorectal Cancer', *Cell Physiol Biochem*, 45, pp. 237-249, doi: 10.1159/000486770.
- Li, L.C. and Dahiya R. (2002) 'MethPrimer: designing primers for methylation PCRs', *Bioinformatics*, 18(11), pp.1427-1431, doi:10.1093/bioinformatics/18.11.1427
- Li, Y. and Tollefsbol, T.O. (2011) 'DNA methylation detection: bisulfite genomic sequencing analysis', *Methods in Molecular Biology*, 791, pp11-21, doi:10.1007/978-1-61779-316-5\_2.
- Liu, L. and Roberts, R.M. (1996) 'Silencing of the gene for the  $\beta$  subunit of human chorionic gonadotropin by the embryonic transcription factor Oct3/4'. *The Journal of Biological Chemistry*, 271(28), pp. 16683–16689, Available at: <http://www.jbc.org/content/271/28/16683.full.pdf> (Accessed: 16 December 2019).
- Livak, K.J. and Schmittgen, T.D.(2001) 'Analysis of relative gene expression data using real-time quantitative PCR and the 2(-Delta Delta C(T)) Method', *Methods*, 25(4), pp. 402-408, doi:10.1006/meth.2001.1262
- Luthra, R., Patel, K.P., Reddy, N.G., Haghshenas, V., Routbort, M.J., Harmon, M.A., Barkoh, B.A., Kanagal-Shamanna, R., Ravandi, F., Cortes, J.E., Kantarjian, H.M., Medeiros, L.J. and Singh, R.R (2014) 'Next-generation sequencing-based multigene mutational screening for acute myeloid leukemia using MiSeq: applicability for diagnostics and disease monitoring', *Haematologica*, 99(3), pp. 465-473, doi:10.3324/haematol.2013.093765.
- Madeira, F., Park, Y.M., Lee, J., Buso, N., Gur, T., Madhusoodanan, N., Basutkar, P., Tivey, A.R.N., Potter, S.C., Finn, R.D. and Lopez, R.I.(2019) 'The EMBL-EBI search and sequence analysis tools APIs in 2019', *Nucleic Acids Research*, 47(W1), pp. W636-W641, doi:10.1093/nar/gkz268.
- Masser, D.R., Berg, A.S. and Freeman, W.M. (2013) 'Focused, high accuracy 5-methylcytosine quantitation with base resolution by benchtop next-

generation sequencing', *Epigenetics Chromatin*, 6(1), doi:10.1186/1756-8935-6-33.

- McCabe, M. T., Brandes, J. C., and Vertino, P. M. (2009) 'Cancer DNA methylation: molecular mechanisms and clinical implications', *Clinical cancer research : an official journal of the American Association for Cancer Research*, 15(12), pp. 3927–3937, doi:10.1158/1078-0432.CCR-08-2784.
- Mikeska, T., Felsberg, J., Hewitt, C., and Dobrovic, A. (2011) *Analysing DNA Methylation Using Bisulphite Pyrosequencing*. In T. Tollefsbol (Ed.), *Epigenetics protocols* (pp. 33-53). Humana Press. doi:10.1007/978-1-61779-316-5\_4.
- Parrott, A. M., Sriram, G., Liu, Y., and Mathews, M. B. (2011) 'Expression of Type II Chorionic Gonadotropin Genes Supports a Role in the Male Reproductive System', *Molecular and Cellular Biology*, 31(2), pp. 287-299. doi:10.1128/MCB.00603-10.
- Pestell, R.G., Hollenberg, A.N., Albanese, C. and Jameson, J.L.(1994) 'c-Jun represses transcription of the human chorionic gonadotropin  $\alpha$  and  $\beta$  genes through distinct types of CREs', *The Journal of Biological Chemistry*, 269(49), pp. 31090–31096, Available at: <http://www.jbc.org/content/269/49/31090.full.pdf> (Accessed: 16 December 2019).
- Poleć, A., Fedorcsák, P., Eskild, A. and Tanbo, T.G.(2014) 'The interplay of human chorionic gonadotropin (hCG) with basic fibroblast growth factor and adipokines on angiogenesis *in vitro*', *Placenta*, 35(4), pp. 249-253, doi:10.1016/j.placenta.2014.02.002.
- Portela, A. and Esteller, M.(2010) 'Epigenetic modifications and human disease', *Nature Biotechnology*, 28, pp. 1057–1068, doi:10.1038/nbt.1685.
- Qui, C., Zhi, Y., Shen, Y., Gong, J., Li, Y., and Li, X. (2015) 'High-Resolution melting analysis of HPV-16 L1 gene methylation: a promising method for prognosing cervical cancer', *Clinical Biochemistry*, 48(13-14), pp. 855-859 doi:10.1016/j.clinbiochem.2015.05.006.
- Rao, C.V. (2016) 'There is no turning back on the paradigm shift on the actions of hCG and LH', *Journal of Reproductive Health and Medicine*, 2(1), pp.4-10 doi:10.1016/j.jrh.2015.07.001.
- Reed, K., Poulin, M., Yan, L., and Parrisenti, A. (2009) 'Comparison of bisulfite sequencing PCR with pyrosequencing for measuring differences in DNA methylation', *Analytical Biochemistry*, 397(1) pp.96-106, doi:10.1016/j.ab.2009.10.021.
- Robbins, J. R., Zeldovich, V. B., Poukchanski, A., Boothroyd, J. C., and Bakardjiev, A. I. (2012) 'Tissue barriers of the human placenta to infection with *Toxoplasma gondii*', *Infection and immunity*, 80(1), pp. 418–428, doi:10.1128/IAI.05899-11.
- Robertson, K. D. (2005) 'DNA methylation and human disease', *Nature Reviews Genetics*, 6, pp. 597-610, doi:10.1038/nrg1655.
- Roeh, S., Wiechmann, T., Sauer, S., Ködel, M., Binder, E.B. and Provençal, N.(2018) 'HAM-TBS: high-accuracy methylation measurements via

targeted bisulfite sequencing', *Epigenetics Chromatin*, 11(1)  
doi:10.1186/s13072-018-0209-x.

- Rull, K. and Laan, M. (2005) 'Expression of  $\beta$ -subunit of HCG genes during normal and failed pregnancy', *Human Reproduction*, 20(12), pp.3360-3368, doi:10.1093/humrep/dei261
- Rull, K., Hallast, P., Uuskula, L., Jackson, J., Punab, M., Salumets, A., Campbell, R.K. and Laan, M. (2008) 'Fine-scale quantification of HCG beta gene transcription in human trophoblastic and non-malignant non-trophoblastic tissues', *Molecular Human Reproduction*, 14(1), pp. 23-31, doi:10.1093/molehr/gam082.
- Schüler-Toprak, S., Treeck, O. and Ortmann, O. (2017) 'Human Chorionic Gonadotropin and Breast Cancer', *International Journal of Molecular Sciences.*, 18(7), doi:10.3390/ijms18071587
- Schumacher, A., Brachwitz, N., Sohr, S., Engeland, K., Langwisch, S., Dolaptchieva, M., Alexander, T., Taran, A., Malfertheiner, S.F., Costa, S., Zimmermann, G., Nitschke, C., Volk, H., Alexander, H., Gunzer, M. and Zenclussen, A. C. (2009) 'Human Chorionic Gonadotropin Attracts Regulatory T Cells into the Fetal-Maternal Interface during Early Human Pregnancy', *The Journal of Immunology*, 182(9), pp. 5488-5497, doi:10.4049/jimmunol.0803177.
- Serranoa, M.A., Maciasb, R.I.R., Brizb, O., Monteb, M.J., Blazquezb, A.G., Williamsonc, C., Kubitzd, R. and Marinb, J.J.G. (2007) 'Expression in Human Trophoblast and Choriocarcinoma Cell Lines, BeWo, Jeg-3 and JAr of Genes Involved in the Hepatobiliary-like Excretory Function of the Placenta', *Placenta*, 28(2–3), pp. 107-117, doi:10.1016/j.placenta.2006.03.009.
- Singh, H., Makino, S.I., Endo, Y. and Nie, G.(2010) 'Inhibition of HTRA3 stimulates trophoblast invasion during human placental development.', *Placenta*, 31(12), pp. 1085–1092. doi:10.1016/j.placenta.2010.10.003.
- Singh, V., Rana, R. K., and Singhal, R. (2013) 'Analysis of repeated measurement data in the clinical trials', *Journal of Ayurveda and integrative medicine*, 4(2), pp. 77–81, doi:10.4103/0975-9476.113872
- Sinnappan, S. M. (2015) *The role of free beta subunit of human chorionic gonadotropin in high-grade serous cancer*. PhD thesis. The University of Sydney. Available at: <http://hdl.handle.net/2123/14706> (Accessed 10.01.2020)
- Śliwa, A., Kubiczak, M., Szczerba, A., Walkowiak, G., Nowak-Markwitz, E., Burczyńska, B., Butler, S., Iles, R., Białas, P. and Jankowska, A. (2019) 'Regulation of human chorionic gonadotropin beta subunit expression in ovarian cancer', *BMC cancer*, 19(1), doi:10.1186/s12885-019-5960-2.
- Sohr, S., and Engeland, K. (2011) 'The tumor suppressor p53 induces expression of the pregnancy-supporting human chorionic gonadotropin (hCG) *CGB7* gene', *Cell cycle*, 10(21), pp. 3758–3767, doi:10.4161/cc.10.21.17946
- Soto, J.,Rodriguez-Antolin, C., Vallespín, E., Carpeño, J.C. and Caceres, I.I. (2016) 'The impact of next-generation sequencing on the DNA

- methylation–based translational cancer research’, *Translational Research*, 169, pp. 1-18.e1, doi:10.1016/j.trsl.2015.11.003.
- Stenman, U. H., Tiitinen, A., Alfthan, H. and Valmu, L. (2006) ‘The classification, functions and clinical use of different isoforms of HCG’, *Human Reproduction Update*, 12(6) , pp. 769–784, doi:10.1093/humupd/dml029
- Stenman, U.H., Alfthan, H., and Hotakanien, K. (2004) ‘Human chorionic gonadotropin in cancer’, *Clinical Biochemistry*, 37(7), pp. 549-561, doi:101016/j.clinbiochem.2004.05.008.
- Straussman, R., Nejman, D., Roberts, D., Steinfeld, I., Blum, B., Benvenisty, N., Simon, I., Yakhini, Z., and Cedar, H.(2009) ‘Developmental programming of CpG island methylation profiles in the human genome’. *Nature Structural & Molecular Biology*, 16, pp. 564–571, doi:10.1038/nsmb.1594.
- Szczerba, A., Śliwa, A., Kubiczak, M., Nowak-Markwitz, E., and Jankowska, A. (2016) ‘Human chorionic gonadotropin  $\beta$  subunit affects the expression of apoptosis-regulating factors in ovarian cancer’, *Oncology Reports*, 35, pp. 538-545. doi:10.3892/or.2015.4386
- Tammen, S., Frisco, S., and Choi, S. (2012) ‘Epigenetics: The link Between Nature and Nurture’, *Molecular Aspects of Medicine*, 34(4), pp.753-764, doi:10.1016/j.mam.2012.07.018.
- Thomson, J., Skene, P., Selfridge, J., Clouaire, T., Guy, J., Webb, S., Kerr, A.R., Deaton, A., Andrews, R., James, K.D., Turner, D.J., Illingworth, R. and Bird, A.(2010) ‘CpG islands influence chromatin structure via the CpG-binding protein Cfp1’, *Nature*, 464, pp. 1082–1086, doi:10.1038/nature08924.
- Tsampalás, M., Grídelet, V., Berndt, S., Foidart, J.M., Geenen, V. and d’Hauterive, S.P. (2010) ‘Human chorionic gonadotropin: A hormone with immunological and angiogenic properties’, *Journal of Reproductive Immunology*, 85(1), pp. 93-98, doi:10.1016/j.jri.2009.11.008.
- Tuncay, S., Senol, H., Guler, E.M., Ocal, N., Secen, H., Kocyigit, A. and Topcu, G., (2018) ‘Synthesis of Oleanolic Acid Analogues and Their Cytotoxic Effects on 3T3 Cell Line’, *Medicinal Chemistry*, 14(6), pp. 617-625(9), doi:10.2174/1573406414666180222094544.
- Uuskula, L., Rull, K., Nagirnaja, L., and Laan, M. (2010) ‘Methylation Allelic Polymorphism (MAP) in Chorionic Gonadotropin beta5 (CGB5) and Its Association with Pregarancy Success’, *Clinical Endocrinology Metabolism*, 96(1), pp. e199-e207, doi:10.1210/jc.2010-1647.
- Varela-Rey, M., Iruarrizaga-Lejarreta, M., Lozano, J. J., Aransay, A. M., Fernandez, A. F., Lavin, J. L., Mosen-Ansorena, D., Berdasco, M., Turmaine, M., Luka, Z., Wagner, C., Lu, S.C., Esteller, M., Mirsky, R., Jessen, K.R., Fraga, M.F., Martínez-Chantar, M.L., Mato, J.M. and Woodhoo, A. (2014) ‘S-adenosylmethionine levels regulate the Schwann cell DNA methylome’, *Neuron*, 81(5), pp. 1024–1039, doi:10.1016/j.neuron.2014.01.037.
- Ward, D. G., Baxter, L., Gordon, N.S., Ott, S., Savage, R.S., Beggs, A.D., James, J.D., Lickiss, J., Green, S., Wallis, Y., Wei, W., James, N.D., Zeegers, M.P., Cheng, K.K., Mathews, G.M., Patel, P., Griffiths, M. and Bryan, R.T

- (2016) 'Multiplex PCR and Next Generation Sequencing for the Non-Invasive Detection of Bladder Cancer', *PLoS One*, 11(2), pp. e0149756, doi:10.1371/journal.pone.0149756.
- Warden, C.D., Lee, H., Tompkins, J.D., Li, X., Wang, C., Riggs, A.D., Yu, H., Jove, R. and Yuan, Y.C.(2013) 'COHCAP: an integrative genomic pipeline for single-nucleotide resolution DNA methylation analysis', *Nucleic Acids Research*, 41(11), pp. e117 doi:10.1093/nar/gkt242
- Warnecke, P. M., Stirzaker, C., Song, J., Grunau, C., Melki, J.R. and Clark, S.J. (2002) 'Identification and resolution of artifacts in bisulfite sequencing', *Methods*, 27(2), pp. 101-107, doi:10.1016/S1046-2023(02)00060-9
- Weber, M., Hellmann, I., Stadler, M., Ramos, L., Pääbo, S., Rebhan, M. and Schübeler, D. (2007) 'Distribution, silencing potential and evolutionary impact of promoter DNA methylation in the human genome', *Nat Genet*, 39, pp.457–466, doi:10.1038/ng1990.
- Weinhold, L., Wahl, S., Pechlivanis, S., Hoffmann, P. and Schmid, M. (2016) 'A statistical model for the analysis of beta values in DNA methylation studies', *BMC Bioinformatics*, 17, doi:10.1186/s12859-016-1347-4.
- Wen, Y., Wei, Y., Zhang, S., Li, S., Liu, H., Wang, F., Zhao, Y., Zhang, D. and Zhang, Y. (2017) 'Cell subpopulation deconvolution reveals breast cancer heterogeneity based on DNA methylation signature', *Briefings in Bioinformatics*, 18(3), pp 426–440, <https://doi.org/10.1093/bib/bbw028>
- Whitfield, G. K. and Kourides, I.A. (1985) 'Expression of Chorionic Gonadotropin  $\alpha$ - and  $\beta$ -Genes in Normal and Neoplastic Human Tissues: Relationship to Deoxyribonucleic Acid Structure', *Endocrinology*, 117(1), pp. 231–236, doi:10.1210/endo-117-1-231
- Wojdacz, T. K., and Dobrovic, A. (2007) 'Methylation-sensitive high-resolution melting (MS-HRM): a new approach for sensitive and high-throughput assessment of methylation', *Nucleic Acid Research*, 6, pp. e41, doi:10.1093/nar/gkm013.
- Wojdacz, T. K., Borgbo, T., and Hansen, L. L. (2009) 'Primer design versus PCR bias in methylation independent PCR amplifications', *Epigenetics*, 4(4), pp. 231-234, doi:10.4161/epi.9020.
- Wolfe, M.W. (2006) *Culture and Transfection of Human Choriocarcinoma Cells*. In: Soares M.J., Hunt J.S. (eds) *Placenta and Trophoblast. Methods in Molecular Medicine™*, vol 121. Humana Press doi:10.1385/1-59259-983-4:227
- Wreczycka, K., Godschan, A., Yusuf, D., Grüning, B., Assenov, Y. and Akalin, A. (2017) 'Strategies for analyzing bisulfite sequencing data', *Journal of Biotechnology*, 261, pp. 105-115, doi:10.1016/j.jbiotec.2017.08.007.
- Wu, W., Gao, H., Li, X., Peng, S., Yu, J., Liu, N., Zhan, G., Zhu, Y., Wang, K., and Guo, X. (2019)  $\beta$ -hCG promotes epithelial ovarian cancer metastasis through ERK/MMP2 signalling pathway, *Cell Cycle*, 18(1), pp. 46-59, doi:10.1080/15384101.2018.1558869.
- Xiao, Z., Li, B., Wang, G., Zhu, W., Wang, Z., Lin, J., Xu, A. and Wang, X. (2014) 'Validation of methylation-sensitive high-resolution melting (MS-HRM) for

the detection of stool DNA methylation in colorectal neoplasms', *Clinica Chimica Acta*, 431, pp. 154-163, doi:10.1016/j.caa.2014.01.044.

Xiong, T., Meister, G.E., Workman, R.E., Kato, N.C, Spellberg, M.J., Turker, F., Timp, W., Ostermeier, M. and Novina, C.D (2017) 'Targeted DNA methylation in human cells using engineered dCas9-methyltransferases', *Scientific Reports*, 7, doi:10.1038/s41598-017-06757-0.

Zhong, Y., Wang, Y., Huang, J., Xu, X., Pan, W., Gao, S., Zhang, Y. and Su, M. (2019) 'Association of hCG and LHCGR expression patterns with clinicopathological parameters in ovarian cancer', *Pathology - Research and Practice*, 215(4) , pp. 748-754, doi:10.1016/j.prp.2019.01.001.

Zimmermann, G., Ackermann, W. and Alexander, H. (2012) 'Expression and Production of Human Chorionic Gonadotropin (hCG) in the Normal Secretory Endometrium: Evidence of CGB7 and/or CGB6 Beta hCG Subunit Gene Expression', *Biology of Reproduction*, 86(3), pp. 1-14, doi:10.1095/biolreprod.111.092429

# Appendix

## A1. DNA and RNA samples

**Table A1.** DNA samples with Quantity and Quality values from Nanodrop and Qbit

Cell Line	Tissue of origin	Qbit	Nanodrop						
		Conc.	Concentration		a260	a280	260/280	260/230	
MDA-MB-468	breast cancer	110 ng/μl	89.65	ng/μl	1.793	0.9515	1.885	2.49	
MCF-7	breast cancer	804 ng/μl	200.9	ng/μl	4.019	2.152	1.87	2.23	
Breast-DNA	Normal breast	N/A							
HeLA	cervical cancer	93.6ng/μl	110.8	ng/μl	2.2155	1.1705	1.89	2.23	
HT-3	cervical cancer	95.6ng/μl	170.55	ng/μl	3.411	1.797	1.9	2.39	
C-33a	cervical cancer	82.2ng/μl	55.25	ng/μl	1.105	0.59	1.875	2.215	
Cervix-DNA	Normal cervix	N/A							
BeWo	choriocarcinoma	93.2ng/μl	265.35	ng/μl	5.308	2.755	1.93	2.04	
JEG-3	choriocarcinoma	106ng/μl	172.85	ng/μl	3.457	1.823	1.895	2.315	
HCT116	colon cancer	94.4ng/μl	241.6	ng/μl	4.832	2.5345	1.905	2.445	
CRL-1790	colon normal	104 ng/μl	29.3	ng/μl	0.586	0.313	1.86	4.61	
3T3	mousefibroblast	104 ng/μl	115.6	ng/μl	2.3115	1.1955	1.935	2.3	
OAW42	ovarian cancer	76 ng/μl	59.75	ng/μl	1.1955	0.635	1.88	2.695	
OVCAR-3	ovarian cancer	95.4ng/μl	124.1	ng/μl	2.4815	1.309	1.895	2.62	
HEY	ovarian cancer	96.8ng/μl	94.55	ng/μl	1.8905	0.987	1.915	2.575	
SKOV-3	ovarian cancer	288 ng/μl	212.3	ng/μl	4.246	2.235	1.9	2.525	

**Table A2.** RNA samples with Quantity and Quality values from Nanodrop and Qbit

Cell Line	Tissue of origin	Qbit	Nanodrop					
		Conc.	Concentration		a260	a280	260/280	260/230
3T3	mouse fibroblast	166 ng/μl	348.8	ng/μl	8.72	4.049	2.15	0.98
BeWo	choriocarcinoma	400 ng/μl	622.7	ng/μl	15.569	7.301	2.13	2.12
C-33a	cervical cancer	348 ng/μl	400.7	ng/μl	10.017	4.728	2.12	1.86
CRL-1790	colon normal	190 ng/μl	155.55	ng/μl	3.89	1.84	2.12	1.55
HCT116	colon cancer	573 ng/μl	864.3	ng/μl	21.607	10.179	2.12	1.9
HeLA	cervical cancer	300 ng/μl	419.6	ng/μl	10.491	4.916	2.13	1.16
HEY	ovarian cancer	808 ng/μl	781.7	ng/μl	19.543	9.21	2.12	2.07
HT-3	cervical cancer	578 ng/μl	584.6	ng/μl	14.616	6.821	2.14	1.5
JEG-3	choriocarcinoma	799 ng/μl	832.9	ng/μl	20.822	9.776	2.13	2.16
MCF-7	breast cancer	126 ng/μl	258	ng/μl	6.451	3.002	2.15	1.17
MDA-MB-468	breast cancer	1100ng/μl	993.5	ng/μl	24.839	11.682	2.13	1.86
OAW42	ovarian cancer	178 ng/μl	274.2	ng/μl	6.856	3.223	2.13	1.7
OVCAR-3	ovarian cancer	356 ng/μl	554.8	ng/μl	13.869	6.447	2.15	1.74
SKOV-3	ovarian cancer	132 ng/μl	164.6	ng/μl	4.115	1.939	2.12	1.43



## A2. *In silico* analyses

### A2.1 MSA with promoter elements

Below is the Multiple Sequence Alignment of the *CGB* genes. The sequences used are the 1 exon and 1000bp upstream for the *CGB1-9* genes and the *LHB* genes

		TSSs.
<i>CGB1</i> (1, 369)	-----	0
<i>CGB2</i> (1, 359)	-----	0
<i>CGB</i> (1, 377)	-----ACTCTCTGAATTTGAGCTCAATCTCTGCAGGATGGGTGCCACCACA	46
<i>CGB5</i> (1, 341)	-----AGGATGGGTGCCACCACA	18
<i>CGB8</i> (1, 382)	ATCACAAAATCACAACTCTCTGAATTTGAGCTCAGTCTCTGCAGGATGGGTGCCACCACG	60
<i>CGB7</i> (1, 419)	--TCCAGGACGTTAAGTACCTCGA-----GGACCCAGGAAACGCAGGCAAACGCG	46
<i>LHB</i>	-----	0
<i>CGB1</i> (1, 369)	-----	0
<i>CGB2</i> (1, 359)	-----	0
<i>CGB</i> (1, 377)	TGTGGTTTTGAAGGTTGAATAGGAGCTCTCCAGGGGAACCTGAGGGTAATCATGATGAT	106
<i>CGB5</i> (1, 341)	TGGGGTTTTGAAGGTTGAATAGGAGTTCTCCTGGGGGAACCTGAGGATAATCATGATG--	76
<i>CGB8</i> (1, 382)	TGGGGTTTTGAAGGTTGAATAGGAGTTCTCCAGGGGAAATGAGAGTAATCATGATG--	118
<i>CGB7</i> (1, 419)	TGCCCGGTGCGCTCCTTCTAAGGGGTGCTCGCCTGGAAATGCAGGAGTTTGAATGTGCA	106
<i>LHB</i>	-----	0
<i>CGB1</i> (1, 369)	-----	0
<i>CGB2</i> (1, 359)	-----	0
<i>CGB</i> (1, 377)	GATG--ATGATGA---TGATAATAATAATAG-----CCACTATTTACTGAGTGT	150
<i>CGB5</i> (1, 341)	-----ATGA---TGATAATAATAATAG-----GCACTATTTACTGAGTGT	113
<i>CGB8</i> (1, 382)	-----ATGA---TGATGATAATAATAG-----CCACTATTTACTGAGTGT	155
<i>CGB7</i> (1, 419)	GACTCCTTAGATCCCGAGGTCTGAAACTCGTCCCAAGGATCCAGCTGTATCCTCACCAT	166
<i>LHB</i>	-----	0
<i>CGB1</i> (1, 369)	-----	0
<i>CGB2</i> (1, 359)	-----	0
<i>CGB</i> (1, 377)	TTACTCTTTCTAGCCCTAATACATAACTCCTCGGATCAACTCTCATGGATTGATCAT-	209
<i>CGB5</i> (1, 341)	TTACTCTTTCTAGCCCTAATACATAACTCCTCGGATCAACTCTCATGGATTGATCAT-	172
<i>CGB8</i> (1, 382)	TTACTCTTTCTAGCCCTAATACATAACTCCTCAGATCAACTCTCATGGATTGATCAT-	214
<i>CGB7</i> (1, 419)	CCCGCCTGCTCC--CACAGGACCGGAGCCTCGGATACCCCGCAAGGACTACCTGACC	224
<i>LHB</i>	-----	0
<i>CGB1</i> (1, 369)	-----	0
<i>CGB2</i> (1, 359)	-----	0
<i>CGB</i> (1, 377)	TGGTGACCTTTGGTGTAAAGTTGCTGACTGCTCAGTCAC-----AGAGGACACCAC--	260
<i>CGB5</i> (1, 341)	TGGTGACCTTTGGTGTAAAGTTGCTGACTGCTCAGTCAC-----AGAGGACACCAC--	223
<i>CGB8</i> (1, 382)	TGGTGACCTTTGGTGTAAAGTTGCTGACTGCTCAGTCAC-----AGAGGACACCAC--	265
<i>CGB7</i> (1, 419)	TACTGGAGCTTAGAAGAGAAGCCCCAAGTCTGGAGTCAACGACCGCAGCGGAGCCCTGT	284
<i>LHB</i>	-----	0
<i>CGB1</i> (1, 369)	-----	0
<i>CGB2</i> (1, 359)	-----	0
<i>CGB</i> (1, 377)	-CTTGCTCATCCTGGGGAGTGGGAGG---GCACATTTCAAGATGTGCATGGGGGAGGAGG	316
<i>CGB5</i> (1, 341)	-CTTGCTCATCCTGGGGAGTGGGAGG---GCACATTTCAAGATGTGCATGGGGGAGGAGG	279
<i>CGB8</i> (1, 382)	-CTTGCTCATCCTGGGGAGTGGGAGG---GCACATTTCAAGATGTGCATGGGGGAGGAGG	321
<i>CGB7</i> (1, 419)	CTTGCTCTTCCAGGCCTCGAGCGCCGACCGCGGGCCATGTCTCCCGGCTCAGGAAA	344
<i>LHB</i>	-----	0
<i>CGB1</i> (1, 369)	-----	0
<i>CGB2</i> (1, 359)	-----	0
<i>CGB</i> (1, 377)	GAAACTGGAACATGCAAGCAGATGGCCAGGGGACCTTGAGGACAT--GGTCTACAGAAGGC	375
<i>CGB5</i> (1, 341)	GAAACTGGAACATGCAAGCAGATGGCCAGGGGACCTTGAGGACAT--GGTCTACAGAAGGC	338
<i>CGB8</i> (1, 382)	GAAACTGGAACATGCAAGCAGATGGCCAGGGGACCTTGAGGACAT--GGTCTACAGAAGGC	380
<i>CGB7</i> (1, 419)	CCTACAGCTCCTCGCC--GCACCCCGCTCCCGCC--GGCTCGACCGCTTCCCGCCCGCTGGAGGC	402
<i>LHB</i>	-----GAGGC	5
<i>CGB1</i> (1, 369)	-----	0
<i>CGB2</i> (1, 359)	-----	0
<i>CGB</i> (1, 377)	CTTTAAGTATCTGGGAGCTGGGGTTCAAATGAGAAATCTTACTTGGTGAGAGCAGGCAGG	435
<i>CGB5</i> (1, 341)	CTTTCAGTATCTGGGAGCTGGGGTTCAAATGAGAAATCTTACTTGGTGAGAGTGGGCAGG	398
<i>CGB8</i> (1, 382)	CTTTAAGTATCTGGGAGCTGGGGTTCAAATGAGAAATCTTACTTGGTGAGAGCAGGCAGG	440
<i>CGB7</i> (1, 419)	GAC-----TTGGGGTGGC--CCCACTGGAAGCCCTGCAGGGCATAACACAGCGTCC	452
<i>LHB</i>	GCC-----CTGGGGCGGC--CGCACTGGAAGCCCTGCAGGGCATAACACAGCGTCC	55

CGB1 (1, 369)	-----AAAGAGCTACCGATCACACGGG	22
CGB2 (1, 359)	-----TTGTTTTGAGATAAAGAGCTACCGATCACACGGG	34
CGB (1, 377)	GGTTGGCTTAGAATATTTCTGTTTTG-----AGATAAAGAGCTACCGATCACACGGG	486
CGB5 (1, 341)	GGT <b>CGGC</b> TTAGAAATATTTGTTTTG-----AGATAATGAGCTACCGATCACAGGGG	449
CGB8 (1, 382)	GGTTGGCTTAGAATATTTCTGTTTTG-----AGATAATGAGCTACCGATCACAGGGG	491
CGB7 (1, 419)	<b>CGAAAGCCTACAGCACCGAGA</b> ACTCC <b>CGCT</b> CAGGC <b>CGCT</b> GTAAGC <b>CGGGGCTAGTGGGAG</b>	512
LHB	<b>CGAAAGCCTACAGTACCGAGA</b> ACTCCAGCTATGGCAGCTTGAAGC <b>CGCGCTGGTGTGAG</b> *** ** *	115
CGB1 (1, 369)	GAGTATAAGCAAGGTTCAATG-----AGAAGTGATCAGGATGCTGGAGAGTTCAGCCCT	76
CGB2 (1, 359)	GAGTATAAGCAAGGTTCAATG-----AGAAGTGATCAGGATGCTGGAGAGTTCAGCCCT	88
CGB (1, 377)	GAGTATAAGCAAGGTTCAATG-----AGAAGTGATCAGGATGCTGGAGAGTTCAGCCCT	540
CGB5 (1, 341)	GAGTTTAAAGCAAGGTTCAATG-----AGAAG <b>CGAT</b> CAAGATGCTGCACAGTTCAGCCCT	503
CGB8 (1, 382)	GAGTATAAGCAAGGTTCAATG-----AGAAG <b>CGAT</b> CAAGATGCTGCACAGTTCAGCCCT	545
CGB7 (1, 419)	CCTGC <b>CGGCCAGCCCCACCC</b> CAGAC <b>CGCCCCCTGGCTGGG</b> -GG <b>CGGAGCAGAGCTCT</b>	571
LHB	<b>CGCTCAGGGCCAGCCCCACCC</b> CAGACC <b>CGCCCCAGGGCCCGCGCTGC</b> <b>CGAGCGGAGCTCG</b> ** ** * * ** * * ** * * ** * * ** * *	175
CGB1 (1, 369)	GGG <b>CGG</b> -----GGAGCTCAAGTCAGGTTTCTAGCCCTCTCCCTGTGC--CATCCTAT	127
CGB2 (1, 359)	GGG <b>CGG</b> -----GGAGCTCAAGTCAGGTTTCTAGCCCTCTCCCTGTGC--CAACCTAT	139
CGB (1, 377)	GGG <b>CGG</b> -----GGAGCTCAAGTCAGGTTTCTAGCCCTCTCCCTGTGC--CAACCTAT	591
CGB5 (1, 341)	GGGTGG-----GGAGCTCAAGTCAGGTTTCTAGCCCTCTCCCTGTGC--CAACCTAT	554
CGB8 (1, 382)	GGGTGG-----GGAG <b>CGCAAGTCAGGTTTCTAGCCCTCTTTCTGTGC--CAACCTAT</b>	596
CGB7 (1, 419)	GGGCAGC <b>CGCTCACTAC--GCGGTGT</b> <b>CGGACCTAGGTGGGCTCGCACTCATTAA</b> GTCTAT	629
LHB	GGACCT <b>CGCTCACTAGGAAGGGTT</b> <b>CGGACCCAGCCTGAGT</b> <b>CGCACTCATTAC</b> GTCTAT ** *	235
CGB1 (1, 369)	ACCCTACATTGGGAAGA--AACAGACCTTAAAATTTGTCAGCTTGATGGCAT <b>CGCGGG</b>	184
CGB2 (1, 359)	ACCCTACACTGGGAAGA--AACAGACCTTAAAATTTGTCAGCTTGATGGCAT <b>CGCGGG</b>	196
CGB (1, 377)	ACCCTACATTGGGAAGA--AACAGACCTTAAAATTTGTCAGCTTGATGGCAT <b>CGCGGG</b>	648
CGB5 (1, 341)	ACCCTACATTGGGAAGA--AACAGACCTTAAAATTTGTCAGCTTGATGGCAT <b>CGCGGG</b>	611
CGB8 (1, 382)	ACCCTACATTGGGAAGA--AACAGACCTTAAAATTTGTCAGCTTGATGGCAT <b>CGCGGG</b>	653
CGB7 (1, 419)	<b>CGCAGTGTGGGACAGGACTAGCC</b> CAGAC <b>CGCCCACTCAGCTGGCGCTGGATCGCGGG</b>	689
LHB	TGGCA <b>CGTGGGGCGGGACTAGCC</b> CAGACCCA-----CTCAGCT <b>CGGCATCA</b> CGGA *	290
CGB1 (1, 369)	GAAGGGACTAAGTCCAGATAATGTCTCT <b>CGAGGCTGCGGCCTCGGGG</b> CAGGACACCT	244
CGB2 (1, 359)	GAAGGGACTAAGTCCAGATAATGTCTCT <b>CGAGGCTGAGGCCTCGGGG</b> CAGGACACACCT	256
CGB (1, 377)	GAAGGGACTAAGTCCAGATAATGTCTCT <b>CGAGGCTTcgccccatggc</b> <b>AGGACACACT</b>	708
CGB5 (1, 341)	GAAGGGACTAAGTCCAGATAATGTCTCT <b>CGAGGCTCGGCCC</b> CGTGGGCAGGACACACCT	671
CGB8 (1, 382)	GAAGGGACTAAGTCCAGATAATGTCTCT <b>CGAGGCTCGGCCC</b> CGTGGGCAGGACATACCT	713
CGB7 (1, 419)	GAAGGGACTAAGTCCAGACAAATGTCTCT <b>CGAGGCTGCGGCCC</b> <b>CGGGGCAGGACACACCT</b>	749
LHB	GAGGGACTAAGTCCAGATAATGTCTCTTGAGGCTGTGGCCC <b>CGGGGGCAAGACACGCAC</b> *	350
CGB1 (1, 369)	CTT <b>CGGGCCTATTCAATAATCAGTTAAATCACCGAAGCACACGCATTTC</b> <b>CGGGGACCG</b>	304
CGB2 (1, 359)	CTT <b>CGGGCCTATTCAATAATCAGTTAAATCACCGAAGCACACGCATTTC</b> <b>CGGGGACCG</b>	316
CGB (1, 377)	<b>cttggggcctattcaataatcagttaaatcacctgaagcacacgcatttccggggacag</b>	768
CGB5 (1, 341)	CCT <b>CGGGCCTATTCAATAATCAGTTAAATCACCGAAGCACACGCATTTC</b> <b>CGGGGACCG</b>	731
CGB8 (1, 382)	CCT <b>CGGGCCTATTCAATAATCAGTTAAATCACCGAAGCACACGCATTTC</b> <b>CGGGGACAG</b>	773
CGB7 (1, 419)	CCT <b>CGGGCCTATTCAATAATCAGTTAAATCACCGAAGCACACGCATTTC</b> <b>CGGGGACCG</b>	809
LHB	CCT <b>CGGGCGTATTAAATAATGAGTTAAATCACCTGAACCACACCCACTTC</b> <b>CGGG-GACG</b> *	409
CGB1 (1, 369)	CTC <b>CGGGCATCCTGGCTTGAGGGTAGAGTGAGGCGAGGTC</b> CCCTAAGGGAGAGGTGGGGCT	364
CGB2 (1, 359)	CTC <b>CGGGCATCCTGGCTTGAGGGTAGAGTGAGGCGAGGTC</b> CCCTAAGGGAGAGGTGGGGCT	376
CGB (1, 377)	<b>CTCCTGGGCATCCTGGCTTGAGGGTAGAGTGAGGCGAGGTC</b> CCCTAAGGGAGAGGTGGGGCT	828
CGB5 (1, 341)	CTC <b>CGGGCATCCTGGCTTGAGGGTAGAGTGAGGCGAGGTC</b> CCCTAAGGGAGAGGTGGGGCT	791
CGB8 (1, 382)	CTC <b>CGGGCATCCTGGCTTGAGGGTAGAGTGAGGCGAGGTC</b> CCCTAAGGGAGAGGTGGGGCT	833
CGB7 (1, 419)	CTC <b>CGGGCATCCTGGCTTGAGGGTAGGGTGGGCGGAGGTC</b> CCCTAAGGGAGAGGTGGGGCT	869
LHB	CTC <b>CGGGCATCCTGGCTTGAGGGTAGGGTGGGCGGAGGTC</b> CCCTAAGGGAGAGGTGGGGCT *	469
CGB1 (1, 369)	<b>CGGGCTGAATCCCTCGTTGGC-GGCACCAGGGTCAAGTGGCTAACCTGGCAGCACAGTCA</b>	423
CGB2 (1, 359)	<b>CGGGCTGAATCCCTCGTTGGC-GGCACCAGGGTCAAGTGGCTAACCTGGCAGCACAGTCA</b>	435
CGB (1, 377)	<b>CGGGCTGAATCCCTCGTTGGC-GGCACCAGGGTCAAGTGGCTAACCTGGCAGCACAGTCA</b>	887
CGB5 (1, 341)	<b>CGGGCTGAATCCCTCGTTGGG-GGCACCAGGGTCAAGTGGCTAACCTGGCAGCACAGTCA</b>	851
CGB8 (1, 382)	<b>CGGGCTGAATCCCTCGTTGGG-GGCACCAGGGTCAAGTGGCTAACCTGGCAGCACAGTCA</b>	892
CGB7 (1, 419)	<b>CGGGCTGAATCCCTCGTTGGGGGCATCTGGGTCAAGTGGCTAACCTGGCAGCACAGTCA</b>	929
LHB	<b>CGGGCTTAATCCCTCCTTG-GGGGCATCTGGGTCAAGTGGCTAACCTGGCAGCACAGTCA</b> *	528
CGB1 (1, 369)	<b>CGGGAGGCCCTCTCTCATTGGGCGAAACTAAGTCCGAAGC</b> <b>CGCGCCCTCTGGGCGA</b>	483
CGB2 (1, 359)	<b>CGGGAGGCCCTCTCTCATTGGGCGAAACTAAGTCCGAAGC</b> <b>CGCGCCCTCTGGGCGA</b>	495
CGB (1, 377)	<b>CGGGAGGCCCTCTCTCATTGGGCGAAACTAAGTCCGAAGC</b> <b>CGCGCCCTCTGGGAGG</b>	947



CGB5 (1, 341)	CGGGGAGGCCCTCTCTCATTTGGGCAGAAGCTAAGTC	CGAAGCCGCGCCCCCTCTGGGAGG	911
CGB8 (1, 382)	CGGGGAGACCCTCTCTCATTTGGGCAGAAGCTAAGTC	CGAAGCCGCGCCCCCTCTGGGAGG	952
CGB7 (1, 419)	CGGGGAGACCCTCTCTCACTGGGCAGAAGCTAAGTC	CGAAGCCGCGCCCCCTCTGTTAGG	989
LHB	CGGGGAGACCCTCTCTCACTGGGCAGAAGCTAAGTC	CGAAGCCGCGCCCCCTCTGTTAGG	588
	*****	*****	*
CGB1 (1, 369)	GGAGGTTCCACCTCCTAGGTTCCCTGTGATTCTCCTGCCTCAGCC	CGAGTAGTGGGACATC	543
CGB2 (1, 359)	GGAGGTTCCACCTCCTAGGTTCCCTGTGATTCTCCTGCCTCAGCC	CGAGTAGTGGGACATC	555
	-----	-----	
	Ets-2	Ets-2	
CGB (1, 377)	TTGGACTGTGGTGCAGGAAAGCCTCAAGT	AGAGGAGGTTGAG-----GCTTCAGTCCAG	1002
CGB5 (1, 341)	TTGGACTGTGGTGCAGGAAAGCCTCAAGT	AGAGGAGGTTGAG-----GCTTCAGTCCAG	966
CGB8 (1, 382)	TTGGACTGTGGTGCAGGAAAGCCTCAAGT	AGAGGAGGTTGAG-----GCTTCAGTCCAG	1007
CGB7 (1, 419)	TTGGACTGTGGTGCAGGAAAGCCTCAAGT	AGAGGAGGTTGAG-----GCTTCAGTCCAG	1044
LHB	TTGGACTGTGGTGCAGGAAAGCCTCAAGT	AGAGGAGGTTGAG-----GCTTCAGTCCAG	640
	* * * * *	* * * * *	* * * * *
CGB1 (1, 369)	CCACTTGCTCCCGCCATTCTGTTTACCACAGGTGAC	CGACCGCCATGGCTGACAGGCAGGG	603
CGB2 (1, 359)	CCACTTGCTCCCGCCATTCTGTTTACCACAGGTGAC	CGACCGCCATGGCTGACAGGCAGGG	615
CGB (1, 377)	CACCTTTCTCGGTCACCGCCTCCTCC--TGGCTCCAGGACCCACCATAGGCAGAGGC		1060
CGB5 (1, 341)	CACCTTTCTCGGTCACCGCCTCCTCC--TGGCTCCAGGACCCACCATAGGCAGAGGC		1024
CGB8 (1, 382)	CACCTTTCTCGGTCACCGCCTCCTCC--TGGCTCCAGGACCCACCATAGGCAGAGGC		1065
CGB7 (1, 419)	CACCTTTCTCGGTCACCGCCTCCTCC--TGGCTCCAGGACCCACCATAGGCAGAGGC		1102
LHB	CACCTTTCTCGGTCATGGCCTCCTCC--TGGCTCCAGGACCCACAAATGGCAGAGGC		698
	* * * * *	* * * * *	* * * * *
CGB1 (1, 369)	AGGTCCTCCCGAGGACCGAGCAAGCCTCGGTCTCCCAAAA	-----AAAAAAGATACATTGA	663
CGB2 (1, 359)	AGGTCCTCCCGAGGACCGAGCAAGCCTCGGTCTCCCAAAA	-----AAAAAAGATACATTGA	672
CGB (1, 377)	AGGCCTTCTACACCCTAC----TCCCTGTGCCTCCAGGCTCGAC	-----TAGTCCCTAGC	1112
CGB5 (1, 341)	AGGCCTTCTACACCCTAC----TCCCTGTGCCTCCAGGCTCGAC	-----TAGTCCCTAGC	1076
CGB8 (1, 382)	AGGCCTTCTACACCCTAC----TCCCTGTGCCTCCAGGCTCGAC	-----TAGTCCCTAGC	1117
CGB7 (1, 419)	AGGCCTTCTACACCCTAC----TCCCTGTGCCTCCAGGCTCGAC	-----TAGTCCCTAGC	1154
LHB	AGGCCTTCTACACCCTAC----TCCCTGTGCCTCCAGGCTCGAC	-----TAGTCCCTAGC	750
	*** * * * *	*** * * * *	*** * * * *
CGB1 (1, 369)	AGTAATTTAAAAACACTTAGGAAGATGTCATTTCTTCTTCAAGG	CGTCCTCCCTTTAT	723
CGB2 (1, 359)	AGTAATTTAAAAACACTTAGGAAGATGTCATTTCTTCTTCAAGG	CGTCCTCCCTTTAT	732
CGB (1, 377)	A----CTCGACGACTGAGTCTCTGAGGTCACCTC	-----GGTCTCGCCTCA	1160
CGB5 (1, 341)	A----CTCGACGACTGAGTCTCTGAGGTCACCTC	-----GGTCTCGCCTCA	1124
CGB8 (1, 382)	A----CTCGACGACTGAGTCTCTGAGGTCACCTC	-----GGTCTCGCCTCA	1165
CGB7 (1, 419)	A----CTCGACGACTGAGTCTCTGAGGTCACCTC	-----GGTCTCGCCTCA	1202
LHB	A----CTCGACAAGTGGTCTCTGAGGTCACCTC	-----GGTCTCTGCCTCA	798
	* * * * *	* * * * *	* * * * *
CGB1 (1, 369)	GTTTTGTTATATATAGGGAACGATAAAAAAATTTTTT	TCTCACCATGGGGC	783
CGB2 (1, 359)	GTTTTGTTATATATAGGGAACGATAAAAAAATTTTTT	TCTCACCATGGGGC	786
CGB (1, 377)	CCCTTGGCGCTGGACCAGTGAGAGGAGAGGGCTGGGG	CGCTCCGCTGAGCCACTCCTGG	1220
CGB5 (1, 341)	CCCTTGGCGCTGGACCAGTGAGAGGAGAGGGCTGGGG	CGCTCCGCTGAGCCACTCCTGG	1184
CGB8 (1, 382)	CCCTTGGCGCTGGACCAGTGAGAGGAGAGGGCTGGGG	CGCTCCGCTGAGCCACTCCTGG	1225
CGB7 (1, 419)	TCCTTGGCGCTAGACCAGTGAGGGAGAGGACTGGGGT	GCTCCGCTGAGCCACTCCTGTG	1262
LHB	CCTCTGGCGCTAGACCAGTGAGGGAGAGGGCTGGGG	CGCTCTGCTGAGCCACTCCTGG	858
	** * * * *	** * * * *	** * * * *
CGB1 (1, 369)	CCAGGTTGACCTCGAACTCCAGTCCCTCACACCCT	CGCCTAGCCTTGAGAGCCCGAGGGC	843
CGB2 (1, 359)	CCCGTTGGCCCTCGAACTCGTACCC--TCAAAACCTCCCTCCCTGAGGGCCCGAGGGC		843
CGB (1, 377)	CCCCCTGGCCTTG-----TCTACTCTTGCCCCCGGAGGGTTAGTG-TC		1265
CGB5 (1, 341)	CCCCCTGGCCTTG-----TCTACTCTTGCCCCCGGAGGGTTAGTG-TC		1229
CGB8 (1, 382)	CCCCCTGGCCTTG-----TCTACTCTTGCCCCCGGAGGGTTAGTG-TC		1270
CGB7 (1, 419)	CCTCCCTGGCCTTG-----TCTACTCTTGCCCCCGGAGGGTTAGTG-TC		1307
LHB	CCTCCCTGGCCATG-----TGCACCTCTCGCCCCGGGGGATAGTG-TC		903
	** * * * *	** * * * *	** * * * *
CGB1 (1, 369)	AGGCTCAATCGCAGGAGCCACAATGGCTCGC	CGTTCAGGCCCACATCTCTCTCTTT	903
CGB2 (1, 359)	ACGCGCAACCGGTGCGAGCCACAATAGCTCGGGTGT	CGGGGATCTCCTTTCTCTCTTT	903
CGB (1, 377)	GAGCTCACCCAGC---ATCCTATCACCTCCTGGTGGCCT	TGCGCCCCACAACCCCGA	1322
CGB5 (1, 341)	GAGCTCACCCAGC---ATCCTACAACCTCCTGGTGGCCT	TGCGCCCCACAACCCCGA	1286
CGB8 (1, 382)	GAGCTCACTCCAGC---ATCCTACAACCTCCTGGTGGCCT	TGCGCCCCACAACCCCGA	1327
CGB7 (1, 419)	CAGCTCACTCCAGC---ATCCTACAACCTCCTGGTGGCCT	TGCGCCCCACAACCCCGA	1364
LHB	CAGGTTACCCAGC---ATCCTATCACCTCCTGGTGGCCT	TGCGCCCCACAACCCCGA	960
	* * * * *	* * * * *	* * * * *
CGB1 (1, 369)	GACCTTACGAGGGTGTGGAGCCAATCAGGAGAGGCT	CACCCCTGACGTCACCCAGTCC	963
CGB2 (1, 359)	GACCTTACGAGGGTGTGGAGCCAATCAGGAGAGGCT	CACCCCTGACGTCACCCAGTCC	963
CGB (1, 377)	GGTATAAAGCCAGGTA-----CACGAGGCAGG	-----GGACGCA	1356
CGB5 (1, 341)	GGTATAAAGCCAGGTA-----CACGAGGCAGG	-----GGACGCA	1320

<i>CGB8</i> (1, 382)	GGTTTAAAGCCAGGTA-----CACGAGGCAGG-----GGACACA	1361
<i>CGB7</i> (1, 419)	GGTATAAAGCCAGGTA-----CACCAGGCAGG-----GGA <b>CG</b> CA	1398
<i>LHB</i>	GGTATATAGCCAGATA-----CAC <b>CG</b> AGGCAGG-----GGATGCA	994
	* * * * * * * * * * * * * * * * * * * *	
<i>CGB1</i> (1, 369)	CCAGGGCCAGT <b>CG</b> GAGGGCCCT <b>CG</b> TTCC <b>CG</b> TGG <b>CG</b> CCCCCTGGAGGGAGGAAGGGGA <b>ACTGC</b>	1023
<i>CGB2</i> (1, 359)	CCAGGGCCAGT <b>CG</b> GAGGGCCCT <b>CG</b> TTCC <b>CG</b> TGG <b>CG</b> CCCCCTGGAGGGAGGAAGGGGA <b>ACTGT</b>	1023
<i>CGB</i> (1, 377)	CCAAGGATGGAGATGTTCCAG-----	1377
<i>CGB5</i> (1, 341)	CCAAGGATGGAGATGTTCCAG-----	1341
<i>CGB8</i> (1, 382)	CCAAGGATGGAGATGTTCCAG-----	1382
<i>CGB7</i> (1, 419)	CCAAGGATGGAGATGTTCCAG-----	1419
<i>LHB</i>	CCAAGGATGGAGATGCTCCAG-----	1015
	*** ** * * * * * * * *	
<i>CGB1</i> (1, 369)	ATCTGAGAGAGAGCAGCCAATTGGGT <b>CG</b> CTGACTCTGGCCAGGTTCC <b>CG</b> TGG <b>CG</b> CGCTCC	1083
<i>CGB2</i> (1, 359)	ATCTGAGAGAGAGCAGCCAATTGGGT <b>CG</b> CTGACTCTGGCCAGGTTCC <b>CG</b> TGG <b>CG</b> CGCTCC	1083
<i>CGB</i> (1, 377)	-----	1377
<i>CGB5</i> (1, 341)	-----	1341
<i>CGB8</i> (1, 382)	-----	1382
<i>CGB7</i> (1, 419)	-----	1419
<i>LHB</i>	-----	1015
<i>CGB1</i> (1, 369)	AACACCCCTCACTCCCTGTCTCACTCCCCCA <b>CG</b> GAGACTCAATTTACTTTCCATGTCAC	1143
<i>CGB2</i> (1, 359)	AACACCCCTCACTCCCTGTCTCACTCCCCCA <b>CG</b> GAGACTCAATTTACTTTCCATGTCAC	1143
<i>CGB</i> (1, 377)	-----	1377
<i>CGB5</i> (1, 341)	-----	1341
<i>CGB8</i> (1, 382)	-----	1382
<i>CGB7</i> (1, 419)	-----	1419
<i>LHB</i>	-----	1015
<i>CGB1</i> (1, 369)	ATCCCAGT <b>CG</b> CTT <b>CG</b> GAAGATATCC <b>CG</b> CTAAGAGAGAGACATGTCAAAGGTAGGGTAGA	1203
<i>CGB2</i> (1, 359)	ATCCCAGT <b>CG</b> CTT <b>CG</b> GAAGATATCC <b>CG</b> CTAAGAGAGAGACATGTCAAAGGTAGGGTAGA	1203
<i>CGB</i> (1, 377)	-----	1377
<i>CGB5</i> (1, 341)	-----	1341
<i>CGB8</i> (1, 382)	-----	1382
<i>CGB7</i> (1, 419)	-----	1419
<i>LHB</i>	-----	1015
<i>CGB1</i> (1, 369)	TCCACATT <b>CG</b> CGGCCACCAAAGATGGAGATGTTCCAGGAAAGACTGCAGGGCCCCCTGGGC	1263
<i>CGB2</i> (1, 359)	TCCACATT <b>CG</b> CGGCCACCAAAGATGGAGATGTTCCAGGAAAGACTGCAGGGCCCCCTGGGC	1263
<i>CGB</i> (1, 377)	-----	1377
<i>CGB5</i> (1, 341)	-----	1341
<i>CGB8</i> (1, 382)	-----	1382
<i>CGB7</i> (1, 419)	-----	1419
<i>LHB</i>	-----	1015
<i>CGB1</i> (1, 369)	ACCTTCCACCTCCTTCCAGGCCATCACTGGCATGAGAAGGGGCAGACC <b>CG</b> TGTGAGCTGT	1323
<i>CGB2</i> (1, 359)	ACCTTCCACCTCCTTCCAGGCCATCACTGGCATGAGAAGGGGCAGACCAGTGTGAGCTGT	1323
<i>CGB</i> (1, 377)	-----	1377
<i>CGB5</i> (1, 341)	-----	1341
<i>CGB8</i> (1, 382)	-----	1382
<i>CGB7</i> (1, 419)	-----	1419
<i>LHB</i>	-----	1015
<i>CGB1</i> (1, 369)	GGAAGGAGGCCTCTTTCTGGAGGAG <b>CG</b> TGACCCCCAGTAAGCTCA	1369
<i>CGB2</i> (1, 359)	GGAAGGAGGCCTCTTTCTGGAGGAG <b>CG</b> TGACCCCCA-----	1359
<i>CGB</i> (1, 377)	-----	1377
<i>CGB5</i> (1, 341)	-----	1341
<i>CGB8</i> (1, 382)	-----	1382
<i>CGB7</i> (1, 419)	-----	1419
<i>LHB</i>	-----	1015

**Fig.A1** Multiple Sequence alignment of *CGB1-9* and *LHB*. Legend for MSA: **CG** – CpG site; cggcccc – AP2 binding; CGGCCCC – SP1 binding; **CTCTCATT** Putative promoter *CGB3-9*; **CTCTCATT** Putative promoter *CGB1-2*; **CGGCCCC** - 1<sup>st</sup> exon 5' UTR; **ATGCGG** – 1<sup>st</sup> exon after ATG; **CTCTCATT**CGGC- cAMP response elements; **cctgCGGG**-TSE ; **TCTCATT**-CCAAT box; **TCTCATT** – Ets-2; **TCTCATT**-Oct3/4; **TCTCATT** =*CGB1-2* insert ; **CTCTCATT** snaR-G1 reverse complement; **TGGC** snaR-G2 reverse complement;

## A2.2 CpG Island predictions

### EMBOSS Newcpgreport

Identify and report CpG islands in nucleotide sequence(s)

**STEP 1 - Enter your input sequence**

Enter or paste a nucleic acid sequence in any supported format:

Or, upload a file:  No file selected. [Use a example sequence](#) | [Clear sequence](#) | [See more example inputs](#)

**STEP 2 - Set options**

WINDOW SIZE	MINIMUM LENGTH	MINIMUM OBSERVED	MINIMUM PERCENTAGE
200	200	0.6	50

**Fig.A2** Screen capture of the Newcpgreport tool and its settings used to predict the CGIs for CGB3-8

```
ID  CGB3  1377 BP.
XX
DE  CpG Island report.
XX
CC  Obs/Exp ratio > 0.60.
CC  % C + % G > 50.00.
CC  Length > 200.
XX
FH  Key                               Location/Qualifiers
FT  no islands detected

ID  CGB5  1341 BP.
XX
DE  CpG Island report.
XX
CC  Obs/Exp ratio > 0.60.
CC  % C + % G > 50.00.
CC  Length > 200.
XX
FH  Key                               Location/Qualifiers
FT  no islands detected

ID  CGB8  1382 BP.
XX
DE  CpG Island report.
XX
CC  Obs/Exp ratio > 0.60.
CC  % C + % G > 50.00.
CC  Length > 200.
XX
FH  Key                               Location/Qualifiers
FT  no islands detected
```

**Fig.A3** Output from Newcpgreport tool for CGB3, 5 and 8. ID row is the user defined ID and length of input sequence, DE- description of test, CC rows – conditions of the test, FH and FT rows present the predicted CpG island in relation to the input sequence.

## A2.3 Primer design and ePCR

### MethPrimer

**NEW!** [Invitation to test MethPrimer 2.0](#)

Paste an ORIGINAL source [sequence](#). Try this [Sample sequence](#)  
 You don't need to modify your sequence (e.g. convert 'C' to 'T') before pasting.

Pick primers for [bisulfite sequencing PCR](#) or [restriction PCR](#) .  
 Pick [MSP](#) primers.

Use [CpG island prediction](#) for primer selection?
 
 Window: 100   
 Shift: 1   
 Obs/Exp: 0.6   
 GC%: 50

General Parameters for Primer Selection	
Sequence name (optional):	<input type="text"/>
Target (optional):	<input type="text"/> "start, size", such as (560, 30)
Excluded Regions (optional):	<input type="text"/> "start, size", such as (160, 50 1100, 50)
Number of output pairs (optional):	5 <input type="text"/>

Product Size:	Min: 100 <input type="text"/>	Opt: 200 <input type="text"/>	Max: 300 <input type="text"/>
Primer Tm:	Min: 50 <input type="text"/>	Opt: 55 <input type="text"/>	Max: 60 <input type="text"/>
Primer Size:	Min: 20 <input type="text"/>	Opt: 25 <input type="text"/>	Max: 30 <input type="text"/>
Product CpGs:	4 <input type="text"/>	Primer Poly X:	5 <input type="text"/>
Primer non-CpG 'C's:	4 <input type="text"/>	Primer Poly T:	8 <input type="text"/>

Parameters for MSP primers	
3'CpG constraint:	3 <input type="text"/>
CpG in primer:	1 <input type="text"/>
Max Tm difference:	5 <input type="text"/>

**Fig.A4** Screen capture of the MethPrimer tool and its settings used to design primers for CGB3-8 putative promoter

Primer	Start	Size	Tm	GC%	'C's	Sequence
1. Left primer	647	27	59.54	48.15	4	GGGAAGGGATTAAGTTTAGATAATGTT
Right primer	879	25	59.03	64.00	7	CTACCAAAAAAACCCTTAACCCTA
Product size: 233, Tm: 67.2, CpGs in product: 10						

**Fig.A5** Sample output of primer pair with primer characteristics

**Search primer pairs in genome**

Forward primer	<input type="text"/>
Reverse primer	<input type="text"/>
- OR -	
Upload File	<input type="button" value="Browse..."/> No file selected.
Bisulfite	<input checked="" type="checkbox"/>
MSP	<input type="checkbox"/>

**Parameters**

**Database search and fast PCR**

Database	<input type="text" value="Homo sapiens"/>	Mismatches	<input type="text" value="0000000011111111"/>
		Max:	<input type="text" value="4"/>
PCR length	<input type="text" value="1000"/>	PCR product to show	<input type="text" value="100"/>
		Primer matches to show	<input type="text" value="100"/>

**Fig.A6** Screen capture of the BiSearch ePCR page and its settings used to predict PCR products for proposed primer pairs

```

PCR product(s) on the bisulfite transformed sense chain
  Forward primer: GGGAAGGGATTAAGTTTAGATAATGTT
  Reverse primer: CTACCAAAAAAACCCTTAACCCTA
1. Chromosome 19 (CGB2) (len: 233)
  49031105
      GGG AAGGGATTAA GTTTAGATAA
      TGTTTTTTGA GGTGAGGTT TTGGGGGTAG GATATATTTT TTGTGGGTTT
      ATTTAATAAT TAGTTAAATT ATTTGAAGTA TATGTATTTT TGGGGATTGT
      TTTGGGTATT TTGGTTGAG GGTAGAGTGG GTAGAGGTTT TTAAGGGAGA
      GGTGGGGTTT GGGTTGAATT TTTTGTGGT GGTATTAGGG TTAAGTGGTT
      AATTTGGTAG
      49031338
PCR product(s) on the bisulfite transformed antisense chain
  Forward primer: GGGAAGGGATTAAGTTTAGATAATGTT
  Reverse primer: CTACCAAAAAAACCCTTAACCCTA
3 PCR products should be generated.
1. Chromosome 19 (CGB3) (len: 233)
  49024454
      CTAC CAAAAAACC ACTTAACCCT
      AATACCACCA ACAAAAAATT CAACCCAAAC CCCACCTCTC CCTTAAAAAC
      CTCCACCCAC CCTACCCTCA AACCAAAATA CCCAAAACTA TCCCCAAAAA
      TACATATACT TCAAATAATT TAACTAATTA TTAAATAAAC CCACAAAAAA
      TATATCCTAC CCATAAAACC AAAACCTCAA AAAACATTAT CTAAACTTAA
      TCCCTTCCC
      49024687
2. Chromosome 19 (CGB1) (len: 233)
  49037480
      CTACCAA TTAACCACTT AACCTAATA CCACCAACAA AAAATTCAAC
      CCAAACCCCA CCTCTCCCTT AAAAACCTCT ACCACTCTA CCCTCAAACC
      AAAATACCCA AAACAATCCC CAAAAATACA TATACTCAA ATAATTTAAC
      TAATTATTAA ATAAACCAC AAAAAATATA TCCTACCCCC AAAACCACAA
      CCTCAAAAAA CATTATCTAA ACTTAATCCC TTCCC
      49037713
3. Chromosome 19 (CG8) (len: 233)
  49049222
      CTACCA
      AAAAAACCAC TTAACCCTAA TACCCCAA AAAAATTC AACC AAACCC
      CACCTCTCCC TTAAAAACCT CCACCCACTC TACCCTCAA CCAAATACC
      CAAACTATC CCCAAAAATA CATATACTTC AAATAATTTA ACTAATTATT
      AAATAAACCC ACAAAAAATA TATCCTACCC ACAAACCAA AACCTCAAAA
      AACATTATCT AAACCTAATC CCTTCCC
      49049455

```

**Fig.A7** ePCR Predicted PCR products for primer pair 1.

**PCR product(s) on the bisulfite transformed sense chain**  
Forward primer: TTAATAATTAGTTAAATTATTTGAAGTATA  
Reverse primer: AAAAAAATACTAAACTAAAACCTC

1. [Chromosome 19](#) (CGB5) (len: 291)  
49043567 T TAATAATTAG  
TTAAATTATT TGAAGTATAT GTATTTTTGG GGATTGTTTT GGGTATTTTG  
GTTTGAGGGT AGAGTGGGTG GAGGTTTTTA AGGGAGAGGT GGGGTTTGGG  
TTGAATTTTT TGTTGGGGGG TATTTGGGT AAGTGGTTTT TTTGGTAGTA  
TAGTTATGGG GAGGTTTTTT TTTATTGGGT AGAAGTTAAG TTTGAAGTTG  
TGTTTTTTTT GGGAGGTTGG ATTGTGGTGT AGGAAAAGTT TAAGTAGAGG  
AGGGTTGAGG TTTTAATTTA GTATTTTGT 49043858

**PCR product(s) on the bisulfite transformed antisense chain**  
Forward primer: TTAATAATTAGTTAAATTATTTGAAGTATA  
Reverse primer: AAAAAAATACTAAACTAAAACCTC

3 PCR products should be generated.

1. [Chromosome 19](#) (CGB3) (len: 290)  
49024322 AAAAAA  
ATACTAAACT AAAACCTCAA CCCTCCTCTA CTTAAAACCT TCCTACACCA  
CAATCCAACC TCCCAAAAAA AACACAACCT CAAACTTAAT TTCTACCCAA  
TAAAAAAAAA CCTCCCCATA ACTATACTAC CAAAAAAC ACTTAACCCT  
AATACCACCA ACAAAAAATT CAACCCAAAC CCCACCTCTC CCTTAAAAAC  
CTCCACCCAC CCTACCCTCA AACCAAAATA CCCAAAAC TAACCCAAAA  
TACATATACT TCAAATAATT TAACTAATTA TTAA 49024612

2. [Chromosome 19](#) (CGB8) (len: 290)  
49049090 AAAAAAAT ACTAACTAA AACCTCAACC CTCCTCTACT  
TAAAACCTTC CTACACCACA ATCCAACCTC CCAAAAAAAA CACAACCTCA  
AACTTAACTT CTACCCAATA AAAAAAATC TCCCATAAC TATACTACCA  
AAAAAACCCAC TTAACCTAA TACCCCAA AAAAAATCA ACCCAAACCC  
CACCTCTCCC TTAAAAACCT CCACCCACTC TACCCTCAA CCAAATACC  
CAAACTATC CCCAAAATA CATATACTTC AAATAATTTA ACTAATTATT  
AA 49049380

3. [Chromosome 19](#) (CGB7) (len: 291)  
49055726 AA  
AAAAATACTA AACTAAAACC TCAACCTCC TCTACTTAAA CCATTCCTAC  
ACCACAATCC AACCTAACAA AAAAAACACA ACTTCAAAC TAACCTCTAC  
CCAATAAAAA AAAATCTCCC CATAACTATA CTACCAAAAA AACCCTTAA  
CCCAAATACC CCCCAACAAA AAATTCAACC CAAACCCAC CTCTCCCTTA  
AAAACCTCCA CCCACCTAC CCTCAAACCA AAATACCCAA AACCAATCCC  
AAAAATACAT AACTTTCAA TAATTTAACT AATTATTAA 49056017

**Fig.A8** ePCR Predicted PCR products for primer pair 2.



PCR product(s) on the bisulfite transformed sense chain					
Forward primer: TTTAATAATTAGTTAAATTATTTGAAGTAT					
Reverse primer: CTTAATTTCTACCCAATAAAAAAAAA					
<b>2 PCR products should be generated.</b>					
1.	<a href="#">Chromosome 19</a>	(CGB2)	(len: 201)	cgb2	
49031179	TTTAATAAT	TAGTTAAATT	ATTTGAAGTA	TATGTATTTT	TGGGGATTGT
	TTTGGGTATT	TTGGTTTGAG	GGTAGAGTGG	GTAGAGGTTT	TTAAGGGAGA
	GGTGGGGTTT	GGGTTGAATT	TTTTGTTGGT	GGTATTAGGG	TTAAGTGGTT
	AATTTGGTAG	TATAGTTATG	GGGAGGTTTT	TTTTTATTGG	GTAGAAATTA
	AG				49031380
2.	<a href="#">Chromosome 19</a>	(CGB5)	(len: 202)		
49043566				TT	TAATAATTAG
	TTAAATTATT	TGAAGTATAT	GTATTTTTGG	GGATTGTTTT	GGGTATTTTG
	GTTTGAGGGT	AGAGTGGGTG	GAGGTTTTTA	AGGGAGAGGT	GGGGTTTTGGG
	TTGAATTTTT	TGTTGGGGGG	TATTTGGGTT	AAGTGGTTTT	TTTGGTAGTA
	TAGTTATGGG	GAGGTTTTTT	TTTATTGGGT	AGAAGTTAAG	49043768
PCR product(s) on the bisulfite transformed antisense chain					
Forward primer: TTTAATAATTAGTTAAATTATTTGAAGTAT					
Reverse primer: CTTAATTTCTACCCAATAAAAAAAAA					
<b>4 PCR products should be generated.</b>					
1.	<a href="#">Chromosome 19</a>	(CGB3)	(len: 201)		
49024412				CTTAAT	TTCTACCCAA
	TAAAAAAAAA	CCTCCCCATA	ACTATACTAC	CAAAAAAACC	ACTTAACCCT
	AATACCACCA	ACAAAAAATT	CAACCCAAAC	CCCACCTCTC	CCTTAAAAAC
	CTCCACCCAC	CCTACCCTCA	AACCAAAATA	CCCAAAACTA	TCCCCAAAAA
	TACATATACT	TCAAATAAAT	TAACTAATTA	TTAAA	49024613
2.	<a href="#">Chromosome 19</a>	(CGB1)	(len: 201)		
49037438				CTTAATTTCT	ACCCAATAAA
	TACTACCAAA	TTAACCACTT	AACCCTAATA	CCACCAACAA	AAAATTC AAC
	CCAAACCCCA	CCTCTCCCTT	AAAAACCTCT	ACCCACTCTA	CCCTCAAACC
	AAAATACCCA	AAACAATCCC	CAAAAAATACA	TATACTTCAA	ATAATTTAAC
	TAATTATTAA	A			49037639
3.	<a href="#">Chromosome 19</a>	(CGB8)	(len: 201)	cgb8	
49049180	CTTAACTT	CTACCCAATA	AAAAAAAATC	TCCCCATAAC	TATACTACCA
	AAAAAACCAC	TTAACCCCTAA	TACCCCAAAA	AAAAAATTCA	ACCCAAACCC
	CACCTCTCCC	TTAAAAACCT	CCACCCACTC	TACCCCTCAA	CCAAAATACC
	CAAACTATC	CCCCAAAATA	CATATACTTC	AAATAATTTA	ACTAATTATT
	AAA				49049381
4.	<a href="#">Chromosome 19</a>	(CGB7)	(len: 202)		
49055816				CT	TAACCTTCTAC
	CCAATAAAAA	AAAATCTCCC	CATAACTATA	CTACCAAAAA	AACCACTTAA
	CCCAAATACC	CCCCAACAAA	AAATTCAACC	CAAACCCAC	CTCTCCCTTA
	AAAACCTCCA	CCCACCCTAC	CCTCAAACCA	AAATACCCAA	AACAATCCCC
	AAAAATACAT	ATACTTCAAA	TAATTTAACT	AATTATTAAA	49056018

**Fig.A9** ePCR Predicted PCR products for primer pair 3.

PCR product(s) on the bisulfite transformed sense chain					
Forward primer: GGAAGGGATTAAGTTTAGATAATGTT					
Reverse primer: CTTAATTTCTACCCAATAAAAAAAAA					
2 PCR products should be generated.					
1.	<a href="#">Chromosome 19</a>	(CGB2)	(len: 275)		
49031105				GGG AAGGGATTAA	GTTTAGATAA
	TGTTTTTTGA	GGTTGAGGTT	TTGGGGGTAG	GATATATTTT	TTGTGGGTTT
	ATTTAATAAT	TAGTTAAATT	ATTTGAAGTA	TATGTATTTT	TGGGGATTGT
	TTTGGGTATT	TTGGTTTGAG	GGTAGAGTGG	GTAGAGTTT	TTAAGGGAGA
	GGTGGGGTTT	GGGTTGAATT	TTTTGTTGGT	GGTATTAGGG	TTAAGTGGTT
	AATTTGGTAG	TATAGTTATG	GGGAGGTTTT	TTTTTATTGG	GTAGAAATTA
	AG				49031380
2.	<a href="#">Chromosome 19</a>	(CGB5)	(len: 276)		
49043492				GGGAAG GGATTAAGTT	TAGATAATGT
	TTTTGGTTTTG	TGGGTAGGAT	ATATTTTTTG	TGGGTTTATT	TAATAATTAG
	TTAAATTATT	TGAAGTATAT	GTATTTTTGG	GGATTGTTTT	GGGTATTTTG
	GTTTGAGGGT	AGAGTGGGTG	GAGGTTTTTA	AGGGAGAGGT	GGGTTTTGGG
	TTGAATTTTT	TGTTGGGGGG	TATTTGGGTT	AAGTGGTTTT	TTTGGTAGTA
	TAGTTATGGG	GAGGTTTTTT	TTTATTGGGT	AGAAGTTAAG	49043768
PCR product(s) on the bisulfite transformed antisense chain					
Forward primer: GGAAGGGATTAAGTTTAGATAATGTT					
Reverse primer: CTTAATTTCTACCCAATAAAAAAAAA					
5 PCR products should be generated.					
1.	<a href="#">Chromosome 19</a>	(LHB)	(len: 274)		
49017519					CTTAACTTC
	TACCCAATAA	AAAAAATCT	CCCCATAACT	ATACTACCAA	AAAAACCACT
	TAACCCAAAT	ACCCCCAAA	AAAAATTAAA	CCCAAACCC	ACCTCTCCCT
	TAAAAACCTC	CACCCACCCT	ACCCTCAAAC	CAAAATACCC	AAAACATCCC
	CAAAAATAAA	TATAATTCAA	ATAATTTAAC	TCATTATTTA	ATACACCCAC
	AAAATACATA	TCTTACCCCC	AAAACCACAA	CCTACAAAAA	CATTATCTAA
	ACTTAATCCC	CTCTC			49017793
2.	<a href="#">Chromosome 19</a>	(CGB3)	(len: 275)		
49024412				CTTAAT	TTCTACCCAA
	TAAAAAATAA	CCTCCCCATA	ACTATACTAC	CAAAAAAACC	ACTTAACCCT
	AATACCACCA	ACAAAAAATT	CAACCCAAAC	CCCACCTCTC	CCTTAAAAAC
	CTCCACCCAC	CCTACCCTCA	AACCAAAATA	CCCAAAACCTA	TCCCCAAAAA
	TACATATACT	TCAAATAAAT	TAACTAATTA	TTAAATAAAC	CCACAAAAAA
	TATATCCTAC	CCATAAAAACC	AAAACCTCAA	AAAACATTAT	CTAAACTTAA
	TCCCTTCCC				49024687
3.	<a href="#">Chromosome 19</a>	(CGB1)	(len: 275)		
49037438				CTTAATTTCT	ACCCAATAAA
	TACTACCAA	TTAACCACTT	AACCCTAATA	CCACCAACAA	AAAATTCAAC
	CCAAACCCCA	CCTCTCCCTT	AAAAACCTCT	ACCCTACTCA	CCCTCAAACC
	AAAATACCCA	AAACAATCCC	CAAAAATACA	TATACTCAA	ATAATTTAAC
	TAATTATTAA	ATAAACCCAC	AAAAAATATA	TCCTACCCCC	AAAACCACAA
	CCTCAAAAAA	CATTATCTAA	ACTTAATCCC	TTCCC	49037713
4.	<a href="#">Chromosome 19</a>	(CGB8)	(len: 275)		
49049180				CTTAACTT	CTACCCAATA
	AAAAAACCAC	TTAACCTTAA	TACCCCAAAA	AAAAAATTCA	ACCCAAACCC
	CACCTCTCCC	TTAAAAACCT	CCACCCACTC	TACCTCAAA	CCAAAATACC
	CAAACTATC	CCAAAAATA	CATATACTTC	AAATAATTTA	ACTAATTATT
	AAATAAACCC	ACAAAAATA	TATCCTACCC	ACAAAACCAA	AACCTCAAAA
	AACATTATCT	AACTTAATC	CCTTCCC		49049455
5.	<a href="#">Chromosome 19</a>	(CGB7)	(len: 276)		
49055816				CT	TAACCTTCTAC
	CCAATAAAAA	AAAATCTCCC	CATAACTATA	CTACCAAAAA	AACCACTTAA
	CCCAAATACC	CCCCAACAAA	AAATTC AAC	CAAAACCCAC	CTCTCCCTTA
	AAAACCTCCA	CCCACCCTAC	CCTCAAACCA	AAATACCCAA	AACAATCCCC
	AAAAATACAT	ATACTTCAA	TAATTTAACT	AATTATTTAA	TAAACCCACA
	AAAAATATAT	CCTACCACAA	AAACCACAAC	CTCAAAAAAC	ATTATCTAAA
	CTTAATCCCT	TCCC			49056092

Fig.A10 ePCR Predicted PCR products for primer pair 4.

PCR product(s) on the bisulfite transformed sense chain					
Forward primer: TTAATAATTAGTTAAATTATTTGAAGTATA					
Reverse primer: CTTAATTTCTACCCAATAAAAAAAAA					
<b>2 PCR products should be generated.</b>					
1. <a href="#">Chromosome 19</a> (CGB2) (len: 200)					
49031180	TTAATAAT	TAGTTAAATT	ATTTGAAGTA	TATGTATTTT	TGGGGATTGT
	TTTGGGTATT	TTGGTTTGAG	GGTAGAGTGG	GTAGAGGTTT	TTAAGGGAGA
	GGTGGGGTTT	GGGTGAATT	TTTTGTTGGT	GGTATTAGGG	TTAGTGGTT
	AATTTGGTAG	TATAGTTATG	GGGAGGTTTT	TTTTTATTGG	GTAGAAATTA
	AG				49031380
2. <a href="#">Chromosome 19</a> (CGB5) (len: 201)					
49043567				T	TAATAATTAG
	TTAAATTATT	TGAAGTATAT	GTATTTTTGG	GGATTGTTTT	GGGTATTTTTG
	GTTTGAGGGT	AGAGTGGGTG	GAGGTTTTTA	AGGGAGAGGT	GGGGTTTTGGG
	TTGAATTTTT	TGTTGGGGGG	TATTTGGGTT	AAGTGGTTTT	TTTGGTAGTA
	TAGTTATGGG	GAGGTTTTTT	TTTATTGGGT	AGAAGTTAAG	49043768
PCR product(s) on the bisulfite transformed antisense chain					
Forward primer: TTAATAATTAGTTAAATTATTTGAAGTATA					
Reverse primer: CTTAATTTCTACCCAATAAAAAAAAA					
<b>4 PCR products should be generated.</b>					
1. <a href="#">Chromosome 19</a> (CGB3) (len: 200)					
49024412				CTTAAT	TTCTACCCAA
	TAAAAAAAAA	CCTCCCCATA	ACTATACTAC	CAAAAAAACC	ACTTAACCCCT
	AATACCACCA	ACAAAAAATT	CAACCCAAAC	CCCACCTCTC	CCTTAAAAAC
	CTCCACCCAC	CCTACCCTCA	AACCAAAATA	CCCAAAACTA	TCCCCAAAAA
	TACATATACT	TCAAATAATT	TAACTAATTA	TTAA	49024612
2. <a href="#">Chromosome 19</a> (CGB1) (len: 200)					
49037438		CTTAATTTCT	ACCCAATAAA	AAAAAACCTC	CCCATAACTA
	TACTACCAAA	TTAACCACTT	AACCCTAATA	CCACCAACAA	AAAATTC AAC
	CCAAACCCCA	CCTCTCCCTT	AAAAACCTCT	ACCCACTCTA	CCCTCAAACC
	AAAATACCCA	AAACAATCCC	CAAAAAATACA	TATACTTCAA	ATAATTTAAC
	TAATTATTAA				49037638
3. <a href="#">Chromosome 19</a> (CGB8) (len: 200)					
49049180	CTTAACTT	CTACCCAATA	AAAAAAAATC	TCCCATAAC	TATACTACCA
	AAAAAACCAC	TTAACCCCTAA	TACCCCAAAA	AAAAAATTCA	ACCCAAACCC
	CACCTCTCCC	TTAAAAACCT	CCACCCACTC	TACCCCTCAA	CCAAAATACC
	CAAACTATC	CCCCAAAAATA	CATATACTTC	AAATAATTTA	ACTAATTATT
	AA				49049380
4. <a href="#">Chromosome 19</a> (CGB7) (len: 201)					
49055816				CT	TAAC TTCTAC
	CCAATAAAAA	AAAAATCTCCC	CATAACTATA	CTACCAAAAA	AACCACTTAA
	CCCAAATACC	CCCCAACAAA	AAATTCAACC	CAAACCCAC	CTCTCCCTTA
	AAAACCTCCA	CCCACCCTAC	CCTCAAACCA	AAATACCCAA	AACAATCCCC
	AAAAATACAT	ATACTTCAAA	TAATTTAACT	AATTATTAA	49056017

**Fig.A11** ePCR Predicted PCR products for primer pair 5.

PCR product(s) on the bisulfite transformed sense chain				
Forward primer: GGGGAAGGGATTAAGTTTAGA				
Reverse primer: ACTATACTACCAAAAAAACCCTTA				
1.	<a href="#">Chromosome 19</a>	(CGB5)	(len: 241)	
49043492	GGGGAAG	GGATTAAGTT	TAGATAATGT	TTTTTGAGGT
	TTTGGTTTTG	TGGGTAGGAT	ATATTTTTTG	TGGGTTTATT
	TTAAATTATT	TGAAGTATAT	GTATTTTTGG	GGATTGTTTT
	GTTTGAGGGT	AGAGTGGGTG	GAGGTTTTTA	AGGGAGAGGT
	TTGAATTTTT	TGTTGGGGGG	TATTTGGGTT	AAGTGGTTTT
	TAGT			TTTGGTAGTA
				49043732
PCR product(s) on the bisulfite transformed antisense chain				
Forward primer: GGGGAAGGGATTAAGTTTAGA				
Reverse primer: ACTATACTACCAAAAAAACCCTTA				
4 PCR products should be generated.				
1.	<a href="#">Chromosome 19</a>	(LHB)	(len: 239)	
49017556			ACT	ATACTACCAA
	TAACCCAAAT	ACCCCAAAA	AAAAATTAAA	CCCAAACCC
	TAAAAACCTC	CACCCACCT	ACCCTCAAAC	CAAAATACCC
	CAAAAATAAA	TATAATTCAA	ATAATTTAAC	TCATTATTTA
	AAAATACATA	TCTTACCCCC	AAAACCACAA	CCTACAAAAA
	ACTTAATCCC	CTCTCC		CATTATCTAA
				49017794
2.	<a href="#">Chromosome 19</a>	(CGB3)	(len: 240)	
49024449			ACTATACTAC	CAAAAAAACC
	AATACCACCA	ACAAAAAATT	CAACCCAAAC	CCCACCTCTC
	CTCCACCCAC	CCTACCCTCA	AACCAAAATA	CCCAAAATA
	TACATATACT	TCAAATAATT	TAACATAATTA	TTAAATAAAC
	TATATCCTAC	CCATAAAACC	AAAACCTCAA	AAAACATTAT
	TCCCTTCCCC			CTAAACTTAA
				49024688
3.	<a href="#">Chromosome 19</a>	(CGB8)	(len: 240)	
49049217			AC	TATACTACCA
	AAAAAACCAC	TTAACCCTAA	TACCCCAAAA	AAAAAATTCA
	CACCTCTCCC	TTAAAAACCT	CCACCCACTC	TACCCTCAAA
	CAAACTATC	CCCAAAAATA	CATATACTTC	AAATAATTTA
	AAATAAACCC	ACAAAAAATA	TATCCTACCC	ACAAAACCAA
	AACATTATCT	AAACTTAATC	CCTTCCCC	
				49049456
4.	<a href="#">Chromosome 19</a>	(CGB7)	(len: 241)	
49055853			ACTATA	CTACCAAAAA
	CCCAAATACC	CCCCAACAAA	AAATTCAACC	CAAACCCAC
	AAAACCTCCA	CCCACCTTAC	CCTCAAACCA	AAATACCCAA
	AAAAATACAT	ATACTTCAAA	TAATTTAACT	AATTATTTAA
	AAAAATATAT	CCTACCCACA	AAACCACAAC	CTCAAAAAAC
	CTTAATCCCT	TCCCC		ATTATCTAAA
				49056093

**Fig.A12** ePCR Predicted PCR products for primer pair 6.

PCR product(s) on the bisulfite transformed sense chain					
Forward primer: GGGTATTTTGGTTTGAGGG					
Reverse primer: CCTCAACCCTCCTCTACTT					
1.	<a href="#">Chromosome 19</a>	(CGB5)	(len: 220)		
	49043619			GGGTATTTTG	
		GTTTGAGGGT	AGAGTGGGTG	GAGGTTTTTA	AGGGAGAGGT
		TTGAATTTTT	TGTTGGGGGG	TATTTGGGTT	AAGTGGTTTT
		TAGTTATGGG	GAGGTTTTTT	TTTATTGGGT	AGAAGTTAAG
		TGTTTTTTTT	GGGAGGTTGG	ATTGTGGTGT	AGGAAAAGTTT
		AGGGTTGAGG			TAAGTAGAGG
					49043838
PCR product(s) on the bisulfite transformed antisense chain					
Forward primer: GGGTATTTTGGTTTGAGGG					
Reverse primer: CCTCAACCCTCCTCTACTT					
3 PCR products should be generated.					
1.	<a href="#">Chromosome 19</a>	(CGB3)	(len: 219)		
	49024343			CCTCAA	CCCTCCTCTA
		CAATCCAACC	TCCCAAAAAA	AACACAACCTT	CAAACTTAAT
		TAAAAAATAA	CCTCCCCATA	ACTATACTAC	CAAAAAAACC
		AATACCACCA	ACAAAAAATT	CAACCCAAAC	CCCACCTCTC
		CTCCACCCAC	CCTACCCTCA	AACCAAAATA	CCC
					49024561
2.	<a href="#">Chromosome 19</a>	(CGB8)	(len: 219)		
	49049111			CCTCAACC	CTCCTCTACT
		TAAAACTTTC	CTACACCACA	ATCCAACCTC	CCAAAAAATA
		AACTTAACTT	CTACCCAATA	AAAAAAAATC	TCCCCATAAC
		AAAAAACCAC	TTAACCCTAA	TACCCCAAAA	AAAAAATTC
		CACCTCTCCC	TTAAAAACCT	CCACCCACTC	TACCCTCAAA
		C			CCAAAAATACC
					49049329
3.	<a href="#">Chromosome 19</a>	(CGB7)	(len: 220)		
	49055747			CC	TCAACCCTCC
		ACCACAATCC	AACCTAACAA	AAAAAACACA	ACTTCAAACCT
		CCAATAAAAA	AAAATCTCCC	CATAACTATA	CTACCAAAAA
		CCCAAATACC	CCCCAACAAA	AAATTCAACC	CAAACCCAC
		AAAACCTCCA	CCCACCCTAC	CCTCAAACCA	AAATACCC
					49055966

**Fig.A13** ePCR Predicted PCR products for primer pair 7.

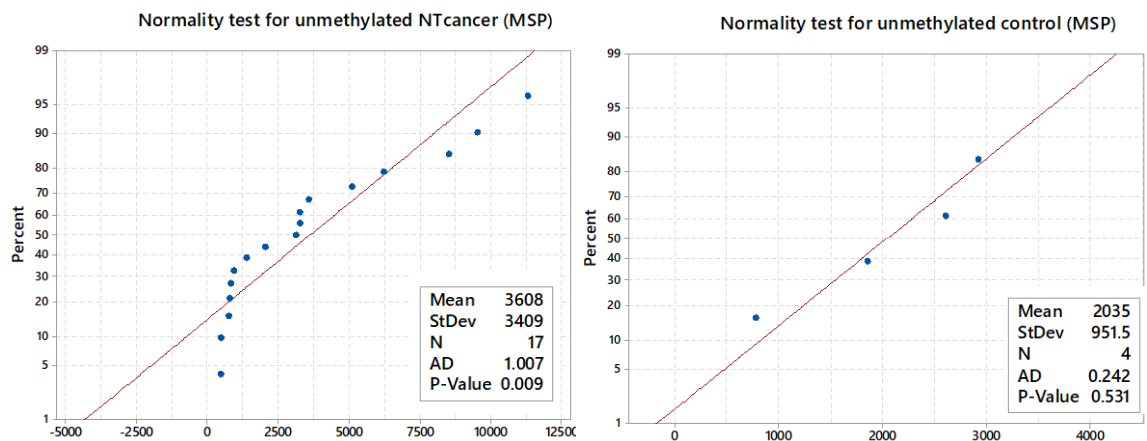
# A3. MSP Densitometry

**Table A3** MSP Densitometry data from ImageJ

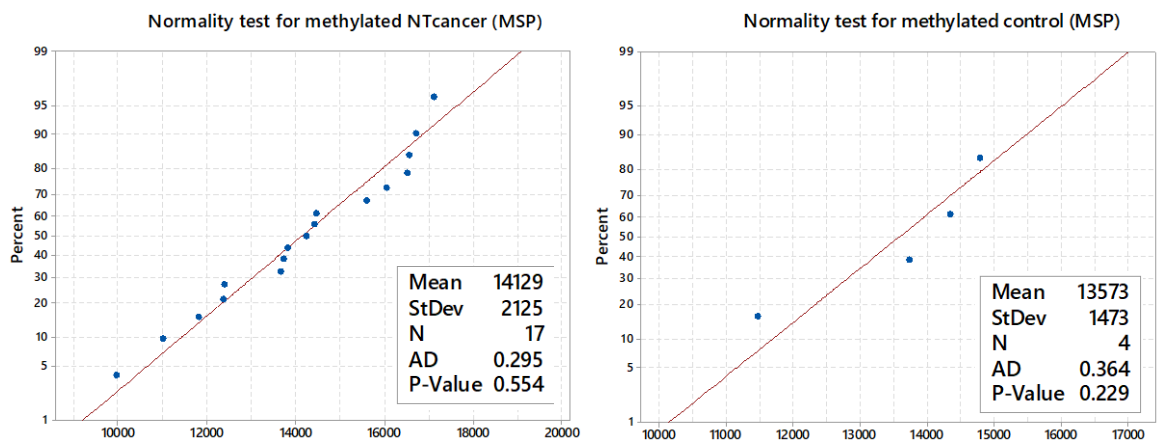
Cell Line	HeLa (NT cancer)		HEY (NT cancer)		SKOV-3 (NT cancer)	
	u	m	u	m	u	m
1	11299.96	16703.4	805.385	17103.69	1370.477	16540.45
2	9506.861	13705.45	917.234	14228.57	473.92	12383.86
3	8492.154	12351.86	755.406	13649.45	3093.205	16031.69
4	6208.548	9947.912	447.335	11001.15	-	-
5	5105.376	16496.05	787.213	14401.64	-	-

Cell Line	C-33a (NT cancer)		CRL-1790 (control)	
	u	m	u	m
1	-	-	-	-
2	3244.426	14456.33	2913.841	14332.91
3	3573.134	13804.98	2603.548	13724.98
4	2019.77	11796.28	1848.184	11460.15
5	3228.497	15594.93	775.749	14774.59



**Fig.A14** Plot for unmethylated densitometry data normality test (Anderson-Darling). Output from Minitab. (Left: non-trophoblastic cancer right: control)



**Fig.A15** Plot for methylated densitometry data normality test (Anderson-Darling). Output from Minitab. (Left: non-trophoblastic cancer right: control)

## Mann-Whitney: unme c, unmectrl Method

$\eta_1$ : median of unme c

$\eta_2$ : median of unmectrl

Difference:  $\eta_1 - \eta_2$

### Descriptive Statistics

Sample	N	Median
unme c	17	3093.20
unmectrl	4	2225.87

### Estimation for Difference

Difference	CI for Difference	Achieved Confidence
542.193	(-1686.31, 5578.31)	95.61%

### Test

Null hypothesis  $H_0: \eta_1 - \eta_2 = 0$

Alternative hypothesis  $H_1: \eta_1 - \eta_2 \neq 0$

W-Value	P-Value
195.00	0.502

## Mann-Whitney: met c, met ctrl

### Method

$\eta_1$ : median of met c

$\eta_2$ : median of met ctrl

Difference:  $\eta_1 - \eta_2$

### Descriptive Statistics

Sample	N	Median
met c	17	14228.6
met ctrl	4	14028.9

### Estimation for Difference

Difference	CI for Difference	Achieved Confidence
590.122	(-1949.05, 2771.07)	95.61%

### Test

Null hypothesis  $H_0: \eta_1 - \eta_2 = 0$

Alternative hypothesis  $H_1: \eta_1 - \eta_2 \neq 0$

W-Value	P-Value
192.00	0.687

**Fig.A16** Output of Mann-Whitney test of difference from Minitab. (Left: unmethylated MSP data right: methylated MSP data) Legend: unme c: unmethylated NT cancer; unmectrl: unmethylated control; met c: methylated NT cancer; met ctrl: methylated control

## A4. Sequencing data

**Table A4** Received Beta-values Output from the MiSeq sequencing

		3T3- mouse	BeWo	breast- DNA	C-33a	DNA	Control- DNA	UCL- 1790	HCT116	HeLA	HEY	HT-3	JEG-3	MCF-7	MIDMBA 468	OAW42	OVCAR-3	SKOV-3	Annotati on
chr12	52538990	NA	NA	NA	NA	NA	NA	NA	NA	NA	NA	NA	NA	NA	0	NA	NA	NA	
chr12	52539026	NA	NA	NA	NA	NA	NA	NA	NA	NA	NA	NA	NA	NA	0	NA	NA	NA	
chr19	49520764	NA	NA	NA	NA	NA	NA	NA	100	NA	NA	100	NA	NA	NA	0	NA	NA	
chr19	49520772	NA	NA	NA	NA	NA	NA	NA	0	NA	NA	100	NA	NA	NA	100	NA	NA	
chr19	49520808	NA	NA	NA	NA	NA	NA	NA	0	NA	NA	100	NA	NA	NA	0	NA	NA	
chr19	49520867	NA	NA	0	NA	0	NA	NA	100	NA	NA	0	NA	NA	NA	0	NA	100	
chr19	49520895	NA	NA	100	NA	NA	NA	NA	100	NA	NA	100	NA	NA	NA	0	NA	NA	
chr19	49520924	NA	NA	0	NA	0	NA	NA	NA	NA	NA	0	NA	NA	NA	0	NA	100	
chr19	49520929	NA	NA	0	NA	0	NA	NA	NA	NA	NA	0	NA	NA	NA	0	NA	100	
chr19	49520935	NA	NA	0	NA	0	NA	NA	NA	NA	NA	0	NA	NA	NA	0	NA	100	
chr19	49520978	NA	NA	0	NA	0	NA	NA	NA	NA	NA	0	NA	NA	NA	0	NA	100	
chr19	49520982	NA	NA	0	NA	0	NA	NA	NA	NA	NA	0	NA	NA	NA	0	NA	100	
chr19	49520991	NA	NA	0	NA	0	NA	NA	NA	NA	NA	0	NA	NA	NA	0	NA	100	
chr19	49521004	NA	NA	100	NA	0	NA	NA	NA	NA	NA	0	NA	NA	NA	0	NA	100	
chr19	49527657	NA	56	88	92	88	90	100	98	34	75	100	44	90	94	92	84	91	CGB3-5'
chr19	49527659	NA	66	88	93	83	88	100	98	27	100	100	49	82	96	98	86	93	CGB3-5'
chr19	49527665	NA	72	100	90	85	87	100	98	26	100	100	55	81	91	91	88	92	CGB3-5'
chr19	49527701	NA	24	79	50	64	68	0	75	10	43	100	25	47	37	64	48	54	CGB3-5'
chr19	49527740	NA	34	100	79	65	78	0	94	54	100	NA	21	48	17	97	74	89	CGB3-5'
chr19	49527746	NA	30	33	49	24	41	17	82	36	57	0	12	16	13	75	51	68	CGB3-5'
chr19	49527760	NA	20	56	46	51	59	50	89	9	100	100	21	39	23	74	45	55	CGB3-5'



chr19	49527788	NA	69	89	96	96	98	75	97	88	100	0	68	92	94	95	90	93	CGB3-5'
chr19	49527817	NA	60	100	84	65	78	50	93	32	100	NA	27	44	46	90	85	81	CGB3-5'
chr19	49527829	NA	73	100	86	75	78	50	94	73	100	NA	58	69	72	84	98	93	CGB3-5'
chr19	49527837	NA	58	100	86	74	100	100	96	66	100	NA	19	66	74	91	93	92	CGB3-5'
chr19	49527876	NA	72	100	75	85	100	100	88	33	100	NA	43	68	75	86	90	79	CGB3-5'
chr19	49527904	NA	87	0	64	82	100	50	82	64	100	NA	74	71	74	82	79	82	CGB3-5'
chr19	49527912	NA	51	NA	54	65	50	100	73	41	100	NA	46	63	64	78	48	67	CGB3-5'
chr19	49546787	NA	76	66	49	74	64	48	86	61	86	87	65	53	72	82	76	73	CGB5 5'
chr19	49546793	NA	64	50	26	52	43	36	81	39	91	85	42	32	54	58	53	54	CGB5 5'
chr19	49546815	NA	67	75	65	82	93	74	84	68	89	84	57	54	83	84	81	76	CGB5 5'
chr19	49546854	NA	61	70	88	77	68	72	96	84	87	93	36	65	81	93	87	87	CGB5 5'
chr19	49546862	NA	77	79	92	82	89	92	98	85	92	93	66	71	87	93	97	86	CGB5 5'
chr19	49546869	NA	82	85	96	89	100	92	94	90	92	94	56	87	95	94	94	94	CGB5 5'
chr19	49546874	NA	81	63	88	71	95	86	97	79	89	96	55	58	43	92	93	84	CGB5 5'
chr19	49546903	NA	72	94	95	96	98	93	96	84	97	96	64	91	96	97	91	93	CGB5 5'
chr19	49546931	NA	20	30	12	32	42	26	69	21	60	81	17	16	9	47	16	46	CGB5 5'
chr19	49546945	NA	16	14	5	12	16	9	50	9	49	65	11	6	5	40	8	26	CGB5 5'
chr19	49546991	NA	28	63	42	56	53	27	87	30	75	92	22	48	44	67	27	71	CGB5 5'
chr19	49547027	NA	79	75	80	81	86	83	97	83	92	99	53	79	93	89	90	90	CGB5 5'
chr19	49547033	NA	75	84	93	87	67	93	97	87	92	95	45	92	96	93	94	94	CGB5 5'
chr19	49547035	NA	66	89	90	92	94	92	97	90	87	97	37	94	93	96	94	92	CGB5 5'
chr19	49552425	100	62	90	91	93	92	90	96	90	96	98	56	93	95	94	90	93	CGB8 5'
chr19	49552427	100	72	87	92	88	84	86	95	89	99	95	59	94	94	94	90	95	CGB8 5'
chr19	49552433	100	75	82	90	83	88	64	92	87	97	97	72	88	82	92	93	91	CGB8 5'
chr19	49552469	0	16	49	29	45	55	21	87	28	79	94	24	55	12	63	23	79	CGB8 5'
chr19	49552528	100	18	28	23	38	44	10	89	18	53	80	22	30	14	59	18	53	CGB8 5'
chr19	49552556	100	79	95	95	97	97	96	97	91	97	99	69	93	95	98	90	96	CGB8 5'
chr19	49552585	NA	70	49	85	65	88	75	94	74	97	91	47	51	41	91	77	77	CGB8 5'

chr19	49552597	NA	72	69	92	78	91	77	96	81	98	95	57	75	77	89	89	89	CGB8 5'
chr19	49552605	NA	55	64	93	70	98	88	98	81	95	93	28	69	65	90	93	92	CGB8 5'
chr19	49552644	NA	72	74	75	84	100	85	89	56	90	90	49	59	69	87	83	82	CGB8 5'
chr19	49552666	NA	64	51	31	55	74	50	83	56	92	90	36	33	56	61	48	56	CGB8 5'
chr19	49552672	NA	74	69	57	79	91	60	89	66	89	90	68	60	71	74	76	82	CGB8 5'
chr19	49552680	NA	60	39	55	61	86	53	69	54	51	68	39	47	55	67	56	73	CGB8 5'
chr19	49559061	NA	52	56	85	79	68	42	95	92	100	96	77	82	82	95	47	92	CGB7 5'
chr19	49559063	NA	65	47	90	62	59	23	86	78	100	89	71	80	82	87	29	90	CGB7 5'
chr19	49559069	NA	55	42	68	57	51	26	80	78	84	89	57	62	100	81	55	77	CGB7 5'
chr19	49559105	NA	31	81	80	89	83	93	23	90	73	90	42	75	71	85	50	84	CGB7 5'
chr19	49559151	NA	3	11	8	18	5	8	10	3	30	14	1	2	35	6	9	9	CGB7 5'
chr19	49559165	NA	2	20	6	26	20	6	12	2	40	22	7	5	10	9	10	12	CGB7 5'
chr19	49559193	NA	49	63	75	79	73	67	50	49	72	56	39	57	35	51	59	58	CGB7 5'
chr19	49559222	NA	51	45	28	2	25	33	49	11	53	50	2	7	5	27	53	15	CGB7 5'
chr19	49559227	NA	57	57	41	11	25	57	45	9	55	50	2	9	0	21	67	10	CGB7 5'
chr19	49559234	NA	57	51	32	27	25	51	54	11	66	49	16	6	5	21	65	24	CGB7 5'
chr19	49559242	NA	40	43	47	19	25	30	51	24	68	59	4	5	13	22	60	21	CGB7 5'
chr19	49559281	NA	67	60	42	56	67	71	65	26	69	66	10	22	25	47	65	39	CGB7 5'
chr19	49559301	NA	46	38	8	7	33	45	39	4	56	45	3	0	0	13	40	0	CGB7 5'
chr19	49559303	NA	58	60	22	24	33	48	63	12	84	72	13	7	10	32	53	22	CGB7 5'
chr19	49559309	NA	61	65	38	59	33	65	64	28	82	72	23	33	17	43	59	35	CGB7 5'
chr19	49559317	NA	55	45	27	52	0	44	49	24	63	65	10	21	24	41	41	30	CGB7 5'
chrM	2333	NA	NA	NA	NA	NA	100	NA	NA	NA	NA	NA	NA	NA	NA	NA	NA	NA	
chrM	2345	NA	NA	NA	NA	NA	0	NA	NA	NA	NA	NA	NA	NA	NA	NA	NA	NA	
chrM	2477	NA	NA	NA	NA	NA	100	NA	NA	NA	NA	NA	NA	NA	NA	NA	NA	NA	
chrM	2492	NA	NA	NA	NA	NA	100	NA	NA	NA	NA	NA	NA	NA	NA	NA	NA	NA	

**Table A5** Calculated M-values based on the Beta-values obtained from sequencing

gene	CpG	BeWo	breast-DNA	C-33a	cervix-DNA	Control-DNA	CRL-1790	HCT116	HeLA	HEY	HT-3	JEG-3	MCF-7	MDA-MB468	OAW42	OVCAR-3	SKOV-3
CGB3	a11	0.332575		3.603341	2.904966	3.246074		5.745955	-0.98682			-0.3322	3.190864	3.926882	3.59856	2.414046	3.415655
CGB3	a10	0.934297		3.662206	2.311732	2.861803		5.915879	-1.44144			-0.07985	2.205749	4.476814	5.559695	2.567475	3.831081
CGB3	a9	1.36257		3.148183	2.478631	2.75619		5.666351	-1.47349			0.296393	2.1165	3.288125	3.29799	2.929064	3.510461
CGB3	a8	-1.66647		-0.02223	0.839823	1.087463		1.613817	-3.10949			-1.6172	-0.19605	-0.79558	0.810428	-0.10516	0.235813
CGB3	d1	-0.95553		1.923152	0.896765	1.807355		4.07227	0.232817			-1.94662	-0.10039	-2.27599	4.897043	1.546374	2.97837
CGB3	c1	-1.25511		-0.04879	-1.6443	-0.52607		2.180121	-0.84643			-2.9169	-2.34845	-2.76129	1.551942	0.070598	1.097429
CGB3	a7	-1.9622		-0.23461	0.079999	0.554762		3.030697	-3.35614			-1.90314	-0.62758	-1.77423	1.544645	-0.2766	0.291531
CGB3	a6	1.173648		4.533432	4.411631	5.300123		5.110614	2.925269			1.109229	3.606658	4.087463	4.145488	3.172213	3.630354
CGB3	a5	0.573735		2.423682	0.870787			3.658544	-1.11171			-1.46778	-0.36463	-0.22125	3.197217	2.525462	2.106622
CGB3	a4	1.450033		2.668192	1.57414			4.058894	1.439006			0.454032	1.131438	1.384664	2.426597	5.930738	3.790638
CGB3	a3	0.478047		2.660251	1.485427			4.542527	0.987289			-2.10109	0.973926	1.506107	3.294304	3.741932	3.441598
CGB3	a2	1.378512		1.566872	2.498548			2.873043	-1.04495			-0.40054	1.065802	1.569366	2.6734	3.215013	1.900867
CGB3	a1	2.717857		0.828888	2.160647			2.233119	0.821663			1.485427	1.310223	1.475733	2.203284	1.876618	2.187627
CGB3	b1	0.068713		0.227667	0.86755	0		1.43024	-0.54749			-0.23704	0.769516	0.814444	1.815575	-0.12102	1.025091
CGB5	a1	1.69883	0.926502	-0.04891	1.501881		-0.09398	2.65966	0.672296	2.625835	2.70955	0.869744	0.177709	1.330308	2.160891	1.655352	1.44859
CGB5	e1	0.841935	-0.013	-1.54027	0.108934		-0.80735	2.050123	-0.64618	3.321928	2.492844	-0.48794	-1.06782	0.202817	0.473371	0.187527	0.254719
CGB5	a2	1.043943	1.584963	0.910139	2.232331		1.520572	2.38054	1.061076	2.946419	2.401716	0.397964	0.23012	2.302882	2.430181	2.088056	1.690045
CGB5	a3	0.666263	1.198451	2.936903	1.756804	1.115477	1.366881	4.756729	2.423542	2.686501	3.82905	-0.83446	0.879231	2.133856	3.679237	2.746068	2.720477
CGB5	a4	1.73954	1.9245	3.59614	2.22037	3.087463	3.571867	5.394124	2.514321	3.455195	3.67013	0.972906	1.294488	2.735066	3.696608	5.08625	2.594947
CGB5	f1	2.233797	2.525462	4.61471	3.036423	6.629357	3.448053	3.97429	3.201634	3.503963	3.923379	0.339052	2.739472	4.264703	4.089435	4.059781	3.880111
CGB5	a5	2.08655	0.740168	2.8391	1.316122	4.169925	2.67184	5.118489	1.942691	2.944423	4.654177	0.266336	0.484909	-0.42951	3.5869	3.736541	2.36257
CGB5	a6	1.349727	4.046142	4.115947	4.449561	5.892796	3.731281	4.753217	2.430634	4.807355	4.72792	0.840588	3.348728	4.448081	4.785329	3.315107	3.675565
CGB5	a7	-1.97199	-1.2387	-2.86262	-1.11038	-0.48294	-1.52202	1.167868	-1.87883	0.565854	2.103138	-2.32729	-2.38355	-3.38702	-0.16381	-2.41504	-0.23792
CGB5	c1	-2.42068	-2.59205	-4.15482	-2.81493	-2.37693	-3.37541	0.018958	-3.28113	-0.06319	0.870549	-2.94642	-3.95675	-4.21214	-0.58187	-3.42909	-1.47926
CGB5	a8	-1.36507	0.766887	-0.4637	0.359972	0.149344	-1.43624	2.718004	-1.20224	1.5479	3.614092	-1.80812	-0.13618	-0.33673	1.039813	-1.41219	1.318271
CGB5	a9	1.868562	1.603341	2.008364	2.050912	2.616572	2.262495	4.863118	2.242201	3.453957	6.191903	0.198183	1.944633	3.729104	2.996593	3.101917	3.098989
CGB5	a10	1.5667	2.352714	3.63743	2.716991	1.052568	3.757513	5.150942	2.695808	3.54432	4.145524	-0.31586	3.462343	4.624491	3.630843	3.987363	4.005294
CGB5	a11	0.966597	3.055444	3.126532	3.504231	4.043422	3.520909	5.148552	3.165465	2.77259	5.101037	-0.76447	3.859402	3.751544	4.539733	4.100137	3.542527
CGB8	a11	0.709704	3.184104	3.40387	3.665336	3.489966	3.160177	4.729104	3.091922	4.672425	5.296617	0.345028	3.754887	4.258734	4.025535	3.14505	3.815415
CGB8	a10	1.375509	2.767728	3.600787	2.941701	2.408876	2.617694	4.380424	3.089694	6.295642	4.16501	0.496153	4.046693	4.053111	3.921246	3.14505	4.220409
CGB8	a9	1.568488	2.158189	3.162939	2.301626	2.812563	0.829751	3.570655	2.776767	4.833574	4.816984	1.397631	2.836732	2.223454	3.59547	3.727095	3.367425
CGB8	a8	-2.39169	-0.07326	-1.25899	-0.27669	0.274251	-1.89707	2.706554	-1.3505	1.906562	4.017922	-1.6429	0.316857	-2.85137	0.787173	-1.74974	1.920128
CGB8	a7	-2.22447	-1.36234	-1.74291	-0.73647	-0.32269	-3.17734	3.086316	-2.18237	0.162615	2.007016	-1.85114	-1.18903	-2.58496	0.506369	-2.17688	0.162166
CGB8	a6	1.937587	4.205114	4.34685	5.147607	4.942983	4.470027	5.061549	3.277766	5.013984	6.576095	1.181256	3.767554	4.219814	5.501252	3.224205	4.599913
CGB8	a5	1.222392	-0.07013	2.522887	0.882867	2.925999	1.621735	3.968951	1.487468	4.925885	3.265345	-0.19071	0.031896	-0.53219	3.426797	1.747019	1.754325
CGB8	a4	1.368445	1.139823	3.546422	1.852193	3.285402	1.724597	4.729404	2.083017	5.29749	4.366782	0.389771	1.577831	1.719794	3.08801	3.087463	3.039966

<b>CGB8</b>	<b>a3</b>	0.283426	0.835597	3.793465	1.215013	5.392318	2.885252	5.590961	2.049244	4.258136	3.673634	-1.39818	1.134961	0.902878	3.232661	3.758276	3.449611
<b>CGB8</b>	<b>a2</b>	1.369695	1.487977	1.603857	2.359081	6.629357	2.488101	2.97537	0.343853	3.097697	3.095157	-0.04108	0.541709	1.174874	2.767091	2.274941	2.203872
<b>CGB8</b>	<b>e1</b>	0.841818	0.061001	-1.17284	0.292409	1.5025	-0.01132	2.271655	0.374589	3.485846	3.111508	-0.8225	-0.99165	0.345135	0.616111	-0.09558	0.350907
<b>CGB8</b>	<b>a1</b>	1.49526	1.135437	0.41622	1.901682	3.321928	0.571842	3.070389	0.97777	3.07298	3.200952	1.114216	0.578703	1.326756	1.495186	1.693684	2.20014
<b>CGB8</b>	<b>b1</b>	0.560715	-0.67479	0.304087	0.663475	2.584963	0.1676	1.162271	0.238288	0.046867	1.092849	-0.62149	-0.15347	0.279617	1.045229	0.36759	1.402098
<b>CGB7</b>	<b>a11</b>	0.106915	0.318822	2.459432	1.944657	1.061776	-0.46467	4.386059	3.449307	6.629357	4.566815	1.731183	2.174498	2.169925	4.380822	-0.16992	3.551796
<b>CGB7</b>	<b>a10</b>	0.881356	-0.152	3.147307	0.719892	0.545968	-1.76867	2.656046	1.8314	6.629357	3.013297	1.31259	1.986061	2.169925	2.697265	-1.26303	3.132156
<b>CGB7</b>	<b>a9</b>	0.263034	-0.46042	1.06114	0.39752	0.08017	-1.50546	2.034646	1.805272	2.432959	2.972693	0.393342	0.693424	6.629357	2.09818	0.263034	1.733756
<b>CGB7</b>	<b>a8</b>	-1.12801	2.124328	2.02526	3.053298	2.307428	3.767339	-1.70974	3.206029	1.447459	3.187244	-0.455	1.57447	1.321928	2.476586	0	2.357279
<b>CGB7</b>	<b>c1</b>	-4.88753	-3.07621	-3.53325	-2.23704	-4.30743	-3.52788	-3.12338	-5.18587	-1.22239	-2.56906	-6.84549	-5.50885	-0.89308	-3.92539	-3.33298	-3.41504
<b>CGB7</b>	<b>a7</b>	-5.94642	-2.04439	-3.90138	-1.49513	-2.01436	-3.89308	-2.88408	-5.47168	-0.58496	-1.80453	-3.83008	-4.37504	-3.22239	-3.39232	-3.16993	-2.84874
<b>CGB7</b>	<b>a6</b>	-0.0813	0.754888	1.584963	1.86994	1.431951	0.993367	-0.01355	-0.03395	1.353637	0.354843	-0.62344	0.424885	-0.90689	0.071553	0.530515	0.454032
<b>CGB7</b>	<b>a5</b>	0.054448	-0.27357	-1.34958	-5.9542		-1.04975	-0.05772	-3	0.167295	0	-5.78136	-3.66297	-4.16992	-1.4458	0.195016	-2.48543
<b>CGB7</b>	<b>f1</b>	0.383329	0.431716	-0.52793	-3.05889		0.380031	-0.28951	-3.36923	0.311944	0.015942	-5.67243	-3.38247	-6.62936	-1.89308	1.013806	-3.11548
<b>CGB7</b>	<b>a4</b>	0.383329	0.08573	-1.09954	-1.4361		0.033553	0.226771	-3.01495	0.958421	-0.03206	-2.35364	-4	-4.16992	-1.86876	0.920566	-1.64386
<b>CGB7</b>	<b>a3</b>	-0.56188	-0.40663	-0.16046	-2.05889		-1.23447	0.057715	-1.65711	1.110054	0.551642	-4.75489	-4.2854	-2.72247	-1.79837	0.606989	-1.89308
<b>CGB7</b>	<b>a2</b>	1	0.593375	-0.47207	0.353637		1.26628	0.91427	-1.5025	1.164387	0.983512	-3.16993	-1.8413	-1.58496	-0.16046	0.906891	-0.63743
<b>CGB7</b>	<b>g1</b>	-0.22239	-0.72085	-3.5025	-3.66297		-0.27563	-0.66558	-4.45943	0.3254	-0.28728	-5.2854	-6.62936	-6.62936	-2.80735	-0.58496	-6.62936
<b>CGB7</b>	<b>e1</b>	0.459432	0.576501	-1.80735	-1.63227		-0.1375	0.747234	-2.93074	2.39689	1.345135	-2.80735	-3.67243	-3.24793	-1.09115	0.17585	-1.848
<b>CGB7</b>	<b>a1</b>	0.616671	0.863938	-0.70454	0.4975		0.880418	0.854149	-1.39593	2.212994	1.394279	-1.78427	-1.03953	-2.32193	-0.37851	0.532874	-0.90689
<b>CGB7</b>	<b>b1</b>	0.289507	-0.27009	-1.44746	0.106915		-0.3388	-0.074	-1.62803	0.792195	0.869939	-3.24793	-1.89308	-1.67807	-0.53051	-0.53051	-1.22239



## A5.2 PCA

```
db<-read.csv("~/b-values3.csv")
pca <- prcomp(t(db<- as.matrix), scale=TRUE)
plot(pca$x[,1], pca$x[,2])
pca.var <- pca$sdev^2
pca.var.per <- round(pca.var/sum(pca.var)*100, 1)
barplot(pca.var.per, main="Scree Plot", xlab="Principal Component", ylab="Percent Variati
on")

library(ggplot2)
pca.data <- data.frame(Sample=rownames(pca$x),
                        X=pca$x[,1],
                        Y=pca$x[,2])

pca.data
ggplot(data=pca.data, aes(x=X, y=Y, label=Sample)) +
  geom_text() +
  xlab(paste("PC1 - ", pca.var.per[1], "%", sep="")) +
  ylab(paste("PC2 - ", pca.var.per[2], "%", sep="")) +
  theme_bw() +
  ggtitle("My PCA Graph")
```

**Fig.A18** Code in R to produce the Scree plot and PCA plot. Code adapted from [https://github.com/StatQuest/pca\\_demo/blob/master/pca\\_demo.R](https://github.com/StatQuest/pca_demo/blob/master/pca_demo.R)

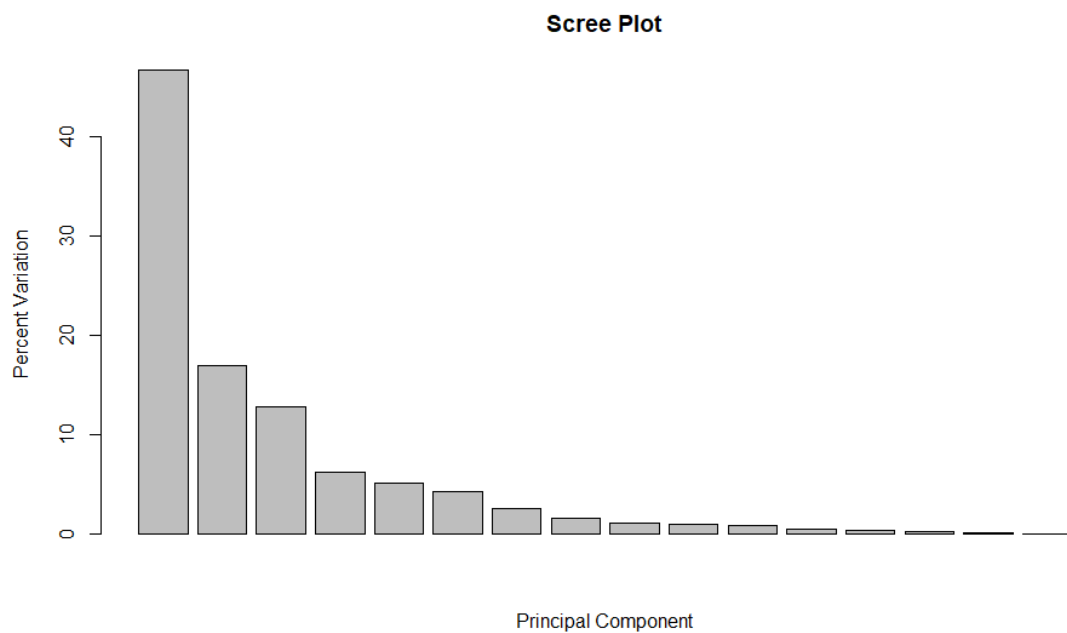


**Fig.A19** Scree plot based on the methylation data used in PCA. Produced with R

## A6. Analyses of difference

### A6.1 Average Promoter methylation

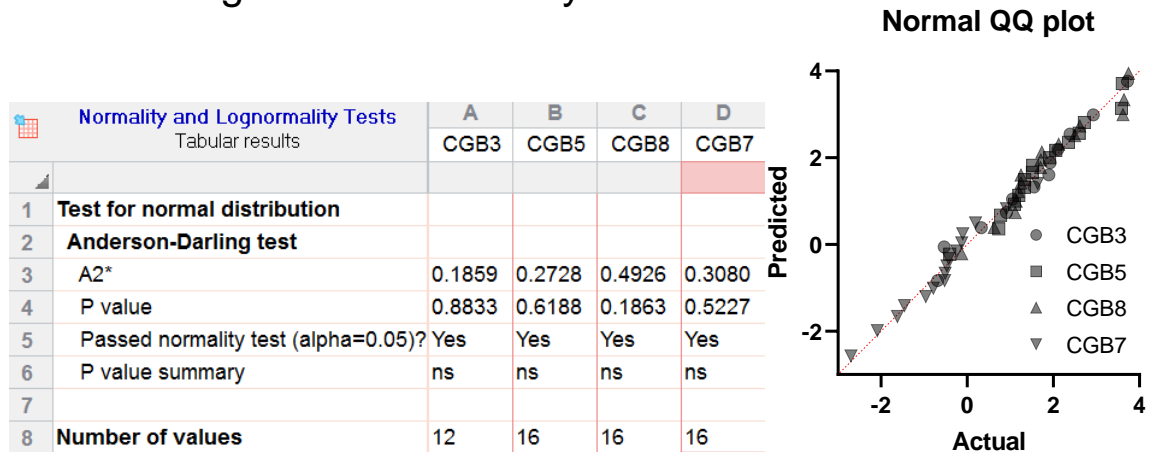


**Fig.A20** Normality test of average promoter methylation. Produced by Prism8 (Left: Anderson-Darling test output; right: plot of Normality test)

	SS	DF	MS	F (DFn, DFd)	P value
23 ANOVA table					
24 Treatment (between columns)	62.88	3	20.96	F (3, 56) = 16	P<0.0001
25 Residual (within columns)	71.83	56	1.283		
26 Total	134.7	59			

**Fig.A21** Ordinary one-way ANOVA output of the average promoter methylation by gene. Produced by Prism8

Ordinary one-way ANOVA						
Multiple comparisons						
1	Number of families	1				
2	Number of comparisons per family	6				
3	Alpha	0.05				
4						
5	Tukey's multiple comparisons test	Mean Diff.	95.00% CI of diff.	Significant?	Summary	Adjusted P Value
6	CGB3 vs. CGB5	-0.2813	-1.427 to 0.8639	No	ns	0.9149
7	CGB3 vs. CGB8	-0.3990	-1.544 to 0.7462	No	ns	0.7929
8	CGB3 vs. CGB7	2.047	0.9016 to 3.192	Yes	****	<0.0001
9	CGB5 vs. CGB8	-0.1176	-1.178 to 0.9426	No	ns	0.9911
10	CGB5 vs. CGB7	2.328	1.268 to 3.388	Yes	****	<0.0001
11	CGB8 vs. CGB7	2.446	1.386 to 3.506	Yes	****	<0.0001

**Fig.A22** Ordinary one-way ANOVA Multiple comparisons output of the average promoter methylation by gene (Tukey's test). Produced by Prism8

## A6.2 Average promoter methylation vs cancer type

Kruskal-Wallis test		
ANOVA results		
1	Table Analyzed	Average methylation of the promoter
2		
3	<b>Kruskal-Wallis test</b>	
4	P value	0.0404
5	Exact or approximate P value?	Exact
6	P value summary	*
7	Do the medians vary signif. (P < 0.05)?	Yes
8	Number of groups	3
9	Kruskal-Wallis statistic	5.698
10		
11	<b>Data summary</b>	
12	Number of treatments (columns)	3
13	Number of values (total)	16

**Fig.A23** Analysis of difference between the average methylation of *CGB3*, 5 & 8 in the 3 groups of cell line cancer type (T, NT, and Control). Kruskal-Wallis Test on Prism8

Kruskal-Wallis test							
Multiple comparisons							
1	Number of families	1					
2	Number of comparisons per family	3					
3	Alpha	0.05					
4							
5	<b>Dunn's multiple comparisons test</b>	<b>Mean rank diff.</b>	<b>Significant?</b>	<b>Summary</b>	<b>Adjusted P Value</b>		
6	trophoblastic cell lines vs. non-trophoblastic cell lines	-8.700	No	ns	0.0550	A-B	
7	trophoblastic cell lines vs. control samples DNA	-6.250	No	ns	0.3887	A-C	
8	non-trophoblastic cell lines vs. control samples DNA	2.450	No	ns	>0.9999	B-C	
9							
10	<b>Test details</b>	<b>Mean rank 1</b>	<b>Mean rank 2</b>	<b>Mean rank diff.</b>	<b>n1</b>	<b>n2</b>	<b>Z</b>
11	trophoblastic cell lines vs. non-trophoblastic cell lines	1.500	10.20	-8.700	2	10	2.359
12	trophoblastic cell lines vs. control samples DNA	1.500	7.750	-6.250	2	4	1.516
13	non-trophoblastic cell lines vs. control samples DNA	10.20	7.750	2.450	10	4	0.8698

**Fig.A24** Multiple comparisons between the average methylation of *CGB3*, 5 & 8 in the 3 groups of cell line cancer type (T, NT, and Control). Dunn's test (Kruskal-Wallis test) on Prism8

Kruskal-Wallis test		
ANOVA results		
1	Table Analyzed	AP2-SP-AP2-Oct3/4 region
2		
3	<b>Kruskal-Wallis test</b>	
4	P value	0.3759
5	Exact or approximate P value?	Exact
6	P value summary	ns
7	Do the medians vary signif. (P < 0.05)?	No
8	Number of groups	3
9	Kruskal-Wallis statistic	2.144
10		
11	<b>Data summary</b>	
12	Number of treatments (columns)	3
13	Number of values (total)	16

**Fig.A25** Analysis of difference between the average 5' promoter region methylation of *CGB3*, 5 & 8 in the 3 groups of cell line cancer type (T, NT, and Control). Kruskal-Wallis Test on Prism8



Kruskal-Wallis test		
ANOVA results		
1	Table Analyzed	AP2-SP1 region
2		
3	<b>Kruskal-Wallis test</b>	
4	P value	0.0634
5	Exact or approximate P value?	Exact
6	P value summary	ns
7	Do the medians vary signif. (P < 0.05)?	No
8	Number of groups	3
9	Kruskal-Wallis statistic	5.080
10		
11	<b>Data summary</b>	
12	Number of treatments (columns)	3
13	Number of values (total)	16

**Fig.A26** Analysis of difference between the average 3' promoter region methylation of *CGB3*, 5 & 8 in the 3 groups of cell line cancer type (T, NT, and Control). Kruskal-Wallis Test on Prism8

Kruskal-Wallis test		
ANOVA results		
1	Table Analyzed	average promoter CGB7
2		
3	<b>Kruskal-Wallis test</b>	
4	P value	0.3428
5	Exact or approximate P value?	Exact
6	P value summary	ns
7	Do the medians vary signif. (P < 0.05)?	No
8	Number of groups	3
9	Kruskal-Wallis statistic	2.345
10		
11	<b>Data summary</b>	
12	Number of treatments (columns)	3
13	Number of values (total)	16

**Fig.A27** Analysis of difference between the average promoter methylation of *CGB7* in the 3 groups of cell line cancer type (T, NT, and Control). Kruskal-Wallis Test on Prism8

Kruskal-Wallis test		
ANOVA results		
1	Table Analyzed	AP2-SP1-AP"-OCT CGB7
2		
3	<b>Kruskal-Wallis test</b>	
4	P value	0.8521
5	Exact or approximate P value?	Exact
6	P value summary	ns
7	Do the medians vary signif. (P < 0.05)?	No
8	Number of groups	3
9	Kruskal-Wallis statistic	0.3750
10		
11	<b>Data summary</b>	
12	Number of treatments (columns)	3
13	Number of values (total)	15

**Fig.A28** Analysis of difference between the average 5' promoter region methylation of CGB7 in the 3 groups of cell line cancer type (T, NT, and Control). Kruskal-Wallis Test on Prism8

Kruskal-Wallis test		
1	Table Analyzed	AP2-SP1 cgb7
2		
3	<b>Kruskal-Wallis test</b>	
4	P value	0.4372
5	Exact or approximate P value?	Exact
6	P value summary	ns
7	Do the medians vary signif. (P < 0.05)?	No
8	Number of groups	3
9	Kruskal-Wallis statistic	1.815
10		
11	<b>Data summary</b>	
12	Number of treatments (columns)	3
13	Number of values (total)	16

**Fig.A29** Analysis of difference between the average 3' promoter region methylation of CGB7 in the 3 groups of cell line cancer type (T, NT, and Control). Kruskal-Wallis Test on Prism8

## A6.3 Average promoter methylation vs cell line origin

### A6.3.1 Choriocarcinoma cell lines

Normality and Lognormality Tests Tabular results	A	B	C
	BeWo	JEG-3	Control-DNA
<b>Test for normal distribution</b>			
<b>Anderson-Darling test</b>			
A2*	0.9541	0.3285	0.2604
P value	0.0118	0.4810	0.6615
Passed normality test (alpha=0.05)?	No	Yes	Yes
P value summary	*	ns	ns
<b>Number of values</b>	16	16	16

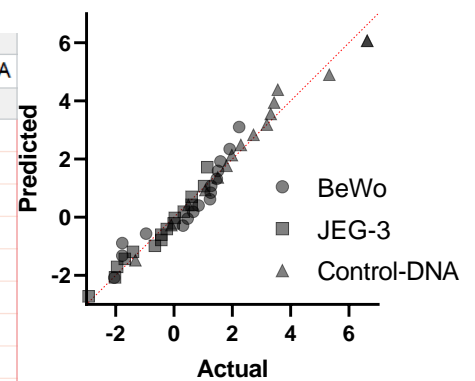


**Fig.A30** Normality test of average promoter methylation for *CGB3*, 5 & 8 in choriocarcinoma group. Produced by Prism8 (Left: Anderson-Darling test output; right: plot of Normality test)

RM one-way ANOVA ANOVA results		
1	Table Analyzed	chorio
2		
3	<b>Repeated measures ANOVA summary</b>	
4	Assume sphericity?	No
5	F	51.56
6	P value	<0.0001
7	P value summary	****
8	Statistically significant (P < 0.05)?	Yes
9	Geisser-Greenhouse's epsilon	0.6067
10	R squared	0.7746

**Fig.A31** RM one-way ANOVA output of the average promoter methylation for *CGB3*, 5 & 8 in choriocarcinoma group. Produced by Prism8

RM one-way ANOVA Multiple comparisons						
1	Number of families	1				
2	Number of comparisons per family	3				
3	Alpha	0.05				
4						
5	<b>Tukey's multiple comparisons test</b>	<b>Mean Diff.</b>	<b>95.00% CI of diff.</b>	<b>Significant?</b>	<b>Summary</b>	<b>Adjusted P Value</b>
6	BeWo vs. JEG-3	1.015	0.6352 to 1.395	Yes	****	<0.0001
7	BeWo vs. Control-DNA	-2.145	-3.069 to -1.222	Yes	****	<0.0001
8	JEG-3 vs. Control-DNA	-3.160	-4.183 to -2.137	Yes	****	<0.0001

**Fig.A32** RM one-way ANOVA Multiple comparisons output of the average promoter methylation for *CGB3*, 5 & 8 in choriocarcinoma group (Tukey's test). Produced by Prism8

### A6.3.2 Ovarian cell lines

Normality and Lognormality Tests Tabular results	A	B	C	D	E
	HEY	OAW42	OVCAR-3	SKOV-3	Control-DNA
<b>Test for normal distribution</b>					
<b>Anderson-Darling test</b>					
A2*	1.438	0.4895	0.7273	0.4963	0.2604
P value	0.0007	0.1898	0.0460	0.1822	0.6615
Passed normality test (alpha=0.05)?	No	Yes	No	Yes	Yes
P value summary	***	ns	*	ns	ns
<b>Number of values</b>	16	16	16	16	16

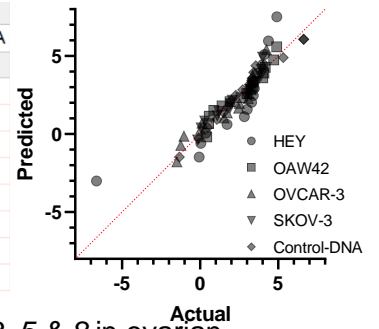


**Fig.A33** Normality test of average promoter methylation for *CGB3*, 5 & 8 in ovarian group. Produced by Prism8 (Left: Anderson-Darling test output; right: plot of Normality test)

RM one-way ANOVA	
ANOVA results	
1	Table Analyzed
2	
3	<b>Repeated measures ANOVA summary</b>
4	Assume sphericity?
5	F
6	P value
7	P value summary
8	Statistically significant (P < 0.05)?
9	Geisser-Greenhouse's epsilon
10	R squared

**Fig.A34** RM one-way ANOVA output of the average promoter methylation for *CGB3*, 5 & 8 in choriocarcinoma group. Produced by Prism8

### A6.3.3 Control group

Normality and Lognormality Tests Tabular results	A	B	C	D
	breast-DNA	cervix-DNA	CRL1790	Control-DNA
<b>Test for normal distribution</b>				
<b>Anderson-Darling test</b>				
A2*	0.5651	0.1468	0.5447	0.2604
P value	0.1193	0.9565	0.1355	0.6615
Passed normality test (alpha=0.05)?	Yes	Yes	Yes	Yes
P value summary	ns	ns	ns	ns
<b>Number of values</b>	16	16	16	16

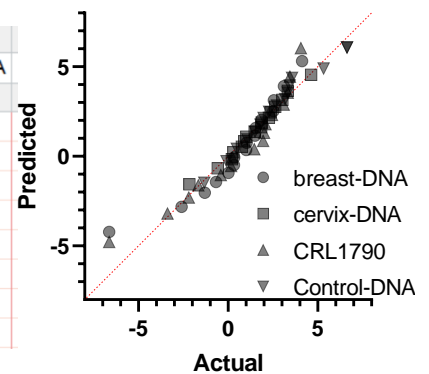


**Fig.A35** Normality test of average promoter methylation for *CGB3*, 5 & 8 in control group. Produced by Prism8 (Left: Anderson-Darling test output; right: plot of Normality test)

RM one-way ANOVA		
ANOVA results		
1	Table Analyzed	control
2		
3	<b>Repeated measures ANOVA summary</b>	
4	Assume sphericity?	No
5	F	9.634
6	P value	0.0014
7	P value summary	**
8	Statistically significant (P < 0.05)?	Yes
9	Geisser-Greenhouse's epsilon	0.5525
10	R squared	0.3911

**Fig.A36** RM one-way ANOVA output of the average promoter methylation for *CGB3*, 5 & 8 in control group. Produced by Prism8

RM one-way ANOVA						
Multiple comparisons						
1	Number of families	1				
2	Number of comparisons per family	6				
3	Alpha	0.05				
4						
5	<b>Tukey's multiple comparisons test</b>	<b>Mean Diff.</b>	<b>95.00% CI of diff.</b>	<b>Significant?</b>	<b>Summary</b>	<b>Adjusted P Value</b>
6	breast-DNA vs. cervix-DNA	-0.9464	-2.236 to 0.3429	No	ns	0.1928
7	breast-DNA vs. CRL1790	-0.07971	-0.7591 to 0.5997	No	ns	0.9862
8	breast-DNA vs. Control-DNA	-2.113	-3.702 to -0.5236	Yes	**	0.0079
9	cervix-DNA vs. CRL1790	0.8667	-0.5643 to 2.298	No	ns	0.3360
10	cervix-DNA vs. Control-DNA	-1.167	-2.089 to -0.2444	Yes	*	0.0114
11	CRL1790 vs. Control-DNA	-2.033	-3.603 to -0.4632	Yes	**	0.0096

**Fig.A37** RM one-way ANOVA Multiple comparisons output of the average promoter methylation for *CGB3*, 5 & 8 in control group (Tukey's test). Produced by Prism8

### A6.3.4 Cervical group

Normality and Lognormality Tests		A	B	C	D
Tabular results		HT3	C33a	HeLA	cervix-DNA
1	<b>Test for normal distribution</b>				
2	<b>Anderson-Darling test</b>				
3	A2*	1.467	0.4873	0.2728	0.1468
4	P value	0.0006	0.1923	0.6188	0.9565
5	Passed normality test (alpha=0.05)?	No	Yes	Yes	Yes
6	P value summary	***	ns	ns	ns
7					
8	Number of values	16	16	16	16

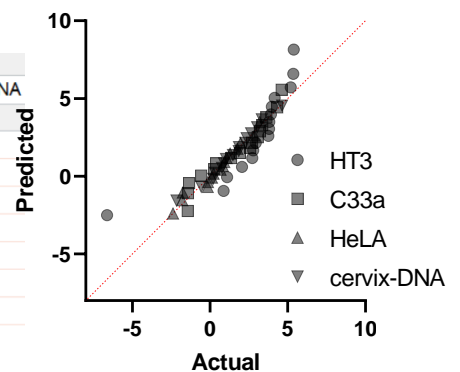


**Fig.A38** Normality test of average promoter methylation for *CGB3*, 5 & 8 in cervical group. Produced by Prism8 (Left: Anderson-Darling test output; right: plot of Normality test)

RM one-way ANOVA ANOVA results		
1	Table Analyzed	cervical
2		
3	<b>Repeated measures ANOVA summary</b>	
4	Assume sphericity?	No
5	F	6.544
6	P value	0.0125
7	P value summary	*
8	Statistically significant (P < 0.05)?	Yes
9	Geisser-Greenhouse's epsilon	0.4485
10	R squared	0.3037

**Fig.A39** RM one-way ANOVA output of the average promoter methylation for *CGB3*, 5 & 8 in cervical group. Produced by Prism8

RM one-way ANOVA Multiple comparisons						
1	Number of families	1				
2	Number of comparisons per family	6				
3	Alpha	0.05				
4						
5	<b>Tukey's multiple comparisons test</b>	<b>Mean Diff.</b>	<b>95.00% CI of diff.</b>	<b>Significant?</b>	<b>Summary</b>	<b>Adjusted P Value</b>
6	HT3 vs. C33a	1.157	-0.9566 to 3.271	No	ns	0.4195
7	HT3 vs. HeLA	2.280	0.3113 to 4.249	Yes	*	0.0209
8	HT3 vs. cervix-DNA	1.330	-0.5197 to 3.180	No	ns	0.2066
9	C33a vs. HeLA	1.122	0.4354 to 1.810	Yes	**	0.0014
10	C33a vs. cervix-DNA	0.1727	-0.6375 to 0.9829	No	ns	0.9259
11	HeLA vs. cervix-DNA	-0.9498	-1.607 to -0.2925	Yes	**	0.0041

**Fig.A40** RM one-way ANOVA Multiple comparisons output of the average promoter methylation for *CGB3*, 5 & 8 in cervical group (Tukey's test). Produced by Prism8

### A6.3.5 Breast group

Normality and Lognormality Tests Tabular results	A	B	C
	MCF-7	MDA468	breast-DNA
<b>Test for normal distribution</b>			
<b>Anderson-Darling test</b>			
A2*	0.2635	0.3135	0.5651
P value	0.6506	0.5131	0.1193
Passed normality test (alpha=0.05)?	Yes	Yes	Yes
P value summary	ns	ns	ns
<b>Number of values</b>	16	16	16

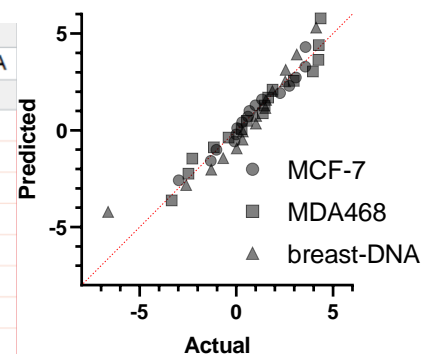


**Fig.A41** Normality test of average promoter methylation for *CGB3*, 5 & 8 in breast group. Produced by Prism8 (Left: Anderson-Darling test output; right: plot of Normality test)

RM one-way ANOVA		
ANOVA results		
1	Table Analyzed	breast
2		
3	<b>Repeated measures ANOVA summary</b>	
4	Assume sphericity?	No
5	F	1.154
6	P value	0.3194
7	P value summary	ns
8	Statistically significant (P < 0.05)?	No
9	Geisser-Greenhouse's epsilon	0.7571
10	R squared	0.07142

**Fig.A42** RM one-way ANOVA output of the average promoter methylation for *CGB3*, 5 & 8 in breast group. Produced by Prism8

### A6.3.6 Colon group

Normality and Lognormality Tests		A	B
Tabular results		CRL1790	HCT116
1	<b>Test for normal distribution</b>		
2	<b>Anderson-Darling test</b>		
3	A2*	0.5289	0.6057
4	P value	0.1611	0.1081
5	Passed normality test (alpha=0.05)?	Yes	Yes
6	P value summary	ns	ns
7			
8	<b>Number of values</b>	27	41

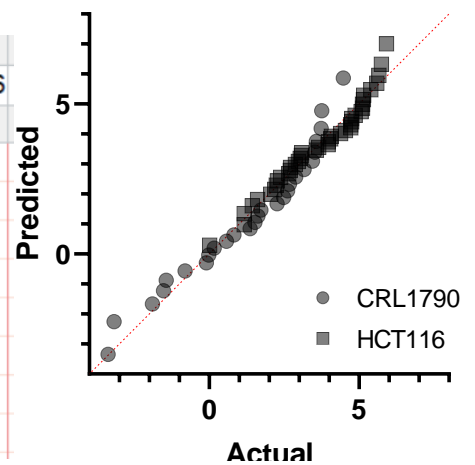


**Fig.A43** Normality test of average promoter methylation for *CGB3*, 5 & 8 in colon group. Produced by Prism8 (Left: Anderson-Darling test output; right: plot of Normality test)

1	Table Analyzed	colon
2		
3	Column B	HCT116
4	vs.	vs.
5	Column A	CRL1790
6		
7	<b>Paired t test</b>	
8	P value	<0.0001
9	P value summary	****
10	Significantly different (P < 0.05)?	Yes
11	One- or two-tailed P value?	Two-tailed
12	t, df	t=9.217, df=26
13	Number of pairs	27
14		
15	<b>How big is the difference?</b>	
16	Mean of differences (B - A)	2.348
17	SD of differences	1.324
18	SEM of differences	0.2547
19	95% confidence interval	1.824 to 2.871
20	R squared (partial eta squared)	0.7657

**Fig.A44** Paired t test output of the average promoter methylation for *CGB3*, 5 & 8 in breast group. Produced by Prism8

### A6.3.7 Choriocarcinoma group (*CGB7*)

Normality and Lognormality Tests Tabular results		A	B	C
		JEG-3	BeWo	CRL1790
1	<b>Test for normal distribution</b>			
2	<b>Anderson-Darling test</b>			
3	A2*	0.2082	2.410	0.3403
4	P value	0.8358	<0.0001	0.4504
5	Passed normality test (alpha=0.05)?	Yes	No	Yes
6	P value summary	ns	****	ns
7				
8	<b>Number of values</b>	16	16	16

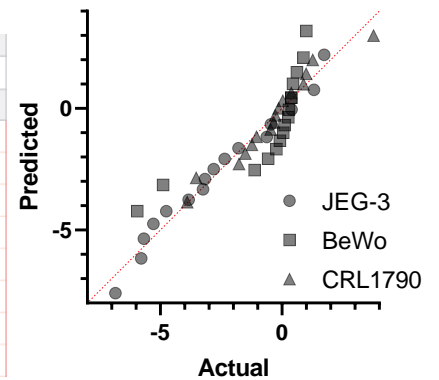


**Fig.A45** Normality test of average promoter methylation for *CGB7* in choriocarcinoma group. Produced by Prism8 (Left: Anderson-Darling test output; right: plot of Normality test)

RM one-way ANOVA ANOVA results		
1	<b>Table Analyzed</b>	chorio cgb7
2		
3	<b>Repeated measures ANOVA summary</b>	
4	Assume sphericity?	No
5	F	9.127
6	P value	0.0020
7	P value summary	**
8	Statistically significant (P < 0.05)?	Yes
9	Geisser-Greenhouse's epsilon	0.8050
10	R squared	0.3783

**Fig.A46** RM one-way ANOVA output of the average promoter methylation for *CGB7* in choriocarcinoma group. Produced by Prism8

RM one-way ANOVA Multiple comparisons						
1	Number of families	1				
2	Number of comparisons per family	3				
3	Alpha	0.05				
4						
5	<b>Tukey's multiple comparisons test</b>	<b>Mean Diff.</b>	<b>95.00% CI of diff.</b>	<b>Significant?</b>	<b>Summary</b>	<b>Adjusted P Value</b>
6	JEG-3 vs. BeWo	-2.174	-3.884 to -0.4638	Yes	*	0.0126
7	JEG-3 vs. CRL1790	-2.269	-4.040 to -0.4974	Yes	*	0.0120
8	BeWo vs. CRL1790	-0.09466	-1.209 to 1.020	No	ns	0.9736

**Fig.A47** RM one-way ANOVA Multiple comparisons output of the average promoter methylation for *CGB7* in choriocarcinoma group (Tukey's test). Produced by Prism8



### A6.3.8 Ovarian group (CGB7)

Normality and Lognormality Tests Tabular results	A	B	C	D	E
	HEY	OAW42	OVCAR-3	SKOV-3	CRL1790
<b>Test for normal distribution</b>					
<b>Anderson-Darling test</b>					
A2*	1.143	0.3843	1.240	0.3352	0.3403
P value	0.0038	0.3516	0.0021	0.4633	0.4504
Passed normality test (alpha=0.05)?	No	Yes	No	Yes	Yes
P value summary	**	ns	**	ns	ns
<b>Number of values</b>	16	16	16	16	16

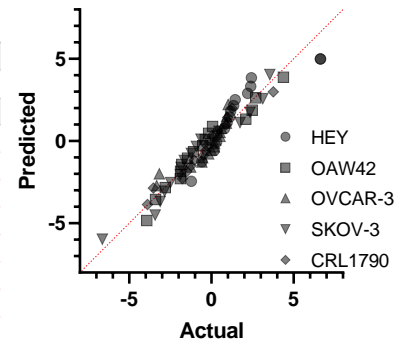


**Fig.A48** Normality test of average promoter methylation for *CGB7* in ovarian group. Produced by Prism8 (Left: Anderson-Darling test output; right: plot of Normality test)

RM one-way ANOVA ANOVA results		
1	Table Analyzed	ovarian cgb7
2		
3	<b>Repeated measures ANOVA summary</b>	
4	Assume sphericity?	No
5	F	6.985
6	P value	0.0047
7	P value summary	**
8	Statistically significant (P < 0.05)?	Yes
9	Geisser-Greenhouse's epsilon	0.4468
10	R squared	0.3177

**Fig.A49** RM one-way ANOVA output of the average promoter methylation for *CGB7* in ovarian group. Produced by Prism8

RM one-way ANOVA Multiple comparisons						
1	Number of families	1				
2	Number of comparisons per family	10				
3	Alpha	0.05				
4						
5	<b>Tukey's multiple comparisons test</b>	<b>Mean Diff.</b>	<b>95.00% CI of diff.</b>	<b>Significant?</b>	<b>Summary</b>	<b>Adjusted P Value</b>
6	HEY vs. OAW42	2.106	1.136 to 3.076	Yes	****	<0.0001
7	HEY vs. OVCAR-3	1.877	0.07284 to 3.681	Yes	*	0.0396
8	HEY vs. SKOV-3	2.596	1.276 to 3.917	Yes	***	0.0002
9	HEY vs. CRL1790	2.062	-0.006638 to 4.132	No	ns	0.0509
10	OAW42 vs. OVCAR-3	-0.2288	-1.999 to 1.542	No	ns	0.9941
11	OAW42 vs. SKOV-3	0.4906	-0.3234 to 1.305	No	ns	0.3777
12	OAW42 vs. CRL1790	-0.04327	-1.821 to 1.734	No	ns	>0.9999
13	OVCAR-3 vs. SKOV-3	0.7194	-1.421 to 2.860	No	ns	0.8341
14	OVCAR-3 vs. CRL1790	0.1856	-0.8010 to 1.172	No	ns	0.9759
15	SKOV-3 vs. CRL1790	-0.5339	-2.698 to 1.630	No	ns	0.9377

**Fig.A50** RM one-way ANOVA Multiple comparisons output of the average promoter methylation for *CGB7* in ovarian group (Tukey's test). Produced by Prism8

### A6.3.9 Control group (CGB7)

Normality and Lognormality Tests Tabular results		A	B	C
		CRL1790	breast-DNA	cervix-DNA
1	Test for normal distribution			
2	Anderson-Darling test			
3	A2*	0.3403	0.6465	0.2515
4	P value	0.4504	0.0747	0.6929
5	Passed normality test (alpha=0.05)?	Yes	Yes	Yes
6	P value summary	ns	ns	ns
7				
8	Number of values	16	16	16

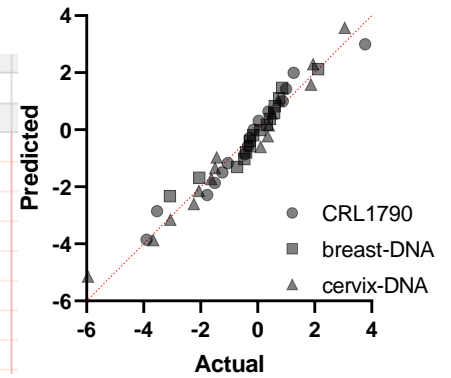


**Fig.A51** Normality test of average promoter methylation for *CGB7* in control group. Produced by Prism8 (Left: Anderson-Darling test output; right: plot of Normality test)

RM one-way ANOVA ANOVA results		
1	Table Analyzed	control cgb7
2		
3	Repeated measures ANOVA summary	
4	Assume sphericity?	No
5	F	1.119
6	P value	0.3188
7	P value summary	ns
8	Statistically significant (P < 0.05)?	No
9	Geisser-Greenhouse's epsilon	0.6185
10	R squared	0.06940

**Fig.A52** RM one-way ANOVA output of the average promoter methylation for *CGB7* in control group. Produced by Prism8

### A6.3.10 Cervical group (CGB7)

Normality and Lognormality Tests Tabular results		A	B	C	D
		C33a	HT3	HeLA	cervix-DNA
1	Test for normal distribution				
2	Anderson-Darling test				
3	A2*	0.2796	0.3506	0.4217	0.2515
4	P value	0.5967	0.4252	0.2835	0.6929
5	Passed normality test (alpha=0.05)?	Yes	Yes	Yes	Yes
6	P value summary	ns	ns	ns	ns
7					
8	Number of values	16	16	16	16

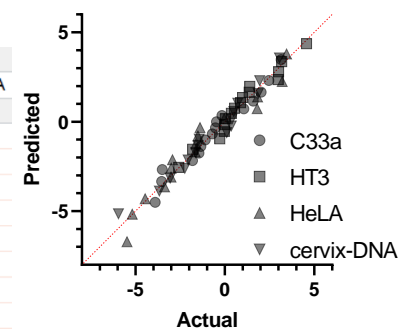


**Fig.A53** Normality test of average promoter methylation for *CGB7* in cervical group. Produced by Prism8 (Left: Anderson-Darling test output; right: plot of Normality test)

RM one-way ANOVA ANOVA results		
1	Table Analyzed	cervix cgb7
2		
3	<b>Repeated measures ANOVA summary</b>	
4	Assume sphericity?	No
5	F	13.38
6	P value	<0.0001
7	P value summary	****
8	Statistically significant (P < 0.05)?	Yes
9	Geisser-Greenhouse's epsilon	0.7434
10	R squared	0.4715

**Fig.A54** RM one-way ANOVA output of the average promoter methylation for *CGB7* in cervical group. Produced by Prism8

RM one-way ANOVA Multiple comparisons						
1	Number of families	1				
2	Number of comparisons per family	6				
3	Alpha	0.05				
4						
5	<b>Tukey's multiple comparisons test</b>	<b>Mean Diff.</b>	<b>95.00% CI of diff.</b>	<b>Significant?</b>	<b>Summary</b>	<b>Adjusted P Value</b>
6	C33a vs. HT3	-1.424	-2.252 to -0.5971	Yes	***	0.0009
7	C33a vs. HeLA	0.9456	0.1427 to 1.749	Yes	*	0.0187
8	C33a vs. cervix-DNA	0.2728	-1.042 to 1.587	No	ns	0.9311
9	HT3 vs. HeLA	2.370	1.445 to 3.295	Yes	****	<0.0001
10	HT3 vs. cervix-DNA	1.697	0.3694 to 3.025	Yes	*	0.0106
11	HeLA vs. cervix-DNA	-0.6728	-1.991 to 0.6457	No	ns	0.4780

**Fig.A55** RM one-way ANOVA Multiple comparisons output of the average promoter methylation for *CGB7* in cervical group (Tukey's test). Produced by Prism8

### A6.3.11 Breast group (*CGB7*)

Normality and Lognormality Tests Tabular results			
	A	B	C
	MCF-7	MDA468	breast-DNA
1	<b>Test for normal distribution</b>		
2	<b>Anderson-Darling test</b>		
3	A2*	0.4268	0.3483
4	P value	0.2752	0.4309
5	Passed normality test (alpha=0.05)?	Yes	Yes
6	P value summary	ns	ns
7			
8	Number of values	16	16

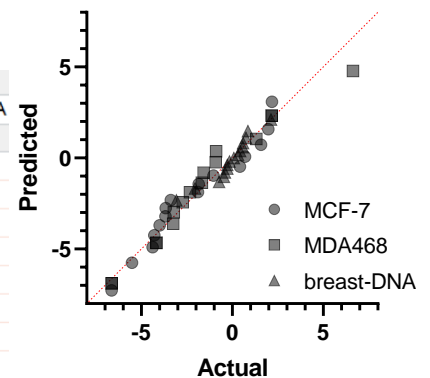


**Fig.A56** Normality test of average promoter methylation for *CGB7* in breast group. Produced by Prism8 (Left: Anderson-Darling test output; right: plot of Normality test)

RM one-way ANOVA		
ANOVA results		
1	Table Analyzed	breast cgb7
2		
3	<b>Repeated measures ANOVA summary</b>	
4	Assume sphericity?	No
5	F	4.573
6	P value	0.0333
7	P value summary	*
8	Statistically significant (P < 0.05)?	Yes
9	Geisser-Greenhouse's epsilon	0.6999
10	R squared	0.2336

**Fig.A57** RM one-way ANOVA output of the average promoter methylation for *CGB7* in breast group. Produced by Prism8

RM one-way ANOVA						
Multiple comparisons						
1	Number of families	1				
2	Number of comparisons per family	3				
3	Alpha	0.05				
4						
5	<b>Tukey's multiple comparisons test</b>	<b>Mean Diff.</b>	<b>95.00% CI of diff.</b>	<b>Significant?</b>	<b>Summary</b>	<b>Adjusted P Value</b>
6	MCF-7 vs. MDA468	-0.4720	-1.889 to 0.9446	No	ns	0.6694
7	MCF-7 vs. breast-DNA	-1.986	-3.494 to -0.4783	Yes	**	0.0100
8	MDA468 vs. breast-DNA	-1.514	-3.806 to 0.7776	No	ns	0.2317

**Fig.A58** RM one-way ANOVA Multiple comparisons output of the average promoter methylation for *CGB7* in breast group (Tukey's test). Produced by Prism8

### A6.3.12 Colon group (*CGB7*)

Normality and Lognormality Tests		A	B
Tabular results		HCT116	CRL1790
1	<b>Test for normal distribution</b>		
2	<b>Anderson-Darling test</b>		
3	A2*	0.4323	0.3403
4	P value	0.2665	0.4504
5	Passed normality test (alpha=0.05)?	Yes	Yes
6	P value summary	ns	ns
7			
8	<b>Number of values</b>	16	16

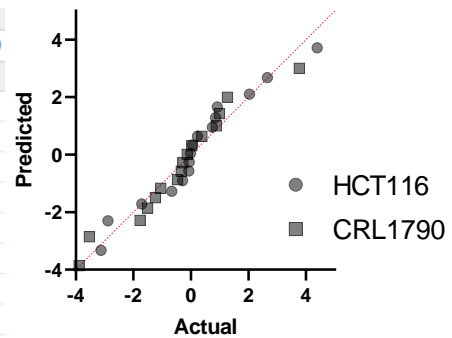


**Fig.A59** Normality test of average promoter methylation for *CGB7* in colon group. Produced by Prism8 (Left: Anderson-Darling test output; right: plot of Normality test)

Paired t test		
1	Table Analyzed	colon cgb7
2		
3	Column B	CRL1790
4	vs.	vs.
5	Column A	HCT116
6		
7	<b>Paired t test</b>	
8	P value	0.3159
9	P value summary	ns
10	Significantly different (P < 0.05)?	No
11	One- or two-tailed P value?	Two-tailed
12	t, df	t=1.038, df=15
13	Number of pairs	16

**Fig.A60** Paired t test output of the average promoter methylation for *CGB7* in colon group. Produced by Prism8

## A7. qRT-PCR data

**Table A6** Cq values obtained from RUN1 of qRT-PCR protocol. Adapted from LightCycler96 software

RUN1							
Analysis Name	Position	Sample Name	Gene Name	Cq	Cq Mean	Cq Error	Dye
Rel Quant	A3	1	CGB3-9	34.22	33.95	0.381838	FAM
Rel Quant	A4	1	CGB3-9	33.68	33.95	0.381838	FAM
Rel Quant	E3	1	GAPDH	15.62	15.58	0.056569	FAM
Rel Quant	E4	1	GAPDH	15.54	15.58	0.056569	FAM
Rel Quant	A5	2	CGB3-9	32.71	33.04	0.46669	FAM
Rel Quant	A6	2	CGB3-9	33.37	33.04	0.46669	FAM
Rel Quant	E5	2	GAPDH	15.88	15.57	0.438406	FAM
Rel Quant	E6	2	GAPDH	15.26	15.57	0.438406	FAM
Rel Quant	A7	3	CGB3-9	32.07	32.18	0.155563	FAM
Rel Quant	A8	3	CGB3-9	32.29	32.18	0.155563	FAM
Rel Quant	E7	3	GAPDH	16.11	16.12	0.014142	FAM
Rel Quant	E8	3	GAPDH	16.13	16.12	0.014142	FAM
Rel Quant	A9	4	CGB3-9	39.63	39.63	0	FAM
Rel Quant	A10	4	CGB3-9				FAM
Rel Quant	E9	4	GAPDH	16.61	16.835	0.318198	FAM
Rel Quant	E10	4	GAPDH	17.06	16.835	0.318198	FAM
Rel Quant	A11	5	CGB3-9	30.55	30.725	0.247487	FAM
Rel Quant	A12	5	CGB3-9	30.9	30.725	0.247487	FAM
Rel Quant	E11	5	GAPDH	15.26	15.51	0.353553	FAM
Rel Quant	E12	5	GAPDH	15.76	15.51	0.353553	FAM
Rel Quant	B1	6	CGB3-9	25.23	25.37	0.19799	FAM
Rel Quant	B2	6	CGB3-9	25.51	25.37	0.19799	FAM
Rel Quant	F1	6	GAPDH	15.07	14.735	0.473762	FAM
Rel Quant	F2	6	GAPDH	14.4	14.735	0.473762	FAM
Rel Quant	B3	7	CGB3-9	26.12	25.79	0.46669	FAM
Rel Quant	B4	7	CGB3-9	25.46	25.79	0.46669	FAM
Rel Quant	F3	7	GAPDH	13.8	14.24	0.622254	FAM
Rel Quant	F4	7	GAPDH	14.68	14.24	0.622254	FAM
Rel Quant	B5	8	CGB3-9	29.92	29.84	0.113137	FAM
Rel Quant	B6	8	CGB3-9	29.76	29.84	0.113137	FAM
Rel Quant	F5	8	GAPDH	15.79	15.9	0.155563	FAM
Rel Quant	F6	8	GAPDH	16.01	15.9	0.155563	FAM
Rel Quant	B7	9	CGB3-9	37.78	37.195	0.827315	FAM
Rel Quant	B8	9	CGB3-9	36.61	37.195	0.827315	FAM
Rel Quant	F7	9	GAPDH	15.58	15.705	0.176777	FAM
Rel Quant	F8	9	GAPDH	15.83	15.705	0.176777	FAM
Rel Quant	B9	10	CGB3-9				FAM
Rel Quant	B10	10	CGB3-9				FAM
Rel Quant	F9	10	GAPDH	15.86	15.78	0.113137	FAM
Rel Quant	F10	10	GAPDH	15.7	15.78	0.113137	FAM
Rel Quant	B11	11	CGB3-9	34.84	35.24	0.565685	FAM
Rel Quant	B12	11	CGB3-9	35.64	35.24	0.565685	FAM
Rel Quant	F11	11	GAPDH	15.2	15.15	0.070711	FAM
Rel Quant	F12	11	GAPDH	15.1	15.15	0.070711	FAM

Rel Quant	C1	12	CGB3-9	31.35	31.36	0.014142	FAM
Rel Quant	C2	12	CGB3-9	31.37	31.36	0.014142	FAM
Rel Quant	G1	12	GAPDH	16.71	16.67	0.056569	FAM
Rel Quant	G2	12	GAPDH	16.63	16.67	0.056569	FAM
Rel Quant	C3	13	CGB3-9	34.55	33.095	2.057681	FAM
Rel Quant	C4	13	CGB3-9	31.64	33.095	2.057681	FAM
Rel Quant	G3	13	GAPDH	15.95	16.035	0.120208	FAM
Rel Quant	G4	13	GAPDH	16.12	16.035	0.120208	FAM
Rel Quant	C5	14	CGB3-9	30	29.985	0.021213	FAM
Rel Quant	C6	14	CGB3-9	29.97	29.985	0.021213	FAM
Rel Quant	G5	14	GAPDH	15.21	15.685	0.671751	FAM
Rel Quant	G6	14	GAPDH	16.16	15.685	0.671751	FAM
Rel Quant	D3	19	CGB3-9				FAM
Rel Quant	D4	19	CGB3-9				FAM
Rel Quant	H3	19	GAPDH	32.74	32.735	0.007071	FAM
Rel Quant	H4	19	GAPDH	32.73	32.735	0.007071	FAM
Rel Quant	D5	20	CGB3-9	34.31	34.625	0.445477	FAM
Rel Quant	D6	20	CGB3-9	34.94	34.625	0.445477	FAM
Rel Quant	H5	20	GAPDH	15.98	15.885	0.13435	FAM
Rel Quant	H6	20	GAPDH	15.79	15.885	0.13435	FAM
Rel Quant	A1	NTC	CGB3-9				FAM
Rel Quant	A2	NTC	CGB3-9				FAM
Rel Quant	E1	NTC	GAPDH				FAM
Rel Quant	E2	NTC	GAPDH				FAM

**Table A7**  $\Delta\Delta Cq$  values obtained from RUN1.

SAMPLE		Cq CGB		Cq GAPDH		$\Delta Cq$	$\Delta\Delta Cq$	fold difference
ID	Z	Average	SD	Average	SD			
MCF-7	1	33.95	0.381838	15.58	0.056569	18.37	-3.12	8.69
MDAMB468	2	33.04	0.46669	15.57	0.438406	17.47	-4.02	16.22
C-33a	3	32.18	0.155563	16.12	0.014142	16.06	-5.43	43.11
HeLa	4	39.63	0	16.835	0.318198	22.795	1.305	0.40
HT-3	5	30.725	0.247487	15.51	0.353553	15.215	-6.275	77.44
BeWo	6	25.37	0.19799	14.735	0.473762	10.635	-10.855	1852.17
JEG-3	7	25.79	0.46669	14.24	0.622254	11.55	-9.94	982.29
HCT116	8	29.84	0.113137	15.9	0.155563	13.94	-7.55	187.40
CRL-1790	9	37.195	0.827315	15.705	0.176777	21.49	0	1.00
3T3	10	-	-	15.78	0.113137	-	-	-
HEY	11	35.24	0.565685	15.15	0.070711	20.09	-1.4	2.64
OAW42	12	31.36	0.014142	16.67	0.056569	14.69	-6.8	111.43
OVCAR-3	13	33.095	2.057681	16.035	0.120208	17.06	-4.43	21.56
SKOV-3	14	29.985	0.021213	15.685	0.671751	14.3	-7.19	146.02
NRT	19	-	-	32.735	0.007071	-	-	-
	20	34.625	0.445477	15.885	0.13435	18.74	-2.75	6.73

**Table A8** Cq values obtained from RUN2 of qRT-PCR protocol. Adapted from LightCycler96 software

<b>RUN2</b>							
<b>Analysis Name</b>	<b>Position</b>	<b>Sample Name</b>	<b>Gene Name</b>	<b>Cq</b>	<b>Cq Mean</b>	<b>Cq Error</b>	<b>Dye</b>
Rel Quant	A3	1	CGB3-9	36.65	34.94	2.418305192	FAM
Rel Quant	A4	1	CGB3-9	33.23	34.94	2.418305192	FAM
Rel Quant	E3	1	GAPDH	15.14	15.16	0.028284271	FAM
Rel Quant	E4	1	GAPDH	15.18	15.16	0.028284271	FAM
Rel Quant	A5	2	CGB3-9	33.66	33.76	0.141421356	FAM
Rel Quant	A6	2	CGB3-9	33.86	33.76	0.141421356	FAM
Rel Quant	E5	2	GAPDH	15.29	14.96	0.466690476	FAM
Rel Quant	E6	2	GAPDH	14.63	14.96	0.466690476	FAM
Rel Quant	A7	3	CGB3-9	32.88	32.325	0.784888527	FAM
Rel Quant	A8	3	CGB3-9	31.77	32.325	0.784888527	FAM
Rel Quant	E8	3	GAPDH	15.29	15.49	0.282842712	FAM
Rel Quant	H9	3	GAPDH	15.69	15.49	0.282842712	FAM
Rel Quant	A9	4	CGB3-9	38.22	38.22	0	FAM
Rel Quant	A10	4	CGB3-9				FAM
Rel Quant	E9	4	GAPDH	16.21	16.2	0.014142136	FAM
Rel Quant	E10	4	GAPDH	16.19	16.2	0.014142136	FAM
Rel Quant	A11	5	CGB3-9	30.22	30	0.311126984	FAM
Rel Quant	A12	5	CGB3-9	29.78	30	0.311126984	FAM
Rel Quant	E11	5	GAPDH	14.5	14.68	0.254558441	FAM
Rel Quant	E12	5	GAPDH	14.86	14.68	0.254558441	FAM
Rel Quant	B1	6	CGB3-9	24.47	24.67	0.282842712	FAM
Rel Quant	B2	6	CGB3-9	24.87	24.67	0.282842712	FAM
Rel Quant	F1	6	GAPDH	14.73	14.67	0.084852814	FAM
Rel Quant	F2	6	GAPDH	14.61	14.67	0.084852814	FAM
Rel Quant	B3	7	CGB3-9	25.96	25.915	0.06363961	FAM
Rel Quant	B4	7	CGB3-9	25.87	25.915	0.06363961	FAM
Rel Quant	F3	7	GAPDH	14.27	14.105	0.233345238	FAM
Rel Quant	F4	7	GAPDH	13.94	14.105	0.233345238	FAM
Rel Quant	B5	8	CGB3-9	29.51	28.805	0.997020561	FAM
Rel Quant	B6	8	CGB3-9	28.1	28.805	0.997020561	FAM
Rel Quant	F5	8	GAPDH	15.64	15.35	0.410121933	FAM
Rel Quant	F6	8	GAPDH	15.06	15.35	0.410121933	FAM
Rel Quant	B7	9	CGB3-9	34.4	35.16	1.074802307	FAM
Rel Quant	B8	9	CGB3-9	35.92	35.16	1.074802307	FAM
Rel Quant	F7	9	GAPDH	15.18	15.125	0.077781746	FAM
Rel Quant	F8	9	GAPDH	15.07	15.125	0.077781746	FAM
Rel Quant	B9	10	CGB3-9				FAM
Rel Quant	B10	10	CGB3-9				FAM
Rel Quant	F9	10	GAPDH	15.65	15.36	0.410121933	FAM
Rel Quant	F10	10	GAPDH	15.07	15.36	0.410121933	FAM
Rel Quant	B11	11	CGB3-9	35.06	34.675	0.544472222	FAM
Rel Quant	B12	11	CGB3-9	34.29	34.675	0.544472222	FAM
Rel Quant	F11	11	GAPDH	14.86	14.74	0.169705627	FAM
Rel Quant	F12	11	GAPDH	14.62	14.74	0.169705627	FAM
Rel Quant	C1	12	CGB3-9	31.35	31.8	0.636396103	FAM
Rel Quant	C2	12	CGB3-9	32.25	31.8	0.636396103	FAM



Rel Quant	G1	12	GAPDH	15.7	15.925	0.318198052	FAM
Rel Quant	G2	12	GAPDH	16.15	15.925	0.318198052	FAM
Rel Quant	C3	13	CGB3-9	34.56	34.735	0.247487373	FAM
Rel Quant	C4	13	CGB3-9	34.91	34.735	0.247487373	FAM
Rel Quant	G3	13	GAPDH	15.24	15.28	0.056568542	FAM
Rel Quant	G4	13	GAPDH	15.32	15.28	0.056568542	FAM
Rel Quant	C5	14	CGB3-9	30.06	29.515	0.770746391	FAM
Rel Quant	C6	14	CGB3-9	28.97	29.515	0.770746391	FAM
Rel Quant	G5	14	GAPDH	15.02	15.195	0.247487373	FAM
Rel Quant	G6	14	GAPDH	15.37	15.195	0.247487373	FAM
Rel Quant	D3	19	CGB3-9				FAM
Rel Quant	D4	19	CGB3-9				FAM
Rel Quant	H3	19	GAPDH	32.77	33.345	0.813172798	FAM
Rel Quant	H4	19	GAPDH	33.92	33.345	0.813172798	FAM
Rel Quant	D5	20	CGB3-9	26.8	28.645	2.609224023	FAM
Rel Quant	D6	20	CGB3-9	30.49	28.645	2.609224023	FAM
Rel Quant	H5	20	GAPDH	15.92	15.78	0.197989899	FAM
Rel Quant	H6	20	GAPDH	15.64	15.78	0.197989899	FAM
Rel Quant	A1	NTC	CGB3-9				FAM
Rel Quant	A2	NTC	CGB3-9				FAM
Rel Quant	E1	NTC	GAPDH				FAM
Rel Quant	E2	NTC	GAPDH				FAM

**Table A9**  $\Delta\Delta Cq$  values obtained from RUN2.

SAMPLE		Cq CGB		Cq gapdh		$\Delta Cq$	$\Delta\Delta Cq$	fold difference
Z	ID	Average	SD	Average	SD			
1	MCF-7	34.94	2.418305	15.16	0.028284	19.78	-0.255	1.19
2	MDAMB468	33.76	0.141421	14.96	0.46669	18.8	-1.235	2.35
3	C-33a	32.325	0.784889	15.49	0.282843	16.835	-3.2	9.19
4	HeLa	38.22		16.2	0.014142	22.02	1.985	0.25
5	HT-3	30	0.311127	14.68	0.254558	15.32	-4.715	26.26
6	BeWo	24.67	0.282843	14.67	0.084853	10	-10.035	1049.15
7	JEG-3	25.915	0.06364	14.105	0.233345	11.81	-8.225	299.21
8	HCT116	28.805	0.997021	15.35	0.410122	13.455	-6.58	95.67
9	CRL-1790	35.16	1.074802	15.125	0.077782	20.035	0	1.00
10	3T3			15.36	0.410122			
11	HEY	34.675	0.544472	14.74	0.169706	19.935	-0.1	1.07
12	OAW42	31.8	0.636396	15.925	0.318198	15.875	-4.16	17.88
13	OVCAR-3	34.735	0.247487	15.28	0.056569	19.455	-0.58	1.49
14	SKOV-3	29.515	0.770746	15.195	0.247487	14.32	-5.715	52.53
19	NRT			33.345	0.813173			
20		28.645	2.609224	15.78	0.19799	12.865	-7.17	144.01

**Table A10** Cq values obtained from RUN3 of qRT-PCR protocol. Adapted from LightCycler96 software

<b>Run3</b>							
<b>Analysis Name</b>	<b>Position</b>	<b>Sample Name</b>	<b>Gene Name</b>	<b>Cq</b>	<b>Cq Mean</b>	<b>Cq Error</b>	<b>Dye</b>
Rel Quant	A3	1	CGB3-9	33.46	33.325	0.190919	FAM
Rel Quant	A4	1	CGB3-9	33.19	33.325	0.190919	FAM
Rel Quant	E3	1	GAPDH	15.09	15.06	0.042426	FAM
Rel Quant	E4	1	GAPDH	15.03	15.06	0.042426	FAM
Rel Quant	A5	2	CGB3-9	33.79	33.82	0.042426	FAM
Rel Quant	A6	2	CGB3-9	33.85	33.82	0.042426	FAM
Rel Quant	E5	2	GAPDH	14.77	14.73	0.056569	FAM
Rel Quant	E6	2	GAPDH	14.69	14.73	0.056569	FAM
Rel Quant	A7	3	CGB3-9	32.07	32.1	0.042426	FAM
Rel Quant	A8	3	CGB3-9	32.13	32.1	0.042426	FAM
Rel Quant	E7	3	GAPDH	15.74	15.725	0.021213	FAM
Rel Quant	E8	3	GAPDH	15.71	15.725	0.021213	FAM
Rel Quant	A9	4	CGB3-9				FAM
Rel Quant	A10	4	CGB3-9	39.51	39.51	0	FAM
Rel Quant	E9	4	GAPDH	16.37	16.29	0.113137	FAM
Rel Quant	E10	4	GAPDH	16.21	16.29	0.113137	FAM
Rel Quant	A11	5	CGB3-9	31.03	31.005	0.035355	FAM
Rel Quant	A12	5	CGB3-9	30.98	31.005	0.035355	FAM
Rel Quant	E11	5	GAPDH	15.27	15.43	0.226274	FAM
Rel Quant	E12	5	GAPDH	15.59	15.43	0.226274	FAM
Rel Quant	B1	6	CGB3-9	24.47	24.455	0.021213	FAM
Rel Quant	B2	6	CGB3-9	24.44	24.455	0.021213	FAM
Rel Quant	F1	6	GAPDH	14.08	14.05	0.042426	FAM
Rel Quant	F2	6	GAPDH	14.02	14.05	0.042426	FAM
Rel Quant	B3	7	CGB3-9	26.54	26.65	0.155563	FAM
Rel Quant	B4	7	CGB3-9	26.76	26.65	0.155563	FAM
Rel Quant	F3	7	GAPDH	14.07	13.93	0.19799	FAM
Rel Quant	F4	7	GAPDH	13.79	13.93	0.19799	FAM
Rel Quant	B5	8	CGB3-9	29.88	29.98	0.141421	FAM
Rel Quant	B6	8	CGB3-9	30.08	29.98	0.141421	FAM
Rel Quant	F5	8	GAPDH	15.1	14.965	0.190919	FAM
Rel Quant	F6	8	GAPDH	14.83	14.965	0.190919	FAM
Rel Quant	B7	9	CGB3-9	36.8	36.955	0.219203	FAM
Rel Quant	B8	9	CGB3-9	37.11	36.955	0.219203	FAM
Rel Quant	F7	9	GAPDH	15.14	15.32	0.254558	FAM
Rel Quant	F8	9	GAPDH	15.5	15.32	0.254558	FAM
Rel Quant	B9	10	CGB3-9				FAM
Rel Quant	B10	10	CGB3-9				FAM
Rel Quant	F9	10	GAPDH	15.07	15.2	0.183848	FAM
Rel Quant	F10	10	GAPDH	15.33	15.2	0.183848	FAM
Rel Quant	B11	11	CGB3-9	35.31	35.32	0.014142	FAM
Rel Quant	B12	11	CGB3-9	35.33	35.32	0.014142	FAM
Rel Quant	F11	11	GAPDH	14.64	14.58	0.084853	FAM
Rel Quant	F12	11	GAPDH	14.52	14.58	0.084853	FAM
Rel Quant	C1	12	CGB3-9	31.2	31.425	0.318198	FAM
Rel Quant	C2	12	CGB3-9	31.65	31.425	0.318198	FAM

Rel Quant	G1	12	GAPDH	15.87	15.795	0.106066	FAM
Rel Quant	G2	12	GAPDH	15.72	15.795	0.106066	FAM
Rel Quant	C3	13	CGB3-9	34.97	35.445	0.671751	FAM
Rel Quant	C4	13	CGB3-9	35.92	35.445	0.671751	FAM
Rel Quant	G3	13	GAPDH	14.56	14.92	0.509117	FAM
Rel Quant	G4	13	GAPDH	15.28	14.92	0.509117	FAM
Rel Quant	C5	14	CGB3-9	29.68	29.89	0.296985	FAM
Rel Quant	C6	14	CGB3-9	30.1	29.89	0.296985	FAM
Rel Quant	G5	14	GAPDH	15.3	15.625	0.459619	FAM
Rel Quant	G6	14	GAPDH	15.95	15.625	0.459619	FAM
Rel Quant	D3	19	CGB3-9	36.29	36.29	0	FAM
Rel Quant	D4	19	CGB3-9				FAM
Rel Quant	H3	19	GAPDH	32.24	32.265	0.035355	FAM
Rel Quant	H4	19	GAPDH	32.29	32.265	0.035355	FAM
Rel Quant	D5	20	CGB3-9	34.8	34.815	0.021213	FAM
Rel Quant	D6	20	CGB3-9	34.83	34.815	0.021213	FAM
Rel Quant	H5	20	GAPDH	15.18	15.17	0.014142	FAM
Rel Quant	H6	20	GAPDH	15.16	15.17	0.014142	FAM
Rel Quant	A1	NTC	CGB3-9				FAM
Rel Quant	A2	NTC	CGB3-9				FAM
Rel Quant	E1	NTC	GAPDH				FAM
Rel Quant	E2	NTC	GAPDH				FAM

**Table A11**  $\Delta\Delta Cq$  values obtained from RUN3

SAMPLE		Cq CGB		Cq gapdh		$\Delta Cq$	$\Delta\Delta Cq$	fold difference
Z	ID	Average	SD	Average	SD			
1	MCF-7	33.325	0.190919	15.06	0.042426	18.265	-3.37	10.34
2	MDAMB468	33.82	0.042426	15.725	0.056569	18.095	-3.54	11.63
3	C-33a	32.1	0.042426	15.725	0.021213	16.375	-5.26	38.32
4	HeLa	39.51		15.725	0.113137	23.785	2.15	0.23
5	HT-3	31.005	0.035355	15.43	0.226274	15.575	-6.06	66.72
6	BeWo	24.455	0.021213	14.05	0.042426	10.405	-11.23	2401.97
7	JEG-3	26.65	0.155563	13.93	0.19799	12.72	-8.915	482.71
8	HCT116	29.98	0.141421	14.965	0.190919	15.015	-6.62	98.36
9	CRL-1790	36.955	0.219203	15.32	0.254558	21.635	0	1.00
10	3T3			15.2	0.183848			
11	HEY	35.32	0.014142	14.58	0.084853	20.74	-0.895	1.86
12	OAW42	31.425	0.318198	15.795	0.106066	15.63	-6.005	64.22
13	OVCAR-3	35.445	0.671751	14.92	0.509117	20.525	-1.11	2.16
14	SKOV-3	29.89	0.671751	15.625	0.459619	14.265	-7.37	165.42
19	NRT			32.265	0.035355			
20		34.815	0.021213	15.17	0.014142	19.645	-1.99	3.97

## A7.1 Correlation

**Table A12** Association between the transcription data and averaged methylation.

Spearman's rho produced in Minitab. The grey rows contain Spearman's coefficient and the no-fill rows contain the p-value for the respective coefficient.

	FOLD DIFF.		FOLD DIFF.		FOLD DIFF.
<b>WHOLE</b>	0.038	<b>CGB358_WHOLE</b>	0.000	<b>CGB7_WHOLE</b>	-0.121
	0.901		1.000		0.694
<b>5 REGION</b>	0.049	<b>CGB358_5 REGION</b>	0.225	<b>CGB7_5 REGION</b>	0.038
	0.873		0.459		0.901
<b>3 REGION</b>	-0.099	<b>CGB358_3 REGION</b>	-0.044	<b>CGB7_3 REGION</b>	-0.088
	0.748		0.887		0.775

## A8. ELISA data

**Table A13** Free-beta hCG ELISA OD values used to calculate the concentration of the subunit in media. Values are 450nm reading subtracted from the 650nm reading

	ID	Run1		Run 2		
standards	0 ng/ml	0.011	0.012	0.009	0.008	-
	1.25ng/ml	-	-	0.077	0.07	-
	2.5ng/ml	0.171	0.169	0.139	0.123	-
	5ng/ml	0.298	0.302	0.261	0.198	-
	10ng/ml	0.498	0.479	0.414	0.384	-
	25ng/ml	0.934	0.932	0.816	0.844	-
	50ng/ml	1.421	1.462	1.219	1.225	-
	100ng/ml	2.08	1.95	-	-	-
	200ng/ml	2.377	2.298	-	-	-
	low standard	0.716	0.684	0.563	0.559	-
samples	CRL-1790	0.011	0.012	0.009	0.009	0.008
	SKOV-3	0.194	0.197	0.192	0.177	0.174
	C-33a	0.012	0.011	0.01	0.01	0.007
	MDAMB468	0.012	0.01	0.009	0.009	0.01
	OVCAR-3	0.012	0.011	0.01	0.008	0.008
	HEY	0.076	0.077	0.077	0.065	0.072
	OAW42	0.023	0.016	0.017	0.013	0.016
	MCF-7	0.011	0.01	0.012	0.007	0.008
	BeWo	0.199	0.161	0.162	0.153	0.142
	JEG-3	0.091	0.093	0.085	0.072	0.078
	HeLa	0.014	0.014	0.013	0.009	0.01
	3T3	0.012	0.013	0.01	0.008	0.009

**Table A14** Intact hCG ELISA OD values used to calculate the concentration of the hormone in media.

	ID	OD (460nm-650nm)	
standards	0 mIU/ml	0.021	0.019
	5 mIU/ml	0.021	0.019
	10 mIU/ml	0.052	0.055
	50 mIU/ml	0.17	0.203
	200 mIU/ml	0.899	0.932
	500 mIU/ml	1.855	1.834
Samples	CRL-1790	0.018	0.017
	SKOV-3	0.019	0.019
	C-33a	0.018	0.018
	MDAMB468	0.02	0.019
	OVCAR-3	0.019	0.018
	HEY	0.021	0.019
	OAW42	0.021	0.018
	MCF-7	0.021	0.021
	BeWo	0.511	0.523
	JEG-3	0.535	0.54
	HeLa	0.02	0.018
	3T3	0.018	0.017

**Regression Formula:**  $y = d + \frac{a-d}{1+(x/c)^b}$

**Inverse Formula:**  $x = c\left(\frac{a-d}{y-d} - 1\right)^{\frac{1}{b}}$

Where:

y = Response Value eg. OD

x = Dose Value eg. Concentration

and the constants/parameters are as follows:

a	b	c	d
2.062	-1.147	36.998	0.038

**R<sup>2</sup> value:** 0.998

**Fig.A61** Regression formula and R<sup>2</sup> calculated based on free beta hCG ELISA standards from Run 1 used to calculate concentration of samples. Curve equation calculated by 4 parameter fit model. Calculation done using <https://elisaanalysis.com>

**Regression Formula:**  $y = d + \frac{a-d}{1+(x/c)^b}$

**Inverse Formula:**  $x = c\left(\frac{a-d}{y-d} - 1\right)^{\frac{1}{b}}$

Where:

y = Response Value eg. OD

x = Dose Value eg. Concentration

and the constants/parameters are as follows:

a	b	c	d
2.9654991	-1.4387708	356.9563315	0.0242282

**R<sup>2</sup> value:** 0.9996244

**Fig.A62** Regression formula and R<sup>2</sup> calculated based on intact hCG ELISA standards. Curve equation calculated by 4 parameter fit model used to calculate concentration of samples. Calculation done using <https://elisaanalysis.com>